NASA Conference Publication 3318

First Moderate Resolution Imaging Spectroradiometer (MODIS) Snow and Ice Workshop

Edited by
Dorothy K. Hall
NASA Goddard Space Flight Center
Greenbelt, Maryland

Proceedings of a workshop sponsored by the
NASA/Goddard Space Flight Center and
held at the U.S. Geological Survey
in Reston, Virginia and at
Goddard Space Flight Center in
Greenbelt, Maryland
September 13-14, 1995

National Aeronautics
and Space Administration

Goddard Space Flight Center
Greenbelt, Maryland 20771

1995

Preface

On 13-14 September 1995, a workshop was held in Reston, Virginia and Greenbelt, Maryland at which snow and ice scientists met to discuss the Earth Observing System (EOS) Moderate Resolution Imaging Spectroradiometer (MODIS) snow and ice products. The workshop was sponsored by NASA/Goddard Space Flight Center. The first morning of the workshop was held at the U.S. Geological Survey in Reston in conjunction with the Arctic Climate Systems Study (ACSYS) workshop which, on that day, was focusing on solid precipitation. On the second day, the MODIS snow and ice workshop was held at Goddard Space Flight Center. Thirty six people registered. Eighteen presentations were made dealing with various aspects of snow and ice and snow-cover mapping. During the remainder of the second day, attendees participated in one of four working groups, each of which discussed different aspects of MODIS snow and ice products. During the working group sessions, participants also discussed a set of questions provided to them at the beginning of the workshop. The chairperson of each working group summarized results at the end of the workshop in the closing plenary session.

Executive Summary

The objectives of the First MODIS Snow and Ice Workshop were to: inform the snow and ice scientific community of potential MODIS products, ensure that the snow and ice products meet the needs of future users, seek advice from the participants regarding the utility of the products, and determine the needs for future post-launch MODIS snow and ice products.

After hearing descriptions of the algorithm-development efforts from the MODIS snow and ice algorthim-development team, discussions were held regarding the utility of the planned products. At the beginning of the workshop, the snow and ice maps were envisioned to be global, 1-km daily, and weekly-composited maps, with snow and ice (both sea ice and ice on large, inland lakes) being identified using an algorithm that employs thresholding to identify snow or ice. Nearly everyone (both operational and research-oriented people) expressed the desire to have the snow maps at better than 1-km resolution). People who were involved in operational aspects of snow and ice monitoring expressed a desire to receive both snow and ice maps in 24 hours or less, but indicated that a 48-hour turnaround time is still useful.

The MODIS snow and ice products will be modified in the pre-launch time frame as a result of the workshop recommendations. Exact details of the changes will evolve over the next few months. However it has been decided that the snow map and the maps of the large, inland lakes will have 500-m spatial resolution instead of 1-km resolution. Additionally, a scheme will be devised wherein the user can select his/her own time period for compositing. In regard to the sea ice product, we will work to implement the sea ice algorithms that were identified during the workshop discussions. Interim results of the algorithm changes will be presented over the next year at scientific meetings.

Brief summaries of the working group recomendations are given below. One theme that was brought out in all of the group discussions was the importance of a good cloud mask. This is considered essential to the successful utilization of the MODIS data. The MODIS cloud mask can be validated with other EOS data, such as the Advanced Spaceborne Thermal Emission and Reflection Radiometer (ASTER).

MODIS At-Launch Snow Products Working Group

There was much discussion about the planned MODIS snow maps. It was generally agreed that daily maps would be useful as would composite maps. However, there was no agreement on the time period of the compositing. People involved in long-term climate studies were interested in monthly snow maps, while others wanted maps composited for a period of a few days or a week. There was also agreement that fractional snow cover is desirable and is possible to accomplish using some image-processing techniques today, in small basins. However, for the production of global maps, these advanced techniques are not yet available. In the pre-launch time frame, when the algorithm has to be finalized, no-one suggested a way to do fractional snow cover globally.

For operational studies, 250-500-m spatial resolution is optimal with a 24-48-hour turnaround time after data acquisition. However, 500-m resolution with 48-hour turnaround is acceptable. The daily snow map is necessary for operational use. A monthly product would be good for climatological studies. It was concluded that the user should decide the compositing period of the daily maps.

MODIS At-Launch Ice Products Working Group

In regard to the sea ice product, the participants concluded that a binary map of sea ice was only marginally useful because RADARSAT synthetic aperture radar (SAR) data are expected to be available in the near future. However MODIS will have better coverage of the Antarctic than will RADARSAT. Additionally, optical data are important and can provide information not available using microwave data, especially when the sea ice is wet. If RADARSAT data are not always available due to failure of the satellite or the sensor, it would be necessary to have other data available. Furthermore, thermal-infrared data, to be available on the MODIS, can provide sea ice temperature, which cannot be obtained using microwave data.

While it was generally agreed that optical data were important for sea ice studies, it was concluded that ice type and concentration information was needed as well as information on the location of sea ice. The group identified a sea ice algorithm, developed by Koni Steffen, that may be useful for that purpose. The group concluded that 1-km spatial resolution is adequate for sea ice studies.

In regard to large inland lakes, discussion indicated that 500-m resolution daily maps would be useful and an important advance over the 1-km resolution data that are currently available.

Post-Launch MODIS Snow and Ice Products

For a post-launch snow product, subpixel snow mapping is needed at local and regional scales. Additionally, combining Multi-Angle Imaging Spectroradiometer (MISR) and MODIS data, and utilizing the pointing capabilities of the MISR, may increase accuracy of snow mapping in forests. In a post-launch product, albedo, temperature and wetness are also desired.

For sea ice, knowledge of albedo, surface temperature, open water fraction, ice type and ice motion is desired.

There was also a discussion about gridding. The group concluded that the planned use of the International Satellite Cloud Climatology Project (ISCCP)-derived grid for EOS Level 3 products may not be suitable for polar applications of the MODIS Snow and Ice products. More information is needed to determine the best approach (one that is efficient while preserving scientific integrity) to routinely produce these data for the polar community.

Utility of MODIS Snow and Ice Products

MODIS snow and ice products will be useful for input to snowmelt-runoff models, to validate other sources of snow data, for ice navigation, for ice-jam monitoring, and to study air/sea interaction among other things. A monthly snow or ice product would be useful for climatologists. MODIS data will likely be useful for operational needs especially if 250-m and 500-m resolution data are available within 48 hours.

Additionally, the MODIS data will be especially useful when combined with other data, such as passive-microwave data for determination of snow water equivalent.

Metadata that will be required with the snow and ice products include information on: georeferencing, ephemeris data, calibration and orbit parameters and information on quality of data.

Table of Contents

Session 3: Mapping Ice and Clouds with Optical Sensors

Session 4: Miscellaneous Topics

Working Group Reports

FIRST MODIS SNOW AND ICE WORKSHOP

Final Agenda

Wednesday, September 13, 1995

7:45 - 8:45 A.M. Bus ride from Greenbelt, Maryland to Reston, Virginia

COMBINED ACSYS/MODIS SESSION ON SNOW

U.S.G.S. Auditorium, Reston, VA

8:45 - 9:00	Sign in
9:00 - 9:15	Refreshments
9:15 - 9:25	R.G. Barry and D. K. Hall - Welcome to combined ACSYS/MODIS Workshop
9:25 - 9:55	T. Carroll - Remote sensing of snow in the cold regions
9:55 - 10:25	D.K. Hall - Satellite snow-cover mapping: a brief review
10:25 - 10:40	B. Ramsay - Interactive multisensor snow and ice mapping system
10:40 - 10:50	Break
10:50 - 11:05	C. Bertoia - Use of satellite data for operational sea ice and lake ice studies
11:05 - 11:20	M. Baumgartner - An integrated analysis system for monitoring snow cover variations in the Alps using NOAA/AVHRR data
11:20 - 11:35	A. Nolin - Fractional snow-covered area mapping using spectral mixture analysis
11:35 - 11:45	Discussion/Questions on morning presentations
11:45 - 12:45	Lunch

MODIS SESSION ON SNOW COVER MAPPING
D. Hall, Chair

Conference room at U.S. Geological Survey (Rm. 1B215)

12:50 - 1:00	D. Hall - Presentation of key MODIS snow/ice issues to be discussed
1:00 - 1:30	G. Riggs - MODIS snow and ice algorithm development
1:30 - 1:45	Discussion
1:45 - 2:00	D. Robinson - An analysis of the NOAA satellite-derived snow-cover record, 1966 - present for polar AVHRR
2:00 - 2:15	R. Green - Snow distribution, grain size and melting properties remotely measured and validated in the solar reflected spectrum
2:15 - 2:30	Break

MAPPING ICE AND CLOUDS WITH OPTICAL SENSORS
D. Hall, Chair

2:30 - 2:45	J. Key - The cloud and surface parameters retrieval (CASPR) system
2:45 - 3:00	R. Welch - Polar cloud and surface classification using Landsat data
3:00 - 3:15	K. Steffen - Potential MODIS applications for ice surface studies based on AVHRR experience
3:15 - 3:30	J. Comiso - Cloud masking and surface temperature distribution in the polar regions using AVHRR and other satellite data
3:30 - 3:45	Break
3:45 - 4:00	G. Leshkevich - Satellite mapping of Great Lakes ice cover
4:00 - 4:15	S. Ackerman - Development of the MODIS Cloud Mask
4:15 - 4:50	Discussion of sea ice and lake ice algorithm development
5:00 - 6:00	Bus ride to Greenbelt.

Thursday, September 14, 1995

Goddard Space Flight Center, Greenbelt, Maryland

8:00 - 8:30 Refreshments

8:30 - 8:35 D. Hall - Day 2 opening comments

8:35 - 8:50 T. Anderson - SNOWSAT - Operational snow mapping in Norway

8:50 - 9:05 K. Seidel - Multisensor analysis of satellite images for regional snow distribution

9:05 - 9:20 G. Scharfen - MODIS activities at the NSIDC DAAC

9:20 - 9:30 Break/Form working groups in various conference rooms

Working Groups*:

I. MODIS at-launch snow products working group - M. Baumgartner, Chair

T. Anderson
R. Armstrong
J. Foster
D. Hall
B. Ramsay
W. Rosenthal
K. Seidel

II. MODIS at-launch ice products working group - C. Bertoia, Chair

L. Brigham
D. Cavalieri
J. Comiso
D. Hall
J. Key
G. Leshkevich
C. Parkinson
K. Steffen

III. Post-launch MODIS snow and ice products - R. Welch, Chair

J. Dozier
R. Green
J. Key
A. Nolin
G. Riggs
G. Scharfen
L. Smith

IV. Utility of MODIS snow and ice products - A. Walker, Chair

S. Ackerman
M. Baumgartner
T. Carroll
E. Josberger
A. Rango
G. Riggs
D. Robinson

9:15 - 12:00 Discuss MODIS snow and ice algorithms in working groups and provide written comments

12:00 - 1:00 Lunch

Afternoon session

1:00 - 1:45 Finish writing comments for workshop proceedings

1:45 - 3:15 Oral reports from working group chairs, and discussion

1:45 - 2:00 R. Welch, Group III Chair

2:00 - 2:20 M. Baumgartner, Group I Chair

2:20 - 2:40 C. Bertoia, Group II Chair

2:40 - 3:00 A. Walker, Group IV Chair

3:00 - 3:10 D. Hall - Closing remarks including a discussion of the need for a future MODIS snow and ice workshop

3:10 Adjourn

SESSION I: MODIS/ACSYS PLENARY

~~~~~~
NATIONAL OPERATIONAL HYDROLOGIC REMOTE SENSING CENTER
Office of Hydrology
National Weather Service, NOAA
1735 Lake Drive West
Chanhassen, Minnesota 55317-8582
~~~~~~
Telephone: (612) 361-6610 ex 225 MCI Mail: NOHRSC
Facsimile: (612) 361-6634 CCMail: Tom Carroll
Internet: tc@nohrsc.nws.gov
http://www.nohrsc.nws.gov
~~~~~~

REMOTE SENSING OF SNOW IN THE COLD REGIONS

by

Thomas R. Carroll

National Operational Hydrologic Remote Sensing Center
Office of Hydrology
National Weather Service
1735 Lake Drive West
Chanhassen, Minnesota 55317-8582

1. ABSTRACT

The National Weather Service (NWS) maintains the National Operational Hydrologic Remote Sensing Center, based in Minneapolis, to generate operational hydrologic products from in situ and remotely sensed snow cover data sets. The Center maintains an Airborne Snow Survey Program, a Satellite Hydrology Program, and a Snow Estimation and Updating Program. In all three programs, the Center relies heavily on the use of multiple Geographic Information Systems (GIS) to process, analyze, and distribute spatial snow cover data sets. Real-time, airborne snow water equivalent data and satellite areal extent of snow cover data are used operationally by the National Weather Service, the U.S. Army Corps of Engineers and other Federal, state, and private agencies when issuing spring flood outlooks, water supply outlooks, river and flood forecasts, and reservoir inflow forecasts. The remotely sensed and interpolated, gridded, snow water equivalent data products are generated by hydrologists in the Minneapolis office and distributed electronically, in near real-time, to NWS and non-NWS end-users in both alphanumeric and graphic format. The reliable, real-time, snow water equivalent information is critical to
~~~~~~

water managers and disaster emergency services officials who are required to make decisions with regard to snowmelt
flooding, reservoir regulation, and water supply allocation.

2. AIRBORNE SNOW SURVEY PROGRAM

The ability to make reliable, airborne gamma radiation snow water equivalent measurements is based on the fact that natural terrestrial gamma radiation is emitted from the potassium, uranium, and thorium radioisotopes in the upper 20 cm of soil. The radiation is sensed from a low-flying aircraft flying 150 m above the ground. Water mass in the snow cover attenuates, or blocks, the
terrestrial radiation signal. Consequently, the difference between airborne radiation measurements made over bare ground and snow covered ground can be used to calculate a mean areal snow water equivalent value with a root mean square error of less than one cm. Each flight line is typically 16 km long and 300 m wide covering an area of approximately 5 sq km. Consequently, each
airborne snow water equivalent measurement is a mean areal measure integrated over the 5 sq km area of the flight line. The techniques used to make airborne snow water equivalent measurements in a prairie, forest, and mountain snowpack environment have been reported in detail by Carroll and Carroll (1989A, 1989B, 1990). The physics and calibration of the airborne gamma
radiation spectrometer were developed under contract by EG&G, Inc. in Las Vegas and have been described by Fritzsche (1982). Details of the system hardware and radiation spectral data collection and analysis procedures have been described by Fritzsche (1982) and others and will not be discussed here.

Airborne snow water equivalent measurements are made using the relationship given in equation (1).

$$SWE = \frac{1}{A}\left[\ln\frac{Co}{C} - \ln\frac{100 + 1.11\,M}{100 + 1.11\,Mo}\right] \quad g\,cm^{-2} \qquad (1)$$

where:

C and Co = Uncollided terrestrial gamma count rates over snow and bare ground,

M and Mo = Percent soil moisture over snow and bare ground,

A = Radiation attenuation coefficient in water, cm2/g

Extraneous radiation is contributed to the spectra by the Compton tails associated with the peaks of higher energy, the cosmic radiation component, the aircraft and fuel, the pilots, and the detection system itself. The raw radiation count rates for various photopeaks must be "stripped" of the extraneous sources to give the pure, uncollided radiation count rates (Fritzsche, 1982). Air mass between the airborne sensors and the terrestrial radiation source also attenuates the radiation signal. Consequently, air temperature, air pressure, and radar altitude are recorded continuously to calculate and compensate for the intervening air mass. After the appropriate photopeaks have been stripped of extraneous radiation, they are normalized to a standard air mass of 17 g/cm2.

2.1 Airborne Measurement Error and Simulation

The principal sources of error in airborne snow water equivalent calculation using the relationship given in equation (1) are: (1) errors in the normalized count rates (C, Co), (2) errors in the estimate of mean areal soil moisture over the flight line (M, Mo), and (3) errors in the radiation attenuation coefficient (A) derived from calibration data.

Carroll and Carroll (1989B) simulated the principle sources of error for airborne measurements made over forested watersheds with as much as 60 cm of snow water equivalent. The results indicate that airborne snow water equivalent measurements can be made in forest environments with 60 cm of water equivalent with an error of approximately 12 percent. The simulated results agree closely with the empirical errors derived from ground snow survey data collected in a forest environment with 48 cm of snow water equivalent (Carroll and Vose, 1984). In addition, the simulation technique can be used to assess the effect of the principle sources of error on airborne measurements made over agricultural environments with 2.0 to 15.0 cm of snow water equivalent. The results indicate that the error of the airborne snow measurement is, in part, a function of snow water equivalent and ranges from 4 to 10 percent. Again, the errors derived from the simulation agree closely with the errors derived using airborne and ground-based snow survey data collected over an agricultural environment (Carroll, et al., 1983). The simulation procedure and assumptions are described in detail by Carroll and Carroll (1989A and 1989B).

The airborne flight line database has the longitude/latitude coordinates for each flight line identified. Immediately after each airborne snow survey, the snow water equivalent derived for each flight line and the longitude/latitude for the flight line mid-point are used in a GIS to generate a contoured surface of snow water equivalent for the region of the survey. Additionally, the digitized hydrologic basin boundary vector file has been used to generate a raster polygon of each hydrologic basin. A cross-tabulation analysis is conducted on the snow water equivalent data plane and the basin boundary polygon data plane. The

result is an average snow water equivalent for each basin polygon. The GIS produces an alphanumeric cross-tabulation analysis and both digital and hardcopy color contour maps for distribution to end-users electronically or in over-night mail. In this way, the end-user is able to obtain, in near real-time, for each airborne snow survey: (1) a color contour map of snow water equivalent, (2) a color map giving the mean areal snow water equivalent for each basin in the region, and (3) an alphanumeric listing of the mean areal snow water equivalent by basin. The data are made available electronically and in color hardcopy format.

3. SATELLITE HYDROLOGY PROGRAM

In the operational satellite snow cover mapping program, AVHRR data are ingested, radiometrically calibrated, and geographically registered to one of 23 windows. During the summer of 1991, 7 additional windows were added to northern Canada and Alaska to facilitate satellite areal extent of snow cover mapping in those regions. A snow/no-snow/cloud cover byte plane image classification is generated on a digital image processing system and exported to a GIS where digital elevation model (DEM) and hydrologic basin boundary maps reside. DEM and basin boundary data sets have been prepared for 6 windows, in the West, each of which are approximately 1000 km by 1000 km. Percent areal extent of snow cover statistics are calculated for each of approximately 5 elevation zones in each of approximately 400 major river basins in the western U.S. Ten additional windows contain basin boundary data sets and are used to map snow cover for the Upper Midwest, the Great Lakes, New England, and southern Canada. During the 1993 snow mapping season, over 4,000 river basins in North America were mapped on multiple occasions using AVHRR and GOES satellite data.

The snow/no-snow/cloud classified images are the operational output from the satellite data receive station and the image processing system. The classified image is shipped to the GIS where basin boundary polygons reside as described above. Satellite areal extent of snow cover is of critical hydrologic interest in the mountainous West as a function of elevation zone. Consequently, the GIS is used with the 30 arc-second DEM database to generate sub-polygons within each basin polygon that define up to five elevation zones within the each basin. In this way, hydrologists can define specific elevation zones to obtain the percent of areal extent of snow cover, for example, in specific elevation zones that might be defined as 1000 m to 1500 m, 1501 m to 2000 m, 2001 m to 2500 m.

Techniques used to map areal extent of snow cover using AVHRR data are described by Holroyd and Carroll (1990) and Holroyd, et al. (1989) and will not be reviewed here. The refinements to the AVHRR snow mapping techniques have been described and incorporated into the NWS operational snow mapping procedures. The major refinements include: (1) scaling of AVHRR data in bands 1, 2, and synthetic band 6, (2) terrain corrections, and (3) change detection.

Data scaling of bands 1 and 2 within the 0-255 byte data range was originally giving an albedo resolution of 0.5 percent. The comparatively low resolution represented only a 5-bit data range and did not take advantage of the full byte range available for electronic transmission or the 10-bit resolution of the spacecraft data stream. Consequently, bands 1 and 2 have been rescaled to an albedo resolution of 0.25 percent.

The original data scaling of band 6 (i.e., band 3 minus band 4) within the 0-255 byte data range produced a saturation of band 3 and occasionally band 4 at radiative temperatures of 46 degrees Celsius or higher. Modifications were made to arbitrarily classify all pixels as snow-free having a band 3 value greater than 245 (40 degrees Celsius or higher) which is physically reasonable.

Classified images from the early morning NOAA-10 satellite accentuate the snow on the east-facing slopes and under represent snow on the west-facing slopes. Similarly, images from NOAA-11 in the early afternoon and NOAA-9 in the late afternoon have snow cover apparently enhanced on the sunlit slopes and diminished on the shaded slopes.

In order to correct the images in rugged terrain, 30 arcsecond digital terrain data were resampled to the 901 m pixel size and projection of the AVHRR imagery. Slope and aspect of the terrain were then calculated. The solar incidence angle, i, was then calculated by:

$$\cos(i) = \cos(z)\cos(s) + \sin(z)\sin(s)\cos(A-a) \qquad (2)$$

where z is the solar zenith angle, s is the terrain slope angle, a is the terrain aspect angle, and A is the solar azimuth angle. Band 1 values are divided by cos(i) to give the brightness values appropriate to flat terrain and a vertical sun. These terrain corrections reduce the solar azimuth bias associated with the areal extent of snow cover. Of course, the corrections are not perfect because substantial variability of solar incidence angle exists within each pixel as a result of terrain variability.

The GIS is used to generate a cross-tabulation analysis using the snow/no-snow/cloud data plane and the elevation zone basins to give an alphanumeric output of percent of snow, no-snow, and cloud for each elevation zone in each basin. The results are summarized in image and alphanumeric format for electronic distribution to the end-user.

4. AIRBORNE AND SATELLITE END-USER SNOW COVER PRODUCTS

Airborne snow surveys are typically conducted from January through March each year using two aircraft simultaneously to provide data to support spring snowmelt flood outlooks and water supply forecasts. Maps and a user's guide are available

that give the current airborne flight line network, the details of the airborne snow water equivalent measurement technique, and the procedures to access electronically the snow water equivalent data in real-time. Hydrologic basin boundaries are shown and a GIS is used to calculate a mean areal snow water equivalent for each hydrologic basin. The observed, airborne mean areal snow water equivalent is used by the NWS River Forecast Centers to update the simulated snow water equivalent generated by the snow accumulation and ablation model.

The alphanumeric and graphic airborne and satellite snow cover data are distributed over both the National Weather Service computer network and the Remote Sensing Center's electronic bulletin board system approximately 4 hours after the snow survey aircraft land anywhere in the country and 36 hours after the morning and afternoon NOAA satellite overpasses. Areal extent of snow cover maps derived from AVHRR satellite data are generated for all 17 windows approximately once a week, the effect of cloud contamination notwithstanding. Over 4,000 NWS basins are currently mapped in the U.S. (including Alaska) and southern Canada. Additional basins are being added in the West and southern Canada for use in future snow cover mapping.

5. SNOW ESTIMATION AND UPDATING PROGRAM

The National Operational Hydrologic Remote Sensing Center currently ingests the real-time, ground-based snow observation data available across the country on a daily basis between January and June of each year. The Snow Estimation and Updating System (SEUS) is used to develop gridded estimates of snow water equivalent that are then provided to end-users (Day, 1990; McManamon, et al., 1993a, 1993b). NWS River Forecast Centers (RFC) compute areal estimates of snow water equivalent over basin subareas and use this information to update the snow states of the conceptual snow model used in flood and water supply forecasting.

The SEUS consists of three components: (1) the calibration component analyzes historical data and develops the parameters needed to estimate gridded snow water equivalent, (2) the operational component accesses real-time data and uses the calibration parameters to determine gridded snow water equivalent, and (3) the updating component updates the snow water equivalent in the conceptual model based on the relative uncertainties of the simulated model snow states and estimates of the snow states developed using the snow observations.

Much of the methodology involves managing and analyzing point, line, and gridded data. The SEUS uses the Geographic Resources Analysis Support System (GRASS) GIS to perform these tasks. GRASS is a raster-based, public domain GIS developed for UNIX platforms by the U.S. Army Construction Engineering Research Laboratory. Part of the appeal of using GRASS to develop the SEUS is its modularity

and the availability of the source code, so that additions and modifications can easily be made to its existing capabilities. GRASS has many low-level commands that provide the user with the capability to tailor the GIS to the exact function that needs to be performed. In order to isolate the user from as many of the details of the GIS as possible, all the GRASS commands for a particular function are packaged in scripts and accessed through a graphical user interface.

The SEUS, based on the GRASS GIS, provides the tools necessary to ingest, process, analyze, display, distribute, and archive the ground-based and airborne snow water equivalent observations. Additionally, satellite areal extent of snow cover data are used in the GIS to constrain the SEUS interpolation algorithms to the geographic regions where snow cover is present.

6. PRODUCT GENERATION AND DISTRIBUTION

Composite use of ground-based and airborne snow water equivalent data along with multi-source satellite data is now accomplished through the newly developed NOHRSC Operational Product Processing System (OPPS) (Hartman, et al, 1995) OPPS ingests and databases classified (i.e., snow, ground, cloud, and unknown) satellite areal extent of snow cover rasters and all identified point and line samples of snow water equivalent and snow depth. OPPS generative capabilities include user-prioritized composite raster generation and multi-source gridded estimates of snow water equivalent and snow depth. OPPS spatial estimation processes for snow water equivalent and snow depth combine point and line data with composited satellite areal extent of snow cover rasters. OPPS can: (1) output rasters in any of several common GIS formats, (2) create displayable images with user-defined vector overlays, and (3) integrate raster data within basin boundaries to produce alphanumeric data products. OPPS products can be stored and distributed using the NOHRSC electronic bulletin board system, FTP'd over Internet to interested cooperators, and sent to NWS offices over AFOS. OPPS was developed to meet the following design objectives:

1. To streamline, to the greatest extent possible, the production of snow estimation products in an operational environment,

2. To integrate, in an automated and objective manner, a wide variety of input data sources used to produce snow estimation products,

3. To develop and employ state-of-the-art spatial data processing algorithms tailored to the task of producing snow estimation products from integrated input data sources, and

4. To automate the dissemination of generated products.

A major objective in the design of OPPS was to automate data integration. Primarily through the use of spatial interpolation techniques and polygon membership modeling, OPPS is capable of integrating raster data with point, line and areal vector data. The integration of variable resolution raster data is supported by run time data sub- and super-sampling functions allowing OPPS to define a range of output product resolutions without regard to the resolution of the input data.

The spatial integration of raster and vector data is supported by automated procedures which exploit the temporal distribution of the input data. Many OPPS processes are designed to evaluate data within windows of opportunity centered on a target date. Because OPPS is designed to address snow estimation on a continental scale, there is a strong possibility that suitable input data are not available for a given instant in time. For example, processes which require satellite image derived maps of areal extent of snow cover are often hampered by cloud cover. By integrating the cloud-free portions of multiple snow cover maps acquired during a window of opportunity,
OPPS can minimize the impact that cloud cover has on the snow estimation process. Similar mechanisms were designed into OPPS for the treatment of each input data source.

OPPS consists of a series synchronized programs communicating with one another through an INFORMIX database server and system calls. The OPPS programs fall into three classes: Database, Analysis, and Product Development. The OPPS programs are supported by the OPPS database consisting of static and dynamic tabular and graphic data. The dynamic portion of the OPPS database is constantly updated by a wide variety of inputs. The remainder of this paper describes, in some detail, the OPPS components and their relationships in the production of OPPS outputs. OPPS is designed to integrate data from a variety of sources, data- types, structures, and formats. OPPS can handle both raster and vector data types. Raster data can be variable in resolution. Vector data may be either point, line or closed polygon structures. To minimize distortions associated with map-projected coordinates, OPPS requires that all of its inputs be in geodetic (longitude and latitude or Earth) coordinate pairs. All calculations are performed in the geodetic coordinate system. The World Geodetic System 1984 (WGS 84) horizontal datum and the National Geodetic Vertical Datum of 1929 (NGVD 29) were selected for OPPS on the basis of the availability of digital elevation model (DEM) data. Many of the analysis programs in OPPS model orographic processes and, as such, are highly dependent upon DEM data. The highest quality of DEM data available in national coverage are in the WGS 84 and NGVD 29 datums. Point observations of snow water, snow depth, precipitation, and surface air temperature are actively and passively acquired over Internet and are automatically ingested into the INFORMIX database. As airborne survey data become available, they also are ingested into the INFORMIX database.

Raster data inputs include areal extent of snow cover thematic rasters derived from the reclassification of satellite images acquired from the GOES and NOAA polar orbiter satellites. Snow cover rasters are produced on a daily basis and are registered with the OPPS database as they become available. OPPS is capable of ingesting raster data in GRASS, ARC/INFO, and Global Imaging formats. OPPS will be capable of ingesting raster data conforming to the SDTS raster profile in the near future. Point observation data are registered and stored as INFORMIX database records. OPPS is capable of ingesting flat files into the INFORMIX database. All line and areal vector structures are stored in OPPS as individual binary flat files whose headers are stored in the INFORMIX database. Since many spatial data analysis systems (i.e., GIS) are capable of exporting flat files, the OPPS approach for dealing with these types of data allows a great deal of flexibility.

In its present state OPPS consists of the following analysis programs:

1. Raster Compositing: this program generates composites from existing rasters in the OPPS database,

2. Areal Extent of Snow Cover by Elevation: this program produces a new raster in which the snow pixels in an areal extent of snow cover raster are represented by DEM elevationvalues,

3. Inverse Distance Interpolation: this program accepts point and flight line observations as the x, y, and z sample data inputs into the inverse distance weighted mean spatial interpolation algorithm,

4. Temperature Interpolation: this program generates an inverse distance weighted mean interpolation of mean daily surface air temperature,

5. Degree Day Accumulation: this program sums the daily positive differences between interpolated surface air temperature and a specified base temperature for each pixel,

6. Orographic Interpolation: this program estimates snow water equivalent or snow depth in areas in which there are orographic dependencies.

7. Basin Analysis: this program will, on a basin-by-basin analysis, compute mean areal snow values (i.e., snow water equivalent, snow depth, etc.) by predefined elevation bands.

OPPS generates a variety of gridded products derived from raster and vector inputs using processes designed specifically for snow distribution estimation. Basin-integrated values can be summarized into coded Standard Hydrometeorological Exchange Format (SHEF) alphanumeric products specifically tailored to a specific user's needs. OPPS is capable of exporting these rasters into a variety of formats including GRASS, ARC/INFO ASCII grids, and Global Imaging (essentially a flat binary raster with an 80 byte header).

The NOHRSC is an operational center within the National Weather Service Office of Hydrology which has, as one of its major responsibilities, the task of mapping snow cover characteristics for all of the United States and portions of Canada. While the NOHRSC has always employed state-of-the-art techniques in accomplishing this task, OPPS, for the first time, allows the snow hydrologist access to the full value of the available ground-based, airborne, and satellite snow cover input data. Through the integration of a broad variety of input data sources, the exploitation of temporal processes, and the design and implementation of data management and analysis programs tailored to snow distribution analysis OPPS, is capable of providing and distributing near-real time analysis of the highest quality currently available.

7. SUMMARY

Techniques are currently being developed using GIS methodology to incorporate DEM data and forest canopy cover data into the satellite snow cover classification procedures to better estimate snow cover in areas where the snow surface is obscured from view by: (1) cloud cover, or (2) dense forest canopy. Research is also continuing toward improvement of normalization procedures to include corrections for within image effects of terrain and for effects of atmospheric scattering and absorption.

Techniques and procedures are currently being implemented in the West to generate operational, gridded snow water equivalent data sets using: (1) ground-based point snow water equivalent data, (2) airborne line snow water equivalent data, (3) satellite areal extent of snow cover data, (4) digital elevation data, and (5) forest canopy cover data sets. The system uses a GIS to store, analyze, and display point, line and gridded data. The SEUS consists of three components, a calibration component that is used to estimate parametric information and develop derived data planes, an operational component that performs the interpolation of the snow observations in real-time and an updating component that combines the estimated snow water equivalent developed using the system with the model simulated snow water equivalent. Preliminary results indicate that the updating process improves streamflow and water supply forecasting.

As a result, water managers and disaster emergency services officials can have available gridded snow water equivalent data sets that optimally integrate all of the available ground-based, airborne, and satellite snow cover information

available. Hydrologists responsible for generating operational river and flood forecasts, water supply forecasts, and spring snowmelt flood outlooks can use the gridded data sets generated using a GIS in user-specific, conceptual hydrologic modeling procedures.

8. REFERENCES

Carroll, S.S. and Carroll, T.R. (1989A) Effect of uneven snow cover on airborne snow water equivalent estimates obtained by measuring terrestrial gamma radiation. Water Resources Research. 25 (7), 1505-1510.

Carroll, S.S. and Carroll, T.R. (1989B) Effect of forest biomass on airborne snow water equivalent estimates obtained by measuring terrestrial gamma radiation. Remote Sensing of Environment. 27 (3), 313-319.

Carroll, S.S. and Carroll, T.R. (1990) Simulation of airborne snow water equivalent measurement errors in extreme environments. Nordic Hydrology 21, 35-46.

Day, Gerald N., (1990) A Methodology for Updating a Conceptual Snow Model With Snow Measurements. NOAA Technical Report NWS 43, Department of Commerce, Silver Spring, MD, March 1990.

Fritzsche, A.E. (1982) The National Weather Service gamma snow system physics and calibration. Publication No. NWS-8201, EG&G, Inc., Las Vegas, NV, pp.37.

Hartman, R.K., Rost, A.A., Anderson, D.M. (1995) Operational processing of multi-source snow data. Presented at the 63rd Annual Western Snow Conference; Sparks, Nevada; 1995 April 17-19.

Holroyd, E.W. and Carroll, T.R. (1990) Further refinements in the remote sensing of snow-covered areas. Presented at the American Society of Photogrammetry and Remote Sensing annual meeting; Denver, CO; 1990 March.

Holroyd, E.W.,III, Verdin, J.P., and Carroll, T.R. (1989) Mapping snow cover with satellite imagery: comparison of results from three sensor systems. Proceedings of the 57th Western Snow Conference; Fort Collins, CO; April 18-20; pp.10.

McManamon, A., Day, G.N., Carroll, T.R. (1993a) Estimating snow water equivalent using a GIS. Presented at the Federal Interagency Workshop on Hydrologic Modeling: Demands for the 90s; Fort Collins, Colorado; 1993 June 7-9.

McManamon, A., Day, G.N., Carroll, T.R. (1993b) Snow Estimation - A GIS application for water resources forecasting. Presented at the American Society of Civil Engineers International Symposium on Engineering Hydrology; San Francisco, California; 1993 July 25-30.

SATELLITE SNOW-COVER MAPPING: A BRIEF REVIEW

Dorothy K. Hall
Hydrological Sciences Branch
Laboratory for Hydrospheric Processes
NASA/Goddard Space Flight Center
Greenbelt, MD 20771

INTRODUCTION

Satellite snow mapping has been accomplished since 1966, initially using data from the reflective part of the electromagnetic spectrum, and now also employing data from the microwave part of the spectrum. Visible and near-infrared sensors can provide excellent spatial resolution from space enabling detailed snow mapping. When digital elevation models are also used, snow mapping can provide realistic measurements of snow extent even in mountainous areas. Passive-microwave satellite data permit global snow cover to be mapped on a near-daily basis and estimates of snow depth to be made, but with relatively poor spatial resolution (approximately 25 km). Dense forest cover limits both techniques and optical remote sensing is limited further by cloudcover conditions. Satellite remote sensing of snow cover with imaging radars is still in the early stages of research, but shows promise at least for mapping wet or melting snow using C-band (5.3 GHz) synthetic aperture radar (SAR) data.

Algorithms are being developed to map global snow and ice cover using Earth Observing System (EOS) Moderate Resolution Imaging Spectroradiometer (MODIS) data beginning with the launch of the first EOS platform in 1998 (Hall et al., in press). Digital maps will be produced that will provide daily, and maximum weekly global snow, sea ice and lake ice cover at 1-km spatial resolution. Statistics will be generated on the extent and persistence of snow or ice cover in each pixel for each weekly map, cloudcover permitting. It will also be possible to generate snow- and ice-cover maps using MODIS data at 250- and 500-m resolution, and to study and map snow and ice characteristics such as albedo.

Algorithms to map global snow cover using passive-microwave data have also been under development. Passive-microwave data offer the potential for determining not only snow cover, but snow water equivalent, depth and wetness under all sky conditions. A number of algorithms have been developed to utilize passive-microwave brightness temperatures to provide information on snow cover and water equivalent (Kunzi et al., 1982; Chang et al., 1987; Goodison and Walker, 1994). The variability of vegetative

cover and of snow grain size, globally, limits the utility of a single algorithm to map global snow cover.

THE USE OF OPTICAL REMOTE SENSING TECHNIQUES FOR MAPPING SNOW COVER

The National Oceanographic and Atmospheric Administration (NOAA) maps snow cover for North America using satellite data (Matson, 1991). Snow charts are digitized weekly using the National Meteorological Center's standard-analysis grid, an 89 X 89 cell Northern Hemisphere grid with polar-stereographic projection. Cell resolution ranges from 16,000 - 42,000 km^2. Only cells with at least 50 percent snow cover are mapped as snow (Robinson et al., 1993). Regional snow products are produced by NOAA's National Hydrologic Remote Sensing Center for more than 4000 drainage basins in the western United States and Canada on a weekly basis during the snow season using Advanced High Resolution Radiometer (AVHRR) and ancillary data (Carroll et al., 1989; Carroll, 1990; Rango, 1993; also see paper by T. Carroll in this volume). Landsat data, both from the multispectral scanner (MSS) and the thematic mapper (TM), are suitable for measuring snow cover at resolutions of 80 m and 30 m, respectively, and the TM bands are suitable for separating snow and clouds, but TM data are only acquired on a 16-day repeat cycle (cloud-cover permitting) and are therefore not very useful for operational studies. This is especially true because during the melt season, when the snowpack is changing rapidly, a maximum of one image every 16 days is not adequate for operational use.

Planned MODIS algorithm for mapping snow

MODIS is an imaging radiometer that uses a cross-track scan mirror and collecting optics, and a set of individual detector elements to acquire imagery of the Earth's surface and clouds in 36 discrete spectral bands. MODIS will acquire data of the land, atmosphere and oceans on a daily or near-daily basis. Spatial resolution of MODIS varies with spectral band and is 250, 500 or 1000 m. The spectral bands cover parts of the electromagnetic spectrum from about 0.4 - 14.0 μm, thus spanning the visible and thermal-infrared parts of the spectrum. The wide swath (± 55°) of the MODIS instrument will be suitable for large-area coverage. Further information on the MODIS can be found in Salomonson and Barker (1992).

A threshold-based algorithm, designed to map global snow cover, has been developed based on heritage algorithms devised by Kyle et al. (1978), Bunting and d'Entremont (1982) and Dozier (1984). This algorithm is called SNOMAP. The intent in selecting the thresholding approach to mapping snow is to utilize proven methods to map global snow and ice for the EOS at-launch global snow-cover product. More advanced snow-and ice-mapping techniques are also being investigated (e.g. Rosenthal, 1993) for use in developing post-launch products. Such advanced methods are currently useful on local and regional scales for snow and ice mapping.

SNOMAP is an algorithm designed to identify snow, if present, in each MODIS pixel each day. If snow is present in any pixel on any day during a 7-day period, that pixel will be considered to be snow covered; results will be composited for 7 days. There will

be a daily and a weekly snow-cover product. The weekly snow-cover product will represent maximum snow cover for the previous 7-day period (Riggs et al., 1994; Hall et al., in press).

SNOMAP has been tested on approximately 25 Landsat TM scenes. Study of these SNOMAP-derived maps has helped us to identify various sources of error. Additionally, field studies conducted in Montana, Saskatchewan and Alaska have allowed us to validate the algorithm when used on TM scenes acquired nearly simultaneously with the field measurements. Errors are associated with mapping snow in deep shadows of clouds and mountains. There are also errors associated with mapping snow under low-solar-elevation angles using SNOMAP, and with mapping snow in mountainous terrain unless a digital elevation model (DEM) is available (Hall et al., 1995). And, under certain conditions, cumulus clouds can be mistaken for snow, using SNOMAP, and mapped as snow cover whether or not snow is underneath the clouds.

Unique aspects of the MODIS-derived global snow maps include: fully-automated production, anticipated improved spectral discrimination between snow and other features, relative to what is available today for global snow mapping, and statistics describing snow-cover persistence in each pixel of the weekly product. A cloud mask, being developed by other MODIS investigators, will be used as will a water mask.

Having its heritage with the Normalized Difference Vegetation Index (NDVI) (Tucker, 1979), and band-ratioing techniques (Kyle et al., 1978; Bunting and d'Entremont, 1982 and Dozier, 1984), the Normalized Difference Snow Index (NDSI) is the primary component of SNOMAP that is used to identify snow. The utility of the NDSI is based on the fact that snow reflects visible radiation more strongly than it reflects radiation in the middle-infrared part of the spectrum. Since the reflectance of clouds remains high in the middle-infrared region of the spectrum, and the reflectance of snow drops to near-zero values, the NDSI also functions as a snow/cloud discriminator. For the Landsat TM, TM band 5 (1.55 - 1.75 μm) acts as a snow/cloud discriminator band.

THE USE OF PASSIVE-MICROWAVE DATA FOR MAPPING GLOBAL SNOW COVER

Passive-microwave algorithms are very useful for measuring snow-covered area and snow depth in parts of the world where the vegetative cover is not dense. However, where dense forest cover exists, passive-microwave data are less accurate for mapping snow and for estimating snow-water equivalent (Hall et al., 1982; Foster et al. 1994 and Foster, 1995).

The intensity of the microwave radiation that is emitted from a snowpack depends on the physical temperature, grain size, density and the underlying surface conditions of the snowpack. By knowing these parameters, the radiation that emerges from a snowpack can be derived by solving the radiative transfer equation (Chang et al., 1976; Foster et al., 1987). The snow grains scatter the electromagnetic radiation incoherently and are assumed to be spherical and randomly spaced within the snowpack. Although snow particles are generally not spherical in shape, their optical properties can be simulated as

spheres by utilizing Mie theory (Chang et al., 1976). The scattering effect is more pronounced at the shorter wavelengths and for larger particle sizes and drier snow.

The Nimbus series of spacecraft provided passive microwave snow-cover observations beginning in the early 1970s. The Scanning Multichannel Microwave Radiometer (SMMR) data set extends from 1978 to 1987. These passive-microwave observations have been used to map snow-covered area on a hemispheric scale at a scale of 1/2° latitude by 1/2° longitude. Several investigators have attempted to produce reliable global snow-cover algorithms using theoretical calculations (Kunzi et al., 1982; Hallikainen, 1984 and Chang et al., 1987). For example, Chang et al. (1987) developed an algorithm that assumes a snow density of 0.30 and a snow grain size of 0.35 mm for the entire snowpack. The difference between the SMMR 37-GHz and 18-GHz channels is used to derive a snow depth/brightness temperature relationship for a uniform snow field that is expressed as follows:

$$SD = 1.59 * (T_{B18H} - T_{B37H})$$

where SD is snow depth in cm, H is horizontal polarization, and 1.59 is a constant derived by using the linear portion of the 37-GHz frequencies. If the 18-GHz brightness temperature is less than the 37 GHz-brightness temperature, the snow depth is zero and no snow cover is mapped (Foster et al., 1987). This algorithm was used to produce maps of Northern Hemisphere snow-covered area and depth. These maps compare favorably with the NOAA maps except that the SMMR maps may underestimate the snow-covered area relative to the NOAA maps.

Analysis of global passive microwave snow data has revealed that the algorithms tend to underestimate snow mass due, primarily, to the effects of vegetation, especially dense conifers (Hallikainen et al., 1984; Foster et al., 1994). Forests not only absorb some of the radiation scattered by snow crystals, but they emit microwave radiation. Foster et al. (1994) have used a vegetation index derived from satellite data to account for forest cover in a given pixel, and to thus improve estimates of snow depth, especially in North America, using algorithms designed to estimate snow depth globally.

Combining visible/near-infrared and passive-microwave data for snow mapping in the EOS era

Both optical and passive-microwave data should be used in synergy to provide optimum results in snow-cover mapping. In the future, when data sets are gridded to a common grid, this will enable comparison and accurate registration of the data sets. The passive-microwave data are invaluable under conditions of darkness and persistent cloud cover, while the optical data provide a high-resolution view of snow cover. The high-resolution optical data are particularly important near the snowline when thin, dry, or wet snow may not be mapped using passive-microwave techniques, or when snow and frozen ground have similar microwave signatures (see, for example, Salomonson et al., 1995).

The Advanced Microwave Sounding Radiometer (AMSR) is a passive-microwave sensor that will be launched early in the next century and will provide improved spatial resolution relative to the currently-operating Special Sensor Microwave Imager (SSMI). AMSR is a Japanese instrument that senses from 40 GHz to 6.0 GHz with a spatial

resolution ranging from 5 to 20 km^2 and an incidence angle of 45°. It is anticipated that algorithms will be developed to utilize both MODIS and AMSR data to provide optimum snow maps.

THE USE OF IMAGING RADAR DATA FOR MAPPING SNOW COVER

The dielectric properties of snow at a given microwave frequency are generally dependent on the relative proportion of liquid and solid water in the snow by volume. Even a thin layer of liquid water will cause the radar signal to be absorbed. Snow that contains a large amount of liquid water has a high dielectric constant (>35 below 20 GHz) relative to that of dry snow. The dielectric properties of the snow mixture are not only influenced strongly by snow wetness, but by the inhomogeneity in the snow volume introduced by the highly-conductive water particles.

The amount of backscatter received by a radar antenna is the sum of surface scattering at the air/snow interface, volume scattering within the snowpack, scattering at the snow/soil interface and volumetric scattering from the underlying surface (if applicable). In a dry snowpack, the microwave scattering is governed by snow depth and density. Volume scattering in dry snow results from scattering at dielectric discontinuities created by the differences in electrical properties of ice crystals and air (Leconte et al., 1990).

At present, the European ERS-1 and -2, and the Japanese JERS-1 satellites are operating, and Canada's RADARSAT is planned for launch later this year. Because the satellite-borne C-band (5.3 GHz) and L-band (1.275 GHz) wavelengths (5.7 and 23.5 cm, respectively) are much larger than the average snow crystal or grain, it is unclear whether or not C- and L-band synthetic aperture radar (SAR) data are potentially useful for monitoring and measuring dry snow. However, studies have shown that there can be a high contrast between snow-free ground and ground covered with wet snow (Matzler and Schanda, 1984) thus making it possible to distinguish wet and dry snow, and to measure snow-covered area when the snow is wet using ERS-1 data. For example, Way et al. (1990) noted a possible increase in backscatter due to snow becoming moist under thawing conditions in central Alaska. This effect was also observed in northern Alaska using ERS-1 data by Hall (in press).

CONCLUSION

The outlook for improving snow mapping in the near future is excellent. Refinements of passive-microwave algorithms for mapping snow cover and snow depth are leading to improved estimates of these parameters globally. Additionally, EOS will allow an enhanced ability to map global snow cover using future MODIS and AMSR data due to improved spatial and spectral resolution. Algorithms will be developed that use data from both sensors to optimize results. These data will be available as input to general circulation models and hydrologic models.

Long-term studies of global snow cover will also be possible with the EOS data, and will extend the satellite record of North America snow cover that dates back to 1966. Satellite-borne SAR data are still being studied for their utility in snow mapping and in

determining snow water equivalent. If, in the future, higher-frequency SAR sensors are flown on satellites, such data may be more useful for the study of seasonal snow cover than are the currently-available C-band SAR satellite data.

ACKNOWLEDGMENTS

The author wishes to thank Dr. Jim Foster for his review of this paper.

REFERENCES

Bunting, J.T. and d'Entremont, R.P., 1982: Improved cloud detection utilizing defense meteorological satellite program near infrared measurements, Air Force Geophysics Laboratory, Hanscom AFB, MA, AFGL-TR-82-0027, Environmental Research Papers, No. 765, 91 pp.

Carroll, T.R., Baglio, J.V., Jr., Verdin, J.P. and Holroyd, E.W.,III, 1989: Operational mapping of snow cover in the United States and Canada using airborne and satellite data, *Proceedings of the 12th Canadian Symposium on Remote Sensing*, V.3, IGARSS'89, 10-14 July 1989, Vancouver, Canada.

Carroll, T.R., 1990: Operational airborne and satellite snow cover products of the National Operational Hydrologic Remote Sensing Center, *Proceedings of the forty-seventh Annual Eastern Snow Conference*, 7-8 June 1990, Bangor, Maine, CRREL Special Report 90-44.

Chang, A.T.C., Gloersen, P., Schmugge, T., Wilheit, T. and Zwally, H.J., 1976: Microwave emission from snow and glacier ice, *Journal of Glaciology*, 16:23-39.

Chang, A.T.C., Foster, J.L. and Hall, D.K.,1987: Nimbus-7 derived global snow cover parameters, *Annals of Glaciology*, 9:39-44.

Foster, J.L., Hall, D.K. and Chang, A.T.C, 1987: Remote sensing of snow, *EOS Transactions of the American Geophysical Union,* 68:681-684.

Foster, J.L., Chang, A.T.C. and Hall, D.K., 1994: Snow mass in boreal forests derived from a modified passive microwave algorithm, *Proceedings of the European Symposium on Satellite Remote Sensing*, 26-30 September 1994, Rome, Italy.

Foster, J.L., 1995: Improving and evaluating remotely-sensed snow/microwave algorithms and snow output from general circulation models, Ph.D. dissertation, Department of Geography, University of Reading, Reading, England.

Goodison, B.E. and Walker, A.E., 1994: Canadian development and use of snow cover information from passive microwave satellite data, *Proceedings of the ESA/NASA International Workshop*, B.J. Choudhury, Y.H. Kerr, E.G. Njoku and P. Pampaloni (eds.), pp.245-262.

Hall, D.K., Foster, J.L., Chien, J.Y.L. and Riggs, G.A., 1995: Determination of actual snow-covered area using Landsat TM and digital elevation model data in Glacier National Park, Montana, *Polar Record*, 31(177):191-198.

Hall, D.K. in press: Remote sensing of snow and ice using imaging radar, in *Manual of Remote Sensing*, 3rd. edition.

Hall, D.K., Foster, J.L. and Chang, A.T.C., 1982: Measurement and modeling of microwave emission from forested snowfields in Michigan, *Nordic Hydrology*, 13:129-138.

Hall, D.K., Riggs, G.A. and Salomonson, V.V., in press: Development of methods for mapping global snow cover using Moderate Resolution Imaging Spectroradiometer (MODIS) data, *Remote Sensing of Environment.*

Hallikainen, M., 1984: Retrieval of snow water equivalent from Nimbus-7 SMMR data: effect of land-cover categories and weather conditions, *IEEE Journal of Oceanic Engineering*. OE9:372.

Kunzi, K.F., Patil, S. and Rott, H.,1982: Snow-cover parameters retrieved from Nimbus-7 SMMR data, *IEEE Transactions on Geoscience and Remote Sensing*, GE20:452-467.

Kyle, H.L.,. Curran, R.J., Barnes, W.L. and Escoe, D., 1978: A cloud physics radiometer, *Third Conference on Atmospheric Radiation*, Davis, CA, pp.107-109.

Leconte, R., Carroll, T. and Tang, P., 1990: Preliminary investigations on monitoring the snow water equivalent using synthetic aperture radar, *Proceedings of the Eastern Snow Conference*, 7-8 June 1990, Bangor, Maine, pp.73-86.

Matson, M., 1991: NOAA satellite snow cover data, *Paleogeography and Paleoecology,* 90:213-218.

Matzler, C. and E. Schanda, 1984: Snow mapping with active microwave sensors, *International Journal of Remote Sensing*, 5(2):409-422.

Rango, A., 1993: Snow hydrology processes and remote sensing, *Hydrological Processes*, 7:121-138.

Riggs, G.A., Hall, D.K. and Salomonson, V.V., 1994: A snow index for the Landsat Thematic Mapper and Moderate Resolution Imaging Spectroradiometer, *Proceedings of the International Geoscience and Remote Sensing Symposium*, IGARSS '94, 8-12 August, 1994, Pasadena, CA, pp.1942-1944.

Robinson, D.A., Dewey, K.F. and Heim, R.R., Jr., 1993: Global snow cover monitoring: an update. *Bulletin of the American Meteorological Society*, 74:1689-1696.

Rosenthal, C.W., 1993: Mapping montane snow cover at subpixel resolution from the Landsat thematic mapper, M.A. thesis, Department of Geography, University of California at Santa Barbara, 70 p.

Salomonson, V.V. and Barker, J.L., 1992: EOS Moderate Resolution Imaging Spectroradiometer: phase C/D status and comments on calibration and georeferencing approaches, *Proceedings of the 15th Annual Guidance and Control Conference,* 8-12 February 1992, Keystone, Colorado, pp.1-14.

Salomonson, V.V., Hall, D.K. and Chien, J.Y.L., 1995: Use of passive microwave and optical data for large-scale snow-cover mapping, *Proceedings of the Second Topical Symposium on Combined Optical-Microwave Earth and Atmosphere Sensing*, 3-6 April, 1995, Atlanta, GA, pp.35-37.

Tucker, C.J., 1979: Red and photographic infrared linear combinations for mapping vegetation, *Remote Sensing of Environment*, 8:127-150.

Way, J., Paris, J., Kasischke, E., Slaughter, C., Viereck, L., Christensen, N., Dobson, M., Ulaby, F., Richards, J., Milne, A., Seiber, A., Ahern, F., Simonett, D., Hoffer, R., Imhoff, M. and Weber, J., 1990: The effect of changing environmental conditions on microwave signatures of forest ecosystems: preliminary results of the March 1988 Alaskan aircraft SAR experiment, *International Journal of Remote Sensing*, 11(7):1119-1144.

National Oceanic and Atmospheric Administration
National Environmental Satellite, Data, and Information Service

Interactive Multisensor Snow and Ice Mapping System

Presented
by
Bruce H. Ramsay
Interactive Processing Branch (E/SP22)
Room 510, NOAA Science Center
5200 Auth Road
Camp Springs, Maryland 20748

Current Process

The purpose of the snow and ice charting performed by the Synoptic Analysis Branch is to produce timely, high quality analyses depicting northern hemispheric snow and ice cover. The primary data source is visible imagery acquired from NOAA-n polar orbiting satellites and is stored in hardcopy. Secondary data sources include on-line GOES, GMS, and METEOSAT imagery, hardcopy Air Force snow analyses, and surface observations. Data needs are season dependent. Snow and ice cover identification is made by the manual inspection of hardcopy imagery and graphics products, on-line imagery loops, and the previous week's analysis. Chart quality is predicated on the availability of clear sky visible imagery and the meteorologist's experience. After all boundaries have been identified, a finalized hardcopy snow and ice chart is manually prepared by the analyst by transferring the boundary lines to the chart. An electronic version of the finalized snow and ice chart is made for archival storage through the digitization of a gridded acetate overlay of the chart. Quality control is either self-imposed by the meteorologist performing the analysis or by the focal point meteorologist. Upon completion, which takes up to 10 hours during the snow season, the hardcopy snow and ice chart is faxed to users such as the National Meteorological Center, Climate Analysis Center, Department of Agriculture, Universities, Foreign Governments, and a number of other customers.

During the NOAA-K,L,M time period, there will be several automated snowmaps of differing accuracy. These include the Advanced Very High Resolution Radiometer (AVHRR)/3 snowmap from NOAA-K, L, and M, the Advanced Microwave Sounding Unit (AMSU) snowcover map, the Special Sensor Microwave/Imager (SSM/I) snowmap, and the Air Force three-dimensional (3-D) Nephanalysis snow product. All of the products are daily except the AVHRR snowmap, which will be produced weekly. In addition, clear sky imagery from both the POES and GOES show the snowline very well. The problem is that visible and infrared techniques suffer from persistent cloudcover near the snowline. This makes observations difficult and infrequent. The microwave snow products are mostly independent of cloudcover: all may be inaccurate under certain circumstances or over specific types of terrain. With several products of varying accuracy, it is

advantageous to allow an analyst to assess each snowcover map and from them to interactively produce a composite that is a more accurate snowcover map.

Proposed System

The ultimate objective is an interactive system for producing daily global snowmaps on Hewlett Packard 755 UNIX-based workstations from a variety of satellite imagery and derived mapped products in one hour or less, with greater accuracy, for the operational use of the Synoptic Analysis Branch. An analyst working at the workstation must have available image editing tools, such as the capability to draw, erase, and label snowlines on an overlay map. The editing software must allow toggling at will between two or more snowmaps. The software must also allow toggling between snowmaps and other mapped data sets, such as elevation maps, vegetation type maps, land use maps, etc. The workstation software must write out to disk a final snowmap with appropriate header information and with an ancillary map containing information about data sources (SSM/I, AVHRR, etc.), and quality flags.

Attachments

National Oceanic and Atmospheric Administration
National Environmental Satellite, Data, and Information Service

Interactive Multisensor Snow and Ice Mapping System Overview

Background

Product	Weekly northern hemisphere snow and ice map - since 1966
Customers	
SAB	Production of weekly map
NMC	Input to numerical models
CAC	Long term map data aggregation
Suppliers	
IPD	AVHRR, SSM/I, USAF Snow Analysis
SSD	GOES, METEOSAT, GMS
NIC	Arctic Ice Analysis
Process	Multiple independent systems Manual interpretation, id snowline Manually prepared hardcopy Electronic map via digitization Time required - 8 to 12 hours

Critical Design Review

Objectives	
Product	Daily global snow and ice map Produced in one hour or less Improved accuracy
System	Modular development Single platform Common user interface
System Overview	
Input Files	Image, overlay data
User Interface	Push-button, menu-driven
Graphics Abilities	Display, edit, zoom, loop, toggle Difference, data sources, overlays
Output Files	Full resolution analysis map NMC map - GRIB format Coarse analysis map

National Oceanic and Atmospheric Administration
National Environmental Satellite, Data, and Information Service

Interactive Multisensor Snow and Ice Mapping System
System Development Objectives and Milestones

Critical Design Review **1994 - 1995**

Prepare Statement of Work for CDR, Phase I
Critical Design

Phase I System Development **1995 - 1996**

Develop Initial Operating Capability, e.g.:
- SSMI, USAF, NIC maps and imagery
- Create, edit, display maps on HP-755
- Overlays
- Save in 1024x1024, 89x89 formats

Training
Test IOC
Prepare SOW for Phase II

Phase II System Development **1996 - 1997**

Develop essential components, e.g.:
- AVHRR, GOES, GMS, METEOSAT, AMSU data and imagery
- Monthly mean, anomaly, frequency (89x89)
- Log files (anomaly and problem reports)

Training
Parallel system test (daily vs. weekly)
Prepare SOW for Phase III

Phase III System Development **1997 - 1998**

Develop remaining components, e.g.:
- Plot weather station data, forecast fields
- Loop maps and images
- Differencing between same source data

Training
System test
Implement operational system

* Funding, facilities, and staff provided by the National Meteorological Center, Polar Program Office (NOAA-KLM), and the Satellite Services Division. Phase I contracting support provided by SMSRC, Inc. Phase II contracting support is pending budget and procurement action.

National Oceanic and Atmospheric Administration
National Environmental Satellite, Data, and Information Service

Interactive Multisensor Snow and Ice Mapping System Phase-I Processing Flow Diagram

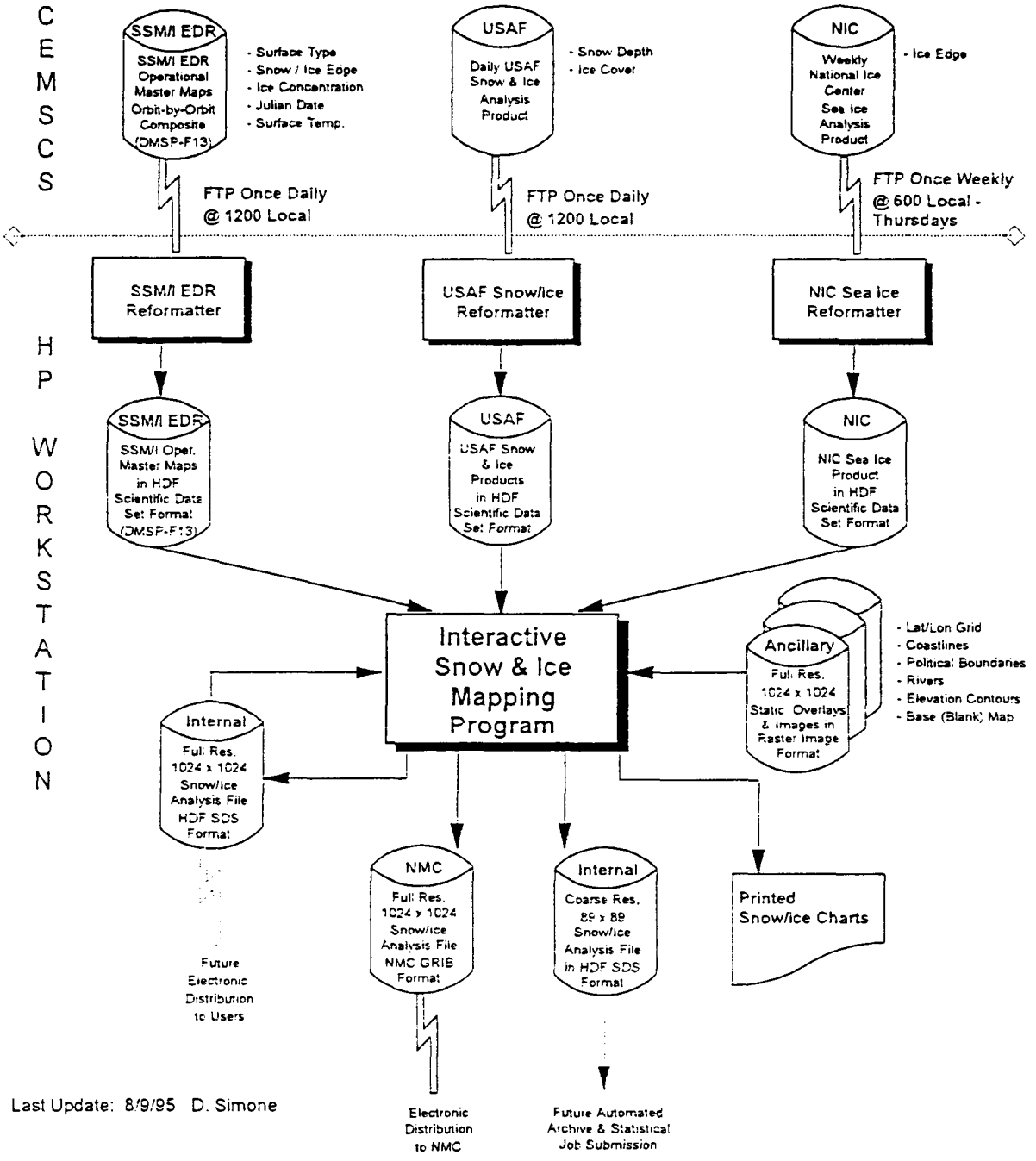

Use of Satellite Data for Operational Sea Ice and Lake Ice Monitoring

First MODIS Snow and Ice Workshop
September 13-14, 1995

Cheryl Bertoia
U.S. National Ice Center
4251 Suitland Road, FOB 4
Washington, D.C. 20395-5120
Voice: 301-457-5314 ext. 302 Fax: 301-457-5300
cbertoia@icecen.fb4.noaa.gov

The U.S. National Ice Center (NIC) is a tri-agency funded organization responsible for providing global sea ice and Great Lakes ice data to military, government, foreign and commercial customers. Sponsoring organizations include the Navy, the National Oceanic and Atmospheric Administration and the U.S. Coast Guard. Satellite derived data are the primary data source for NIC ice analyses and forecast products. During the past fifteen years, analysis techniques have progressed from manual procedures to the integration of multiple sources in a digital workstation environment.

Data Sources

Primary sources of satellite data used at the NIC are the visual and infrared sensors aboard NOAA's polar orbiting TIROS-N series satellites and the visual, infrared and passive microwave sensors aboard the Defense Meteorological Satellite Program satellites (DMSP). Synthetic Aperture Radar (SAR) data from the European Remote Sensing Satellite (ERS-1) have been evaluated over the past three years in an operational demonstration in preparation for use of the more global Radarsat data set.

Products

The NIC routinely produces weekly global scale (1:7,500,000) sea ice analyses of the Arctic and Antarctic as well as regional scale (1:5,000,000) analyses of operationally significant seas. Great Lakes seasonal ice charts and Alaskan regional analyses are produced twice weekly at a scale of 1:3,000,000. Routinely produced ice charts and products are available via either auto-polling facsimile or mail and include ice edge, inner pack concentration boundaries and ice type

identification in standard World Meteorological Organization (WMO) ice symbology. Historical data dating back to 1972 are archived at both the National Snow and Ice Data Center (NSIDC) and the National Climatic Data Center (NCDC). Sea ice support at a higher level of detail is provided upon request for government supported vessels. These specialized requirements range from the depiction of an ice edge for avoidance and safety of navigation to the location and orientation of open water or thin ice-covered polynyas for oceanographic buoy deployments.

Workstation Environment

The bulk of effort in recent years at the NIC has been to develop methods to ingest all data sources digitally using various software packages hosted on Sun workstations. The Naval Satellite Image Processing System (NSIPS) has been adopted as the main image analysis platform and the ingest machine for the NOAA AVHRR data. This PV Wave based system was developed by the Naval Research Laboratory, Stennis Space Center, and has been adapted for use in ice analysis. Current efforts include fine tuning of an egg tool, which allows depiction of the WMO egg code, and adding several ice enhancement curves and multi-channel depictions for AVHRR imagery. NSIPS will be modified to allow ingest of Radarsat images from the Tromso, Gatineau and Alaskan satellite stations. The DMSP OLS images are processed using two commercially available Terascan systems.

Digital Prototype Product

The NIC recently began generating its first fully digital prototype ice product in the Great Lakes. Ingest and analysis of AVHRR and ERS-1 SAR are accomplished and combined with shore station reports and aerial reconnaissance information to produce a digital data field. This information is then transferred into a SUN SPARC station hosting the Geographic Resources Analysis Support System (GRASS) software. This Army Corps of Engineer's GIS displays the information on a UTM projection with 1/8 degree resolution. An analyst tags a portion of the analysis for conversion to ASCII files which are electronically transferred to NOAA's supercomputer for digital input for National Meteorological Center ETA model runs and National Environmental Satellite Data and Information Service Great Lakes Sea Surface Temperature (SST) algorithms. The data field is available to our customers by request via Internet or output from the NIC autopolling system.

Future plans for the NIC include developing a digital product

suite and increasing reliance on SAR data when global Radarsat data become available. This Canadian satellite, scheduled for launch on October 4, 1995, was specifically designed for operational sea ice analysis. SAR imagery is the only high resolution data source capable of penetrating the perpetual cloud cover and illumination conditions unique to the polar regions. Radarsat's C band (5.3 GHz) HH polarized SAR sensor will provide complete arctic coverage at 100 meter resolution. RADARSAT's beam steering capabilities allow coverage over a 500 km swath at 100 meter resolution.

Research Needs

The projected volume of data received from Radarsat precludes manual analysis of the type employed with ERS-1/2 SAR. The NIC anticipates eventually receiving over thirty 500 km^2 Radarsat scenes daily, a data volume of about 3 gigabytes. In order to effectively use Radarsat imagery, automated methods of analysis must be developed. A logical first step is to develop computer assists to the manual analysis process currently employed.

In the ERS era, the NIC directly benefitted from NASA funded SAR research and hopes the trend will continue with Radarsat. NASA funded developmental work at the University of Kansas has resulted in the development of an intelligent ice classification system which addresses ice classification in the summer and in the marginal ice zone. Working with ERS-1 data, they have begun development of an expert system which uses climatology and ice analysis rules to further refine the assignment of backscatter based ice classes. The NIC, working with Ice Services Environment Canada, is working with the University of Kansas to transition some of this work to an operational setting, beginning with development of a rules base for ice classification in the Beaufort Sea.

Long term plans call for development of intelligent methods for fusing all data sources, including visible, infrared, passive and active microwave imagery and ground truth observations in a manner which aids the analyst in determining ice extent and classification.

Monitoring Swiss Alpine Snow Cover Variations Using Digital NOAA-AVHRR Data

Michael F. Baumgartner, Thorbjörn Holzer, Gabriela Apfl

Dept. of Geography, Univ. of Berne, Switzerland; Hallerstr. 12, CH-3012 Berne,
Tel: (++) 31 631 80 20; Fax: (++) 31 631 85 11; E-mail: BAUMGARTNER@giub.unibe.ch

Abstract -- Within a research project and the programm for a *Hydrologic Atlas of Switzerland*, charts of the extent and the variations of the snow cover in Switzerland for two hydrologically and meteorologically different years were derived from digital NOAA-AVHRR data. During the two years, 32 satellite scenes were classified using supervised classification techniques. For the generation of the snow cover charts, up to 12 categories (several sub-categories for vegetation, water, snow, and clouds) were used. The final results were thematic maps differentiating between snow covered and non-snow covered (aper) areas. The snow cover charts were geocoded to the Swiss reference system using a ground-control-point approach allowing the superimposition onto a Digital Elevation Model (DEM) and a digital boundary map of Switzerland within a Geographic Information System (GIS). Based on this data set, the snow coverage and its variations as well as the snowline for the two years under investigation were determined for several river basins in Switzerland. Furthermore, snow cover depletion curves for the two ablation periods, separately for several elevation zones, were generated which were necessary for snowmelt runoff computations in the Rhine-Felsberg basin using the SRM Model.

INTRODUCTION

For a long time, snow cover was a neglected component in the climate system [1]. Recently it became clear, that 80% of the fresh water stems from mountaineous regions. Therefore, it is obvious that alpine snow cover variations are of fundamental importance in hydrology and regional climatology - especially in the context of the climate-change discussion.

Since the mid eighties, weather patterns over Europe have changed considerably influencing the snow cover duration in the Alps and surrounding lowlands. A comparison of NOAA-AVHRR images have shown a drastical reduction of snow covered areas: the prealpine lowlands, the Vosges, the Black Forest, and the Jura used to be snow covered for 40 to 60 days per year whereas today the duration is reduced to a few snow days mainly during end of February and March. As a single event, this situation might be neglected but not if it is lasting for a longer period. The reduction of snow days can be observed since 1988 which is unusual in climate history in Europe during the last 700 years [2][3]. Therefore, the influence of these changes on the hydrologic cycle, the water resources management, the vegetation, the regional climatology, and tourism is of major concern.

In the context of a research project and of the *Hydrologic Atlas of Switzerland*, the snow cover accumulation and ablation patterns for two selected years were studied: the hydrologic year 1983/84 represents a snow-rich year with a large snow cover extent whereas the year 1992/93 was a average year concerning precipitation but with higher temperatures and, therefore, with a significantly smaller snow cover extent (especially in lower elevations).

The paper shows, how snow cover charts, separately for the accumulation and ablation period, can be derived from digital NOAA-AVHRR data. For selected basins, snow cover depletion curves, snowline variations, and snowmelt runoff computations are derived. Furthermore, snow depths data are used for an intercomparison of ground measurements and satellite-derived results. The computations were carried out using the Alpine Snow Cover Analysis System (ASCAS) [4] which integrates the software modules *image processing*, *GIS*, *database*, and *snowmelt runoff modelling*.

GENERATION OF SNOW COVER CHARTS

- Image processing: the NOAA-AVHRR data are retrieved from the archives of the receiving station [5] at the Department of Geography (Univ. of Berne, Switzerland). Based on a classification-by-supervised-learning technique [6], snow cover charts are derived [7]. These raster-based charts - or thematic maps - are geocoded to the Swiss reference system (an oblique Mercator projection) and, finally, are vectorized. These procedures are repeated for a time series of satellite recordings (in this case 32 scenes) during the two selected years.
- GIS analyses: the vectorized snow cover charts are transfered from the image processing to the GIS module within ASCAS for further spatial and temporal analyses [7]. Additionally, topographic, climatologic, and hydrologic data were integrated in the GIS (elevation lines, basin boundaries, location of meteorologic stations, and stream gauges, etc.) by digitizing from topographic maps. In a first step,

elevation zones with an equidistance of 500 m were derived based on the intersection of elevation lines and basin boundaries. Secondly, the layers *elevation zones* were splitted with the layer *basin boundaries* and the snow cover charts resulting in a map (or a statistical table) indicating the snow coverage (in % or in km^2) within a basin and an elevation zone. Repeating these precedures for selected dates, e.g. an ablation (or accumulation) period, the temporal and spatial variations of the snow coverage and the snowline can be extracted and graphically be displayed.

Comparing snow cover accumulation and ablation patterns during the winter 1983/84 and 1992/93, it can be noted that the snow cover extent in 1992/93 was drastically smaller and its duration much shorter than in 1983/84. Lower and middle elevations (below 1200 to 1500 m a.s.l.) showed only a few days with a snow cover. The variations of the snowline elevation (Figure 1) support these findings: by superimposing the snow cover charts with a DEM, the elevation dependent snowline variations show that in 1983/84 the snowline reached for four weeks down to the lowlands (in average) whereas in 1992/93 only two snowfall events caused a descent of the snowline to the lowlands (500 m a.s.l.). All the years since 1988 show a similar behaviour of the snowline variations.

- Snow depths: by comparing these results with snow depths data from meteorological stations it can be seen (Figure 2) that the snow depths of most stations in the Swiss lowlands did significantly decrease (e.g. the station La Dole in Figure 2) between the two years. In higher alpine regions (e.g. the station Saentis in Figure 2) such a decrease can not be detected which suggests that no major change in the amount of precipitation occured up to now.

HYDROLOGIC MODELLING

The snow cover depletion curves [8] for the snowmelt periods of 1984 and 1993, derived from the snow cover charts by interpolation, show the different ablation patterns between the two years (Figure 3). In the latter one, snowmelt takes appoximately three to four weeks earlier place than in 1984 caused basically by a lower snow water equivalent as a consequence of slightly higher temperatures and, therefore, by less snowfall and a shorter duration of the snow coverage.

These differences are influencing the snowmelt runoff and, therefore, production schemes of hydroelectric power companies. Using the SRM snowmelt runoff model [9], snowmelt runoff was simulated for the Rhine-Felsberg basin (Switzerland, 3400 km^2). SRM is based on the degree-day method and asks for snow cover (from remote sensing data), precipitation, and temperatur (minimum, maximum) on a daily basis as input variables.

The simulated runoff reflects the statements made above: the ablation period 1984 is characterized by an increase of the runoff during May, a peak runoff in June, and a typical recession flow during the summer months (Figure 4). In comparison, the snowmelt runoff during the summer half year 1993 (Figure 4) shows significant differences: the increase of snowmelt runoff starts rather early (end of April) but is interrupted by the inflow of cold air masses causing snowfall even during May and June. The snowmelt was often influenced by heavy rainfall especially during summer which was unusual for this time of the year in the past. Due to these rainfall events, the recession flow is interrupted by significant runoff peaks. A typical peak runoff can not be detected as it was usual for alpine regimes. Since 1988, snowmelt runoff is more evenly distributed during the April-through-September period.

CONCLUSIONS

The paper has shown, how snow accumulation and ablation charts for alpine regions can be derived from digital NOAA-AVHRR data using digital image processing and GIS techniques. Due to the higher temperatures during the past hydrologic years, the snowline was for 1992/1993 significantly higher (>1000 m a.s.l.) than for 1983/84 (~500 m a.s.l.). Consequently, in lower and middle elevations a lower snow water equivalent was calculated for 1992/93. The duration of the snow cover was drastically reduced from 40 to 60 snow days to a few days and ablation took three to four weeks earlier place than before 1988. Snowmelt runoff patterns in spring and summer 1993, computed with the SRM model, differ clearly from those in 1984: no typical peak runoff due to snowmelt but many peaks due to rainfall events, and a more evenly distributed seasonal runoff were detected.

The investigations support the idea that after 1988, the situatution regarding alpine snow coverage has changed. Evaluations in other Swiss basins show similar results. The consequences for vegetation and the regional climate as well as for hydroelectric power generation are investigated in a continuation of this project. Currently, a comparison between several basins in the Austrian, French, and Swiss Alps is under investigations. Since the algorithms for extracting snow cover charts are rather expensive, algorithms for an automatic snow cover chart generation are developed which is needed for a permanent monitoring of the snow cover situation in the Alps.

REFERENCES:

[1] NRC, "Opportunities in the Hydrologic Sciences," National Research Council, Washington D.C.: National Academic Press, 1991.

[2] C. Pfister, "Klimageschichte der Schweiz 1525-1860. Das Klima der Schweiz von 1525-1860 und seine Bedeutung in der Geschichte von Bevölkerung und Landwirtschaft," Academia Helvetica 6, Bern: Paul Haupt, 1988.

[3] H. Flohn, A. Kapala, H.R. Knoche, H. Mächler, "Water vapour as amplifier of the greenhouse effect: new aspects," *Meteorologische Zeitschrift*, Neue Folge, No. 1, 1992, pp.122-138.

[4] M.F. Baumgartner and G. Apfl, "Towards an integrated geographic analysis system with remote sensing, GIS, and consecutive modelling for snow cover monitoring," *Int. Journal of Remote Sensing*, Vol. 15, No. 7, 1994, pp.1507-1518.

[5] M.F. Baumgartner and M. Fuhrer, "A Swiss AVHRR and Meteosat receiving station," *Proc. of the 5th European AVHRR User's Meeting* held in Tromso, Norway on the 25th-28th June 1991, EUMETSAT P-09 (Darmstadt: Eumetsat), pp.23-33.

[6] R.O. Duda and P.E. Hart, "Pattern Classification and Scene Analysis," New York: Wiley Interscience, 1973.

[7] M.F. Baumgartner and G. Apfl, "Monitoring snow cover variations in the Alps using the Alpine Snow Cover Analysis System," In: Mountain Environments in Chaning Climates, M. Beniston (Ed.), London: Routledge Publishing Company, 1994, pp.108-120.

[8] J. Martinec, 1985: "Snowmelt runoff models for operational forecasts," *Nordic Hydrology*, Vol. 16, 1985, pp.129-136.

[9] J. Martinec, A. Rango, R. Roberts, "The Snwomelt Runoff Model (SRM) User's Manual," Ed.: M.F.Baumgartner, Geographica Bernensia, P-29, Dept. of Geography, Univ. of Berne, Switzerland, 1994.

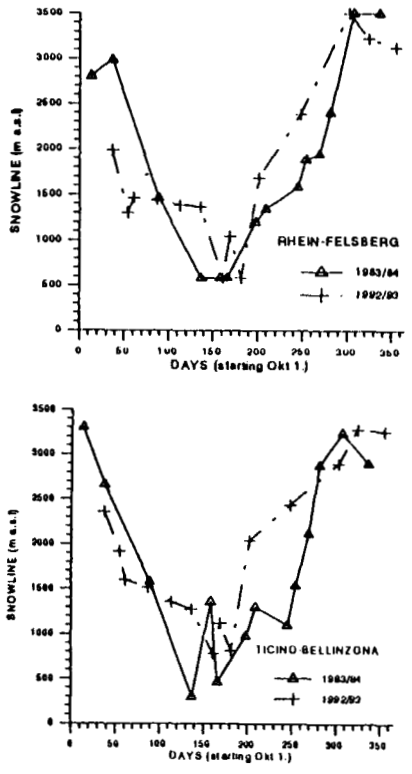

Figure 1: Elevation-dependent variations of the snowline, Rhine-Felsberg and Ticino, Switzerland (1983/84 and 1992/93)

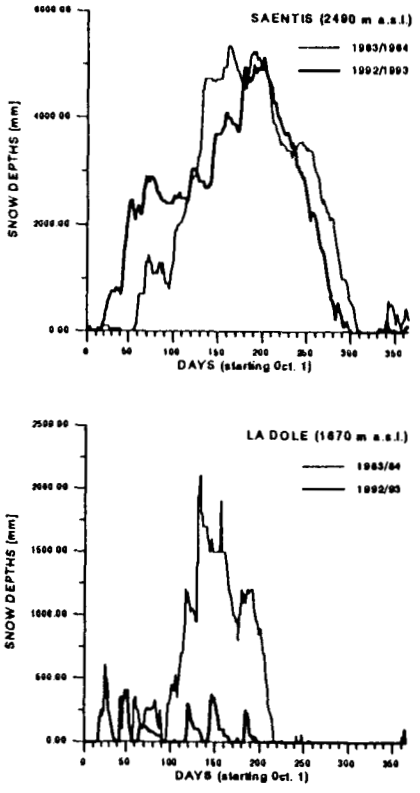

Figure 2: Variations of the snow depths, meteorologic stations La Dôle and Saentis, Switzerland (1983/84 and 1992/93)

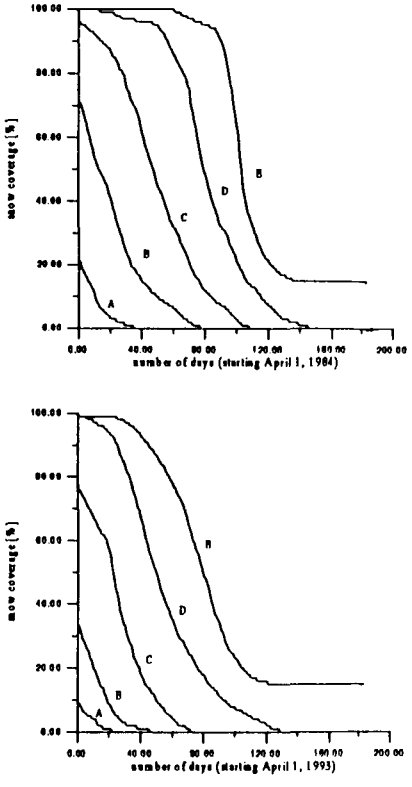

Figure 3: Conventional snow depletion curves for the Rhine-Felsberg basin (Switzerland), 1983/84 and 1992/93

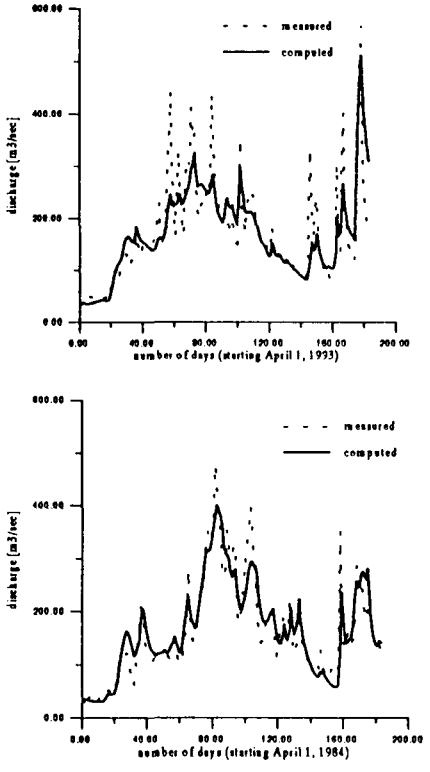

Figure 4: Snowmelt runoff simulations and measurements for the Rhine-Felsberg basin Switzerland (1983/84 and 1992/93) based on the SRM model

Mapping Fractional Snow Covered Area and Sea Ice Concentrations

Anne W. Nolin
CIRES/University of Colorado

1 Introduction

This research assesses the efficacy of using spectral mixture analysis (SMA) as a tool for global mapping of snow-covered area and sea ice concentration at sub-pixel spatial resolution.

The spatial distributions of snowcover and seaice is needed for climate models, where surface albedo is used as a lower boundary condition, and for snowmelt/runoff models, in which snow-covered area is needed for spatially-distributed melt calculations. One of the fundamental difficulties in producing estimates of snow-covered area using remote sensing techniques has been distinguishing snow from other surface covers in a scene. A second major difficulty lies with the mixed pixel effect that arises from the spectral input of different materials (snow, vegetation, liquid water, etc.) in the sensor field-of-view. Binary classifications from remote sensing data categorize pixels as either completely snow-covered or completely non-snow-covered [1, 2, 3, 4]. This simplistic approach may introduce large errors in the estimation of snow covered area, particularly in regions where and at times when snow cover is patchy and discontinuous. One distinct advantage of the SMA technique is that it allows one to estimate the fractional snowcover in a pixel. In addition, the fit of the model to the data can be tested and, unlike most binary classification methods, an error estimate is provided.

SMA uses a linear mixing model in which the sensor response for an image pixel is expressed as a linear combination of the fractional quantity of each component present in the pixel. Thus, each pixel spectrum holds information about both the spectral signature and the fractional abundance of a component. Figure 1 depicts the hypothetical spectrum of a pixel containing 60 In a multispectral image each pixel can be modeled as a linear combination of components identified for that image. Such image components are termed "endmembers" and they are thought to be representative of a finite set of spectrally-unique ingredients in the image. For an atmospherically-corrected, multispectral reflectance image, a linear mixture of the endmembers is calculated using the relationship [5, 6]:

$$R_c = \sum_{i=1}^{N} F_i L_{i,c} + E_c \tag{1}$$

where, R_c is apparent surface reflectance in channel c

F_i is the fraction of endmember i

$R_{i,c}$ is the reflectance of endmember i in channel c

N is the number of spectral endmembers

E_c is the error for channel c of the fit of N spectral endmembers.

To solve for the F_i's the model performs a least-squares fit to the spectrum of each pixel. The fit of the linear mixture model to the spectral data in each pixel is measured by the error term, E_c. Equation 2 calculates the average root mean-squared (RMS) error by squaring and summing E_c over M number of sensor channels to show the model fit.

$$\text{RMS} = \left[M^{-1} \sum_{c=1}^{M} E_c^2 \right]^{1/2} \tag{2}$$

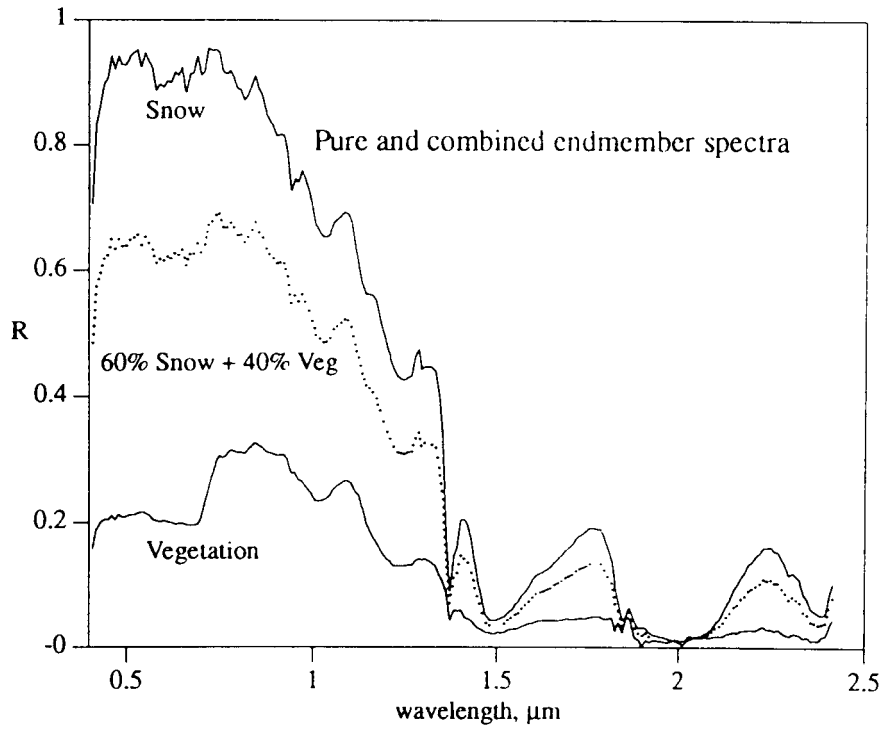

Figure 1: Reflectance spectra (from Mammoth Mountain AVIRIS image) of snow and vegetation and the simulated spectrum of a linear combination of 40% vegetation and 60% snow

Spectral endmembers are chosen from each image and, though the same category of endmember may be the same for many images (eg. rock, snow, vegetation), their spectral characterization is expected to differ from one image to another because of changes in solar illumination, differences in rock, vegetation or snow-type and so on. After atmospheric correction of the image data, using the 5S model, a principal components analysis (PCA) is performed on the multispectral data. PC images are examined and the locations of pixels having the highest value in each PC image are marked. These marked pixels are then located in the reflectance images and the reflectance spectra of these pixels are used as the endmember spectra. The spectral unmixing model is iteratively run (each time solving for the fraction of each endmember in each pixel) with successively fewer endmembers until both the overall RMS error is minimized and the fraction of each endmember lies between the values of 0 and 1.

As part of the Earth Observing System (EOS) project, the Moderate Resolution Imaging Spectrometer (MODIS) will be used to collect data in 36 channels (20 visible and near-infrared channels). Digital maps of global snow-covered area will be produced from MODIS data starting with the launch of EOS in 1998. Towards this end, a global snow-mapping algorithm, SNOMAP, is under development. One proposed approach entails using a normalized difference snow index (NDSI) to produce a binary classification of snowcover. This index, tested with Landsat Thematic Mapper (TM) data, makes use of the fact that snow reflectance is high in the visible and low in the near-infrared. Preliminary tests of the NDSI indicate that it agrees to with 95% with a sub-pixel resolution snowcover map derived with a more complex algorithm [7]. The latter algorithm, based on spectral mixture analysis [8], calculated the fraction of snow-covered area in each pixel providing a higher degree of accuracy for snow mapping. While spectral mixture analysis is a promising tool for snow mapping at regional scales, it is not clear that this more complex method can be justified for use at the global scale.

2 Approach

2.1 Mapping Alpine Snow Cover

Remote Sensing Data

- TM image of Glacier National Park, Montana (March 14, 1995)
- AVIRIS image of Mammoth Mountain, California (January 11, 1993)

In this research, multispectral remotely sensed data from both Landsat Thematic Mapper (TM) and Airborne Visible/Near-Infrared Imaging Spectrometer (AVIRIS) sensors were used as proxy data for MODIS. TM data represent the data having the closest spectral match to the MODIS data and these data have already been used to test both a SMA-based and NDSI-based snow mapping algorithm. So, it is appropriate to use TM data for comparison of the two techniques. Landsat TM has a 30 m spatial resolution while MODIS has 250 m to 1 km spatial resolution.

AVIRIS has a spatial resolution of 20 m a spectral range from 400-2450 nm and a nominal spectral resolution of 10 nm. It is flown in a NASA ER-2 aircraft at an altitude of 20 kmand has a swath width of 12 km. To better characterize the full number of spectral bands that may be used for snow mapping, AVIRIS channels were convolved to MODIS spectral resolution (based on current band characteristics) and results of each algorithm were compared on a spectral basis.

Both regions can be characterized as rugged, mountainous terrain with snow, rock and alpine and subalpine vegetation present. The AVIRIS image is of Mammoth Mountain on January 11, 1993, acquired shortly following a snowfall of about 10-20 cm. The snowpack at the time was approximately 2-3 m deep over most of the mountain. The Glacier National Park TM image, acquired on March 14, 1991, also shows abundant fresh snow.

Because of disk space and computational limitations, subscenes of each image were used. The AVIRIS image was subset so that Mammoth Mountain would be centered in the image. This image is 504 x 342 pixels representing an area 6900 km^2. In the Mammoth Mountain image, AVIRIS channels were convolved to MODIS spectral resolution to create a 20-band synthetic image. Using spectral endmembers chosen from the principal components transformation of the data, the spectral mixture algorithm was applied to the MODIS/AVIRIS synthetic image.

The Glacier National Park image was subset to create a 2500 x 2500 pixel image representing an area of about 562,500 km^2. both the SMA and NDSI methods were used to determine snow covered area.

2.2 Mapping Sea Ice Concentrations

The SMA model was also used in to test its ability to perform sea ice mapping. Two TM images of the Beaufort Sea region of the Canadian Arctic, acquired within a two-day period (April 16, 1992 and April 18, 1992) were used in this part of the analysis. As with the alpine snow images, a PC transformation was run to determine the endmembers for each image. Both images show the pack ice in spring and open water is visible in the cracks between large pieces of sea ice. No wet snow is visible in the April 16 image but, in the April 18 image, melt is just beginning to occur in the snow overlying some of the sea ice. Some clouds are visible in the bottom and the very top of the April 18 image.

2.3 Atmospheric Correction

For each TM image, the uncalibrated data were converted from raw DN values to values of apparent surface reflectance for each of six spectral bands. First, the atmospheric transmittance and path radiance values were calculated for each of the TM spectral bands using the 5S code /citetanre. An example of these values, for the Glacier N. P. image are given in Table 1.

Then, using the transmittance and path radiance values along with the calibration coefficients (gains and offsets) for each TM band, the conversion from DN to reflectance was performed in a single step.

$$\rho = ((offset + (gain * DN)) - L_{path})/(L_{sun} * t_1 * t_2) \quad (3)$$

Table 1: Transmittance, path radiance and solar radiance values used in the atmospheric correction of the Glacier National Park TM scene

Band Number	Path Radiance	Solar Radiance	T_{up}	T_{down}
1	1.747	38.5	0.902	0.822
2	1.043	43.1	0.955	0.913
3	0.475	39.3	0.976	0.954
4	0.013	37.3	0.992	0.984
5	0.018	12.3	0.999	0.999
7	0.001	5.9	1.000	1.000

Where, ρ is apparent surface reflectance, L_{path} is path radiance, L_{sun} is solar radiance at the top of the atmosphere, t_1 and t_2 are the upward and downward transmittances, respectively. In the process of being atmospherically corrected, each TM band is converted from a byte image to a floating point image (thereby increasing its size four-fold).

AVIRIS data were also atmospherically corrected and converted to apparent surface reflectance. This task was accomplished using ATREM, the atmosphere removal program of Gao [9].

3 Results

3.1 Alpine Snow Cover Mapping

The atmospherically-corrected TM image subset (2500 x 2500 pixels) was used for both the spectral mixture analysis and analysis with the NDSI algorithm. In the spectral mixture analysis, three endmembers were chosen: snow, vegetation and shade. These were obtained after running a principal components transformation on the image and examining the scatterplots of the principal components to identify the purest pixels for each endmember and the total number of endmembers. After the image was unmixed into its endmember components, the scaled snow fraction was computed by dividing the snow image by the sum of the snow and vegetation images (see Figure 2). Best results appear to have been obtained for both the snow and shade fraction images with virtually all concentration values falling within the range from 0.0 to 1.0.

Slightly negative values mean that there was some endmember that should have been included that wasn't. However, when additional endmembers were added, the RMS error would increase to an unacceptable level because the added endmember resulted in a greater lack of fit of the model to the data. Slightly super-positive values (greater than 1.0) mean that these pixels were more "pure" than the ones chosen for the endmembers. Changing the endmembers to these "purer" pixels resulted in a worse fit of the model to the data because those pixels were actually less representative of the endmember. The results presented here represent the best fit of the model to the data. Because of the lack of pixels containing only vegetation, this endmember is not particularly representative of "pure" vegetation. This resulted in a greater number of negative and super-positive values in this image. However, the overall RMS error with those chosen endmembers was less than 1

For comparison with the spectral mixture model results, the SNOMAP algorithm was applied the Glacier National Park TM image. The resulting image is shown in Figure 3.

The NDSI binary classification resulted in a total snow covered area of 3979 km^2, slightly exceeding the SMA-derived snow covered area estimate of 3820 km^2, only a 4.2% difference between the two results. Though this difference is not particularly large, it could, depending on the snow depth and spatial distribution, result in a substantially different estimate for the snowmelt/runoff from the snowpack. The snow fraction image produced using SMA is able to show the varying spatial distribution of the snowpack whereas the NDSI binary classification cannot.

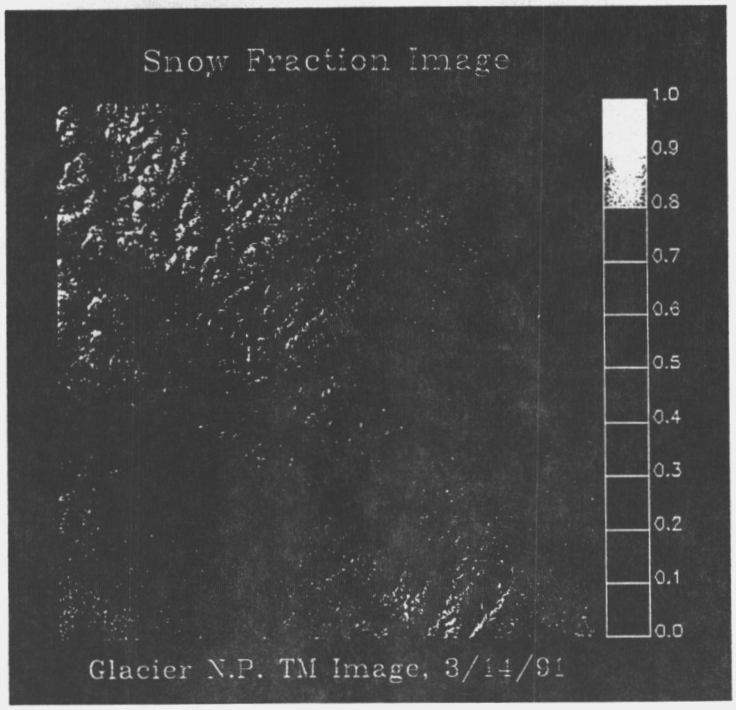

Figure 2: Scaled snow fraction image for Glacier National Park, Montana.

Using spectral endmembers chosen from the principal components transformation of the data, the spectral mixture algorithm was applied to the 20-band MODIS/AVIRIS synthetic image and the results are shown in Figures 4–6.

The snow fraction image has values ranging from 0.0 to 1.0. This closely agrees with results from the application of the spectral mixture model to the original AVIRIS data (which have been validated using aerial photographs [10]. Summing the fractions of snowcover in each pixel gives the total snow covered area for the scene. From the MODIS/AVIRIS synthetic image, the total snow covered area was calculated to be 38.1 km^2 and the total from the original AVIRIS image was 37.3 km^2. Overall RMS error for the unmixed MODIS/AVIRIS scene was 1.1%. Pixels that are insufficiently illuminated have higher RMS error values as do the brightest snowcovered pixels. In general, the spectral mixture model was able to fit the data with very low error.

NDSI estimates of total snow covered area for Mammoth Mountain were significantly lower than those obtained from using the SMA method. The reason for the difference in estimates is the large number of shaded pixels evident in the image, many of which are assigned values of no snow from the SNOMAP algorithm. The NDSI method is not able to express the spatial distribution of snowcover in this rugged alpine area. SMA results from the MODIS-convolved AVIRIS image compared closely with SMA results from the original AVIRIS image.

3.2 Sea Ice Concentration Mapping

In the Beaufort Sea TM image from 04/18/92, four endmembers were found to best characterize the spectral variability in this six-band image: sea ice, liquid water, cloud, and wet snow. Figures 7–10 show the fractional proportions of each of these endmembers with white pixels having concentrations near unity and dark pixels having the lowest concentrations. RMS error was very low for this unmixing result (0.4%).

The SMA method was able to map a wide range of sea ice concentrations in this image. In addition, the it appears that the SMA technique can discriminate between thin ice and thick ice since the combination of open water and sea ice fractions appear to have a spatial distribution like that of thin ice. While, currently

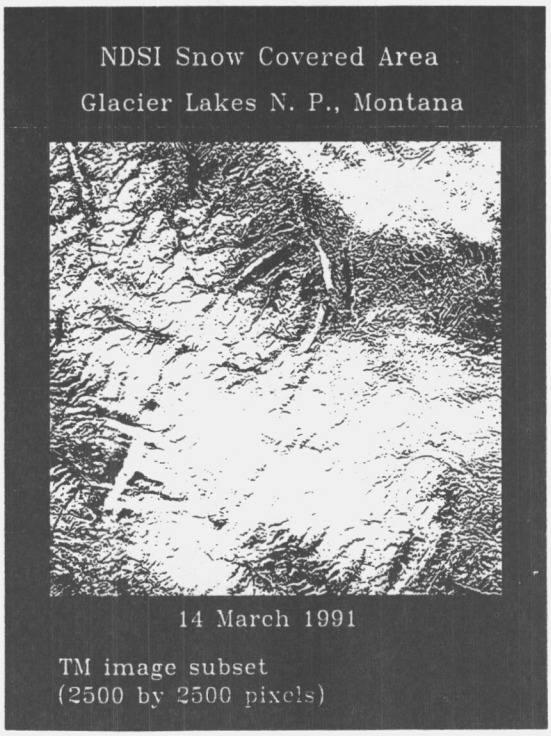

Figure 3: SNOMAP-derived binary classification of snowcover for Glacier National Park, Montana. White pixels represent 100% snowcover and black pixels represen t 0% snowcover.

there is no comparison with estimates of sea ice concentrations and ice types from an NDSI-like method, we expect to produce this comparison in the near future.

The SMA method was also applied to the 04/16/92 sea ice image. Two endmembers were found to describe the range of spectral variations in each pixel: sea ice and liquid water. No clouds were apparent in this image and it appears that surface melt was insignificant. Overall RMS error was about 0.5%.

A test was performed to determine if endmembers could be transferred from one image to another. Because the Beaufort Sea TM images are close in both space and time, it was thought that the seaice and liquid water endmembers from the 4/18/92 image could be used to map those components in the 4/16/92 image. However, the average RMS error for the newly analyzed 4/16/92 image jumped to 10%, an increase of more than one order of magnitude. This case study demonstrates that spectral endmembers need to be chosen from the image data themselves for best results.

3.3 Automated Selection of Endmembers

Further analysis needs to be performed to determine how endmembers can best be selected. This is perhaps the largest constraint on the use of this method as an operational approach to sub-pixel snow and sea ice mapping. Constrained Energy Minimization (CEM), a newly developed technique used for mapping geologic materials has shown promise for discriminating between a spectrum of interest, "foreground", and the spectra of other components in the image, "background". One of the apparent advantages of mapping snow and ice with the CEM technique is that these components have high signal-to-noise and high contrast with other image components. Future research on snow cover mapping will explore the use of the CEM technique.

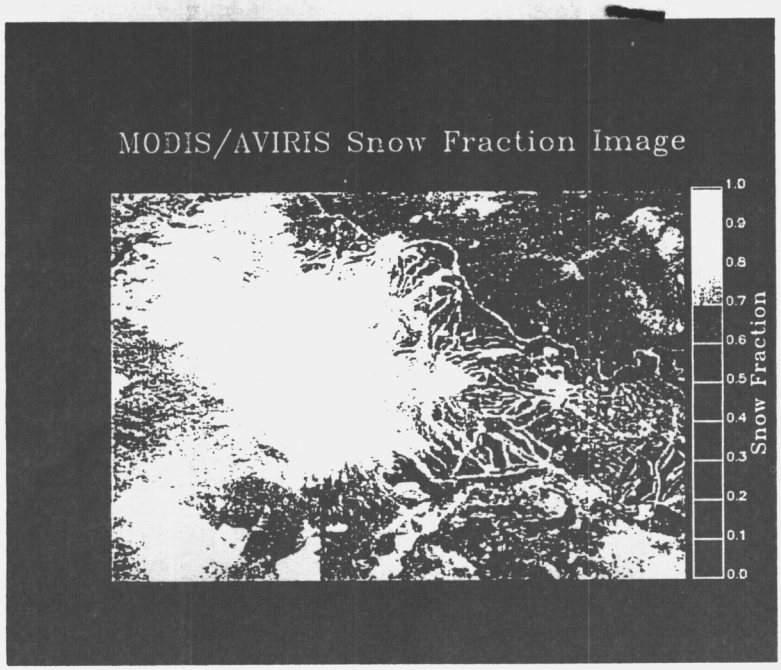

Figure 4: Snow fraction image for the MODIS-convolved AVIRIS data, Mammoth Mountain, California. The original AVIRIS data were acquired on January 11, 1993. North is to the upper right of the 10 km $\times$ 12 km image. Mammoth Mountain isthe large snow-covered region in the center of the image; ski runs are evident on in the north side of the mountain.

4 Conclusions

Snow cover in both the Mammoth Mountain and Glacier National Park images were mapped using the SMA method. Results from the MODIS-convolved AVIRIS image from Mammoth Mountain compared closely with SMA results from the original AVIRIS image. A comparison of SNOMAP-derived snow covered area produced value 4.2% larger than that calculated using the SMA technique. Though this difference is not particularly large for the 2500 $\times$ 2500 image, for snowmelt runoff models, it is crucial to have an accurate measure of the spatial distribution of the fraction of snowcover. Thus, for certain applications such as snowmelt runoff modeling in alpine regions, a binary classification does not provide sufficient information on the spatial distribution of snowcover. One area of significant disagreement between the SMA and NDSI methods was mapping shaded snow. In many pixels in the Glacier National Park image, the NDSI method incorrectly identified shaded snow pixels as non-snowcovered while the SMA method mapped them as containing some fraction of snowcover. So, while the results between the two techniques agreed fairly closely, the accuracy of the NDSI method is in doubt for shaded pixels.

A second important consideration is the possibility that the SNOMAP threshold (currently set at 0.4) may systematically bias the classification results in ways that are not currently understood. For example, if a region has a uniformly patchy snowcover such that each pixel in the image had a snowcover fraction of 0.5, the SNOMAP algorithm may map all those pixels as having zero snowcover. What is needed is a more thorough validation effort for the SNOMAP algorithm to identify possible biases and significant shortcomings.

The SMA method appears to be effective for mapping the spatial distribution of sea ice at a sub-pixel level. Because the range of possible spectral endmembers is small in Arctic scenes this technique holds great promise for accurately characterizing the fine-scale spatial distribution of sea ice, open water,

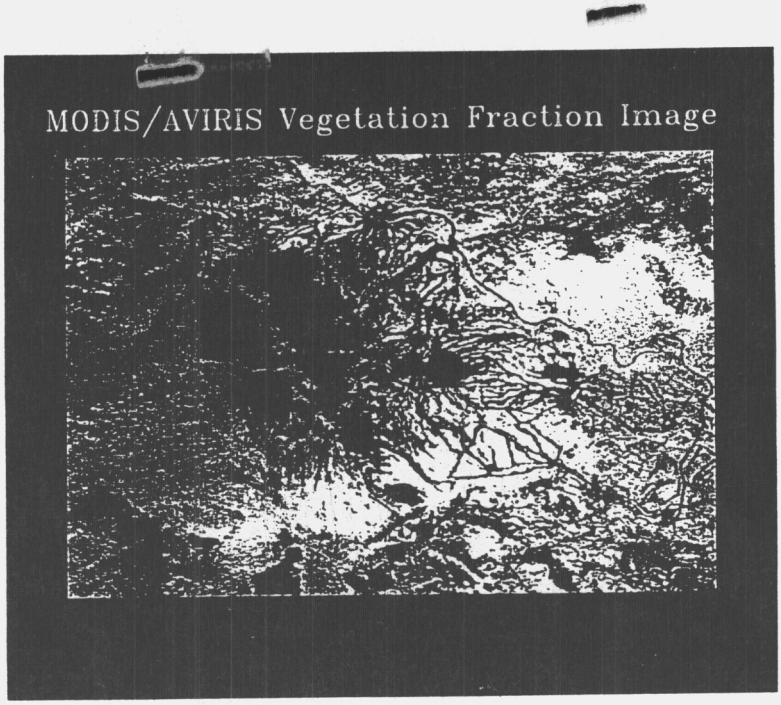

Figure 5: Vegetation fraction image for the MODIS-convolved AVIRIS data, Mammoth Mountain, California.

clouds, and snow.

Cryospheric components in both alpine and arctic were mapped at sub-pixel resolution using the SMA technique. However, because of the need for interactive endmember selection for each image, this technique is remains in a "pre-operational" phase. That is, until automated endmember selection can be carried out in an accurate and computationally reasonable fashion, the SMA method will not be appropriate for global operational snow and ice cover mapping. Future work on this project will focus on developing an automated endmember selection process and work-in-progress indicates that this is a promising line of research.

References

[1] A. Rango, "Assessment of remote sensing input to hydrologic models," *Wat. Res. Bull.*, vol. 21, pp. 423–432, 1985.

[2] J. Dozier and D. Marks, "Snow mapping and classification from Landsat Thematic Mapper data," *Ann. Glaciol.*, vol. 9, pp. 1–7, 1987.

[3] J. Martinec and A. Rango, "Interpretation and utilization of areal snow-cover data from satellites," in *Proc. IAHS Third Int. Assembly, Baltimore, MD*, IAHS, 1987. IAHS Publ. 186.

[4] J. Dozier, R. E. Davis, and A. W. Nolin, "Reflectance and transmittance of snow at high spectral resolution," in *IGARSS '89, Quant. rem. sens.: an economic tool for the Nineties*, (Canada), pp. 662–664, IGARSS '89 12th Can. Symp. on Rem. Sens., 1989. No. 89CH2768-0.

[5] J. B. Adams, M. O. Smith, and P. E. Johnson, "Spectral mixture modeling: a new approach to analysis of rock and soil types at the Viking Lander 1 site," *J. Geophys. Res.*, vol. 91, pp. 8098–8112, 1986.

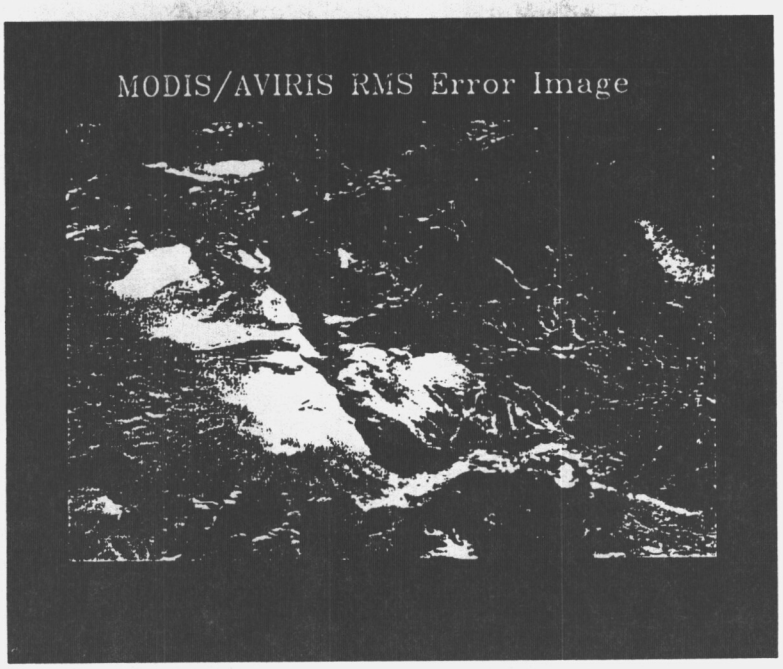

Figure 6: RMS error image for for the MODIS-convolved AVIRIS data, Mammoth Mountain, California.

[6] D. A. Roberts, M. O. Smith, J. B. Adams, and D. E. Sabol, "Isolating woody plant material and senescent vegetation from green vegetation in AVIRIS data," in *Proc. 2nd Ann. JPL Airborne Vis./Infr. Imaging Spectro. (AVIR IS) Workshop* (R. O. Green, ed.), (Pasadena, California), pp. 42–57, Jet Propulsion Laboratory, 1990. JPL Publication 90-54.

[7] D. K. Hall, J. L. Foster, J. Y. L. Chien, and G. A. Riggs, "Determination of actual snow-covered area using Landsat TM and digital elevation model data in Glacier National Park, Montana," *Polar Record*, vol. 31, pp. 191–198, 1995.

[8] W. Rosenthal, "Mapping montane snow cover at subpixel resolution from the Landsat Thematic Mapper," Master's thesis, University of California, Santa Barbara, 1993.

[9] B.-C. Gao, K. Heidebrecht, and A. F. H. Goetz, "Software for the derivation of scaled surface reflectances from AVIRIS data," in *Summ. 3rd Ann. JPL Airborne Geosci. Workshop* (R. O. Green, ed.), (Pasadena, California), pp. 101–103, Jet Propulsion Laboratory, 1992. JPL Publication 92-14, Vol. 1.

[10] A. W. Nolin, "Snowcover mapping with the Airborne Visible/Infrared Imaging Spectrometer," in *Proceedings of the International Geoscience and Remote Sensing Symposium '94*, (Pasadena), pp. 2081–2083, IEEE, 1994. 94CH3378-7.

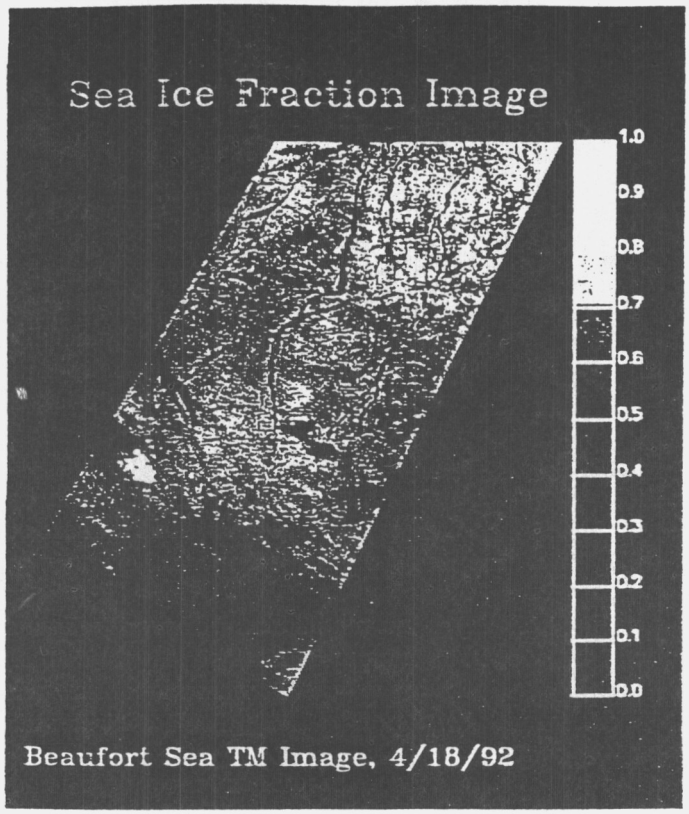

Figure 7: Sea ice fraction image from the Beaufort Sea TM image, 04/18/92.

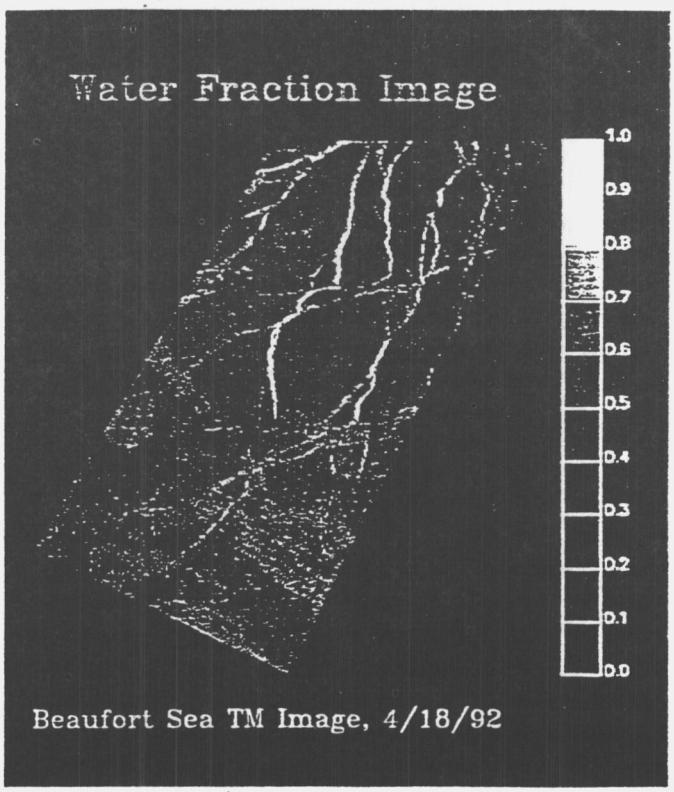

Figure 8: Open water fraction image from the Beaufort Sea TM image, 04/18/92.

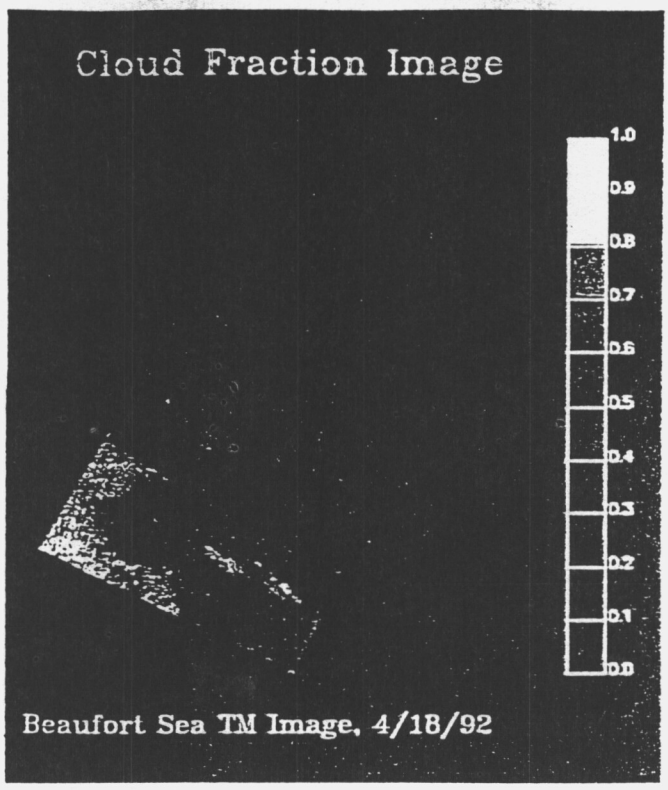

Figure 9: Cloud fraction image from the Beaufort Sea TM image, 04/18/92.

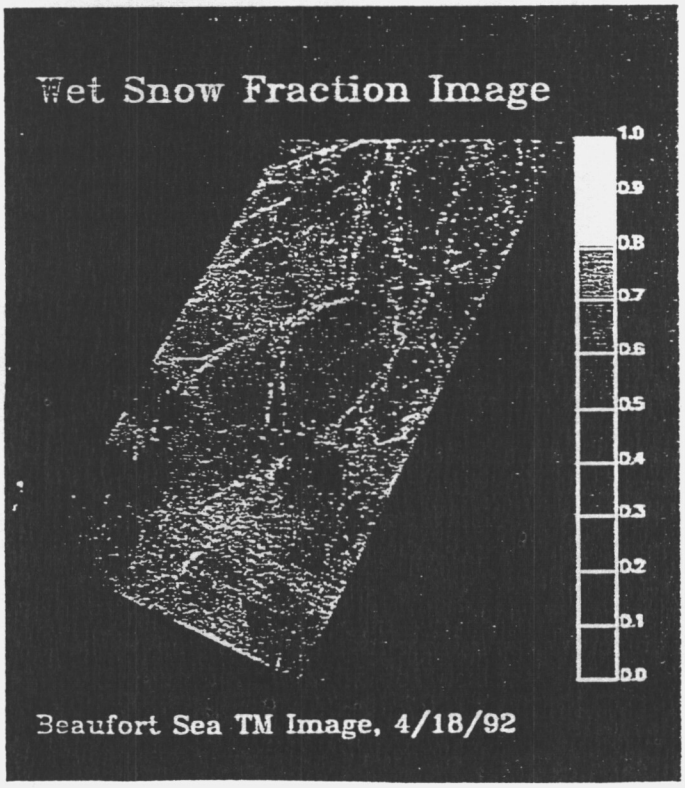

Figure 10: Wet snow fraction image from the Beaufort Sea TM image, 04/18/92.

SESSION II: SNOW-COVER MAPPING

Questions/Issues to be Discussed at the Snow/Ice Workshop

D. K. Hall
Hydrological Sciences Branch
NASA/Goddard Space Flight Center

How soon after acquisition will you need the snow/ice maps?

For the composite maps, which do you prefer, a composite of 7 days, 10 days, other, and why?

What would be the most useful MODIS at-launch and post-launch snow and ice products?

Specifically what would you use the products for?

What metadata should be included with the data products? For example, quality control data are metadata. Image i.d.# and lat/long are also metadata.

What improvements can you suggest to the snow and ice products as currently planned?

MODIS SNOW AND ICE ALGORITHM DEVELOPMENT

George Riggs, Research and Data Systems Corp. Greenbelt, MD email: griggs@ltpmail.gsfc.nasa.gov

Introduction

Context of the Moderate Resolution Imaging Spectroradiometer (MODIS) snow and ice algorithms in EOSDIS is described. Format and content of the data products generated by the algorithms are presented. Algorithm techniques and results are discussed. Requirements for and content of metadata and quality assessment data for the products are briefly discussed. Description of current status of algorithms concludes the presentation.

MODIS Objectives

"MODIS will help scientist to understand the Earth as a system, from which they can develop the capability to predict future change and to differentiate between the impact of human activities and natural activities on the environment. ...MODIS will assist policy makers worldwide in making sound decisions concerning protection and management of our environment and resources." (MODIS, NASA's Earth Observing System, NASA, Goddard Space Flight Center, Greenbelt, MD).

Those are the programmatic objectives for MODIS. The objective of the MODIS snow and ice algorithms is to produce standard data products that are consistent, accurate, and well described (product descriptions and quality assessment information) that will contribute to attaining the above objectives. The data products should also be of general or greater usefulness to the scientific community.

MODIS Instrument Description

MODIS employs a conventional imaging radiometer concept, consisting of a cross-track scan mirror and collecting optics, and a set of linear detector arrays with spectral interference filters located in four focal planes. The optical arrangement will provide imagery in 36 discrete bands between 0.4 and 15 um selected for diagnostic significance in Earth science. The different spectral bands have different spatial resolutions of 250 m, 500 m, or 1 km at nadir. MODIS will provide daylight reflection and day/night emission spectral imaging of any point on the Earth at least every 2 days, with continuous duty cycle. Complete description and specification of the MODIS instrument can be found at the MODIS homepage: http://ltpwww.gsfc.nasa.gov/MODIS/MODIS.html.

Algorithms and Products Within EOSDIS

The Earth Observation System Data Information System (EOSDIS) is the system that will collect data, generate data products, archive data and provide access to data. Within EOSDIS is the Science Data Processing Segment (SDPS) located at each Distributed Active Archive Center (DAAC) that will generate standard MODIS products, including the MODIS snow and ice algorithms. These algorithms are being developed at our Science Computing Facility (SCF) using the Science Data Production (SDP) Toolkit to simulate the production environment of the SDPS.

The project has mandated that data products be in Hierarchical Data Format (HDF) and has specified a standard set of metadata for every product. The standard metadata is generally used for processing control and for services such as data searches. Science content and specification of the data products are left to the PI. The PI may

included metadata and quality assessment data specific to a product. This metadata and quality assessment data should provide the user with information relevant to interpretation of the data and quality of the data.

Current MODIS Snow and Ice Data Products

Algorithm development and coding is in progress for these products:

MOD10 Level 2 Snow Cover
MOD10 Level 3 Daily Gridded Snow Cover
MOD 33 Level 3 Weekly Gridded Snow Cover
(maximum snow cover extent, mean snow cover, snow line)

MOD29 Level 2 Ice Extent (Ice on seas and lakes)
MOD29 Level 3 Daily Gridded Ice Extent
MOD42 Level 3 Weekly Gridded Ice Extent
(maximum ice extent, ice edge)

Level 2 is defined as a data product that remains in the MODIS data granule format no manipulation of the data is done other than to generate a geophysical result for a 'pixel'. A Level 3 data product has been manipulated in any manner, e.g. spatially and or temporally averaged, in the process of generating a product. The weekly products contain one or more HDF scientific data sets.

Snow and ice data products are currently specified to have a 1 km spatial resolution. (Can be gridded to other resolutions and map projections.) The products contain coded values of algorithm results, e.g. 200 = snow, 50 = not snow. Data product files are in HDF composed of global metadata (file attributes) and scientific data sets (SDS) with metadata (dataset attributes).

An ISCCP mapping grid is the current grid used for mapping of MODIS data products.

Specification of metadata, quality assessment metadata and gridding scheme are topics open for discussion at this workshop.

Snow Algorithm

Snow is identified by reflectance characteristics in the visible and near-infrared regions of the electromagnetic spectrum. Key characteristic of snow is the high *reflectance in the visible coupled with very low reflectance in the infrared about* 1.6 um. These characteristics are combined in the Normalized Difference Snow Index (NDSI).

For TM data the NDSI is calculated as;
(TM 2 - TM 5) / (TM 2 + TM 5)

For MODIS the NDSI is calculated as;
(MODIS 4 - MODIS 6) / (MODIS 4 + MODIS 6)

Snow typically has been found to have NDSI values of 0.4 or greater. Open water also has been found to have similarly high NDSI values but can be discriminated from snow with a near infrared reflectance test. In the near infrared snow typically has high reflectance and water absorbs. Thus a near infrared reflectance threshold test serves to distinguish between snow and water.

The NDSI also functions as a snow and cloud discriminator for many types of clouds. Cirrus clouds are very difficult to distinguish from snow. Cirrus clouds are inconsistently distinguished from snow.

A pixel is identified as snow if conditions of the criteria tests for snow are met. The hatched region in Figure 1 is the snow identification region created by the intersection of the criteria tests thresholds.

Figure 1. Snow identification region. The cross hatched area is the snow identification region. Samples are from TM scenes covering Glacier National Park, MT, USA on 14 March 1991, except the water and summer forest samples from a 03 September 1990 scene.

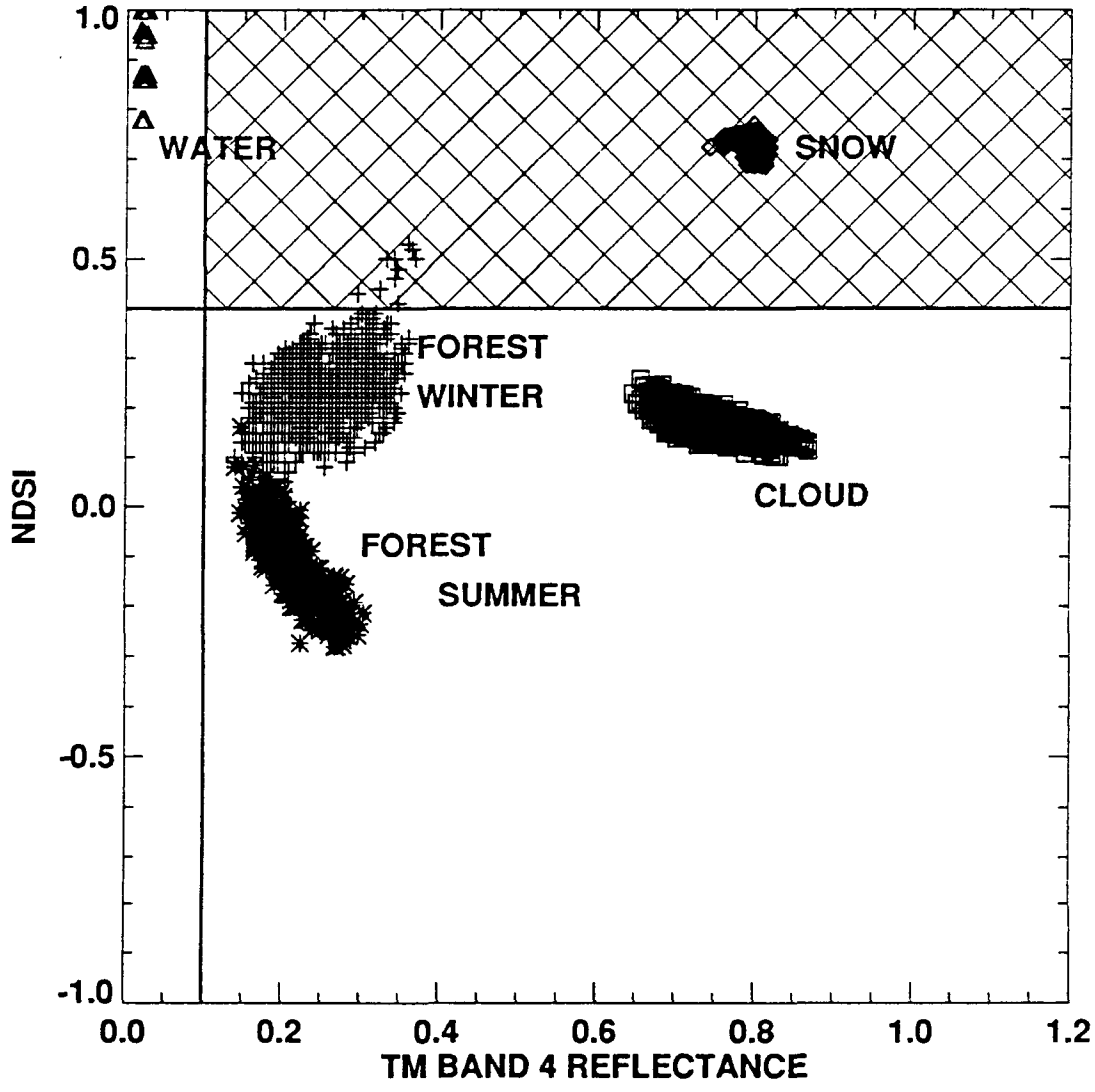

The snow algorithm has produced good results on 25 TM scenes from different seasons with varied surface features. Results of the snow algorithm have compared very favorably with ground observations, visual analysis of imagery, with spectral mixture modelling results, and with supervised classification. A comparison study of Ron Welch's (SDSMT) polar scene classification technique is underway. Comparisons have shown that the extent of snow cover is accurately identified by the snow algorithm. Comparisons also reveal errors of the snow algorithm.

Omission errors of snow in topographic shade and snow under dense forest canopies are not uncommon. Cirrus clouds are a source of confusion with snow.

Commission errors of identifying very bright surfaces, or glacial sediment laden rivers as snow have been observed.

Ice Algorithm

The ice algorithm employs the same criterion test for ice as that used for snow detection on land. Significant reflectance differences between open water and most ice types allow for detection of ice using the same algorithm. The ice algorithm simply identifies a pixel as ice or not ice. Results with the algorithm on over 15 TM scenes have been acceptable. Thick ice and snow covered ice are identified as ice as well as some situations of thin ice. Thin ice types are detected less reliably. A comparative study of polar classification techniques is in progress with Ron Welch.

Weekly Snow Cover

A weekly snow cover product is produced by compositing the previous seven daily snow cover data products. Included in this product are datasets of maximum snow cover extent, a snow persistence index, and continental snow line. Local metadata are also generated with the datasets.

Definition and expression of these data set are not yet fixed. Definition of a snow mapping week and definition of an annual snow year are to be determined.

Weekly Ice Extent

A weekly ice cover product is generated by compositing the previous seven daily ice data products. Two datasets of data on maximum ice extent, and ice edge are planned within this product. Definition and expression of these data sets are not yet fixed. And as with snow definition of an ice week and ice year are to be determined.

Metadata and Quality Assessment

The purpose of metadata and quality assessment (QA) is to provide users with pertinent data and information that will enable them to better understand and evaluate the data products for their purposes. Metadata is any data that is not the geophysical value, i.e. the result, generated by the algorithm. Metadata generated for a run of the snow cover algorithm is;

Percentage of snow cover = 0-100%
Percentage_snow = %
Percentage_not_snow = %
Above_range_NDSI = 0 - count
Below_range_NDSI = 0 - count
Division_by_zero = 0 - count
Out_of_range_input = 0 - count
No_decision = 0 - count

Two types of QA data may be generated for a product. Automated QA generates and compiles statistics regarding errors, limits and summary results obtained during algorithm execution on a granule of data. Interactive QA occurs after routine processing. Interactive QA is where an analyst/scientist visual analyzes the data product, does validation, etc. Results of the interactive QA are then appended to the data product.

The QA data may be contained in numerous pieces of metadata or it may be condensed to a few general QA flags such as; Data quality is-good, acceptable, unacceptable, freakish. These general flags may be derived from numerous other flags and so on. Conceptually there is a pyramid of QA metadata that can accompany a data product.

Current State of Development

Beta-3 versions of the algorithms have been delivered to the project for integration and test. The beta-3 versions contain the snow and ice identification techniques described in this presentation and were integrated with the SDP toolkit. The next step in development will be integrating gridding functions with the algorithms to generate the L2G and L3 gridded data products. Simulated MODIS data is used for coding development of the algorithms.

An ongoing task is the development of a function to take the 250 m and 500 m spatial resolution MODIS bands used in the algorithms to a common spatial resolution.

Integration of the MODIS cloud mask product developed by Paul Menzel et. al., at U. Wisconsin with the algorithms is progressing. Integration of a land/water mask of 1 km resolution derived from the DCW and generated by EDC is progressing.

The conceptual processing flow diagram for the snow algorithm is shown in Figure 2. Rounded corner rectangles are data inputs. Rectangular boxes are functions in the algorithms that process data and generated product outputs. Ellipses are the data products archived at the DAAC. The SDP Toolkit, not shown, is used for I/O and processing control.

Figure 2. MODIS Snow Algorithm Processing Flow

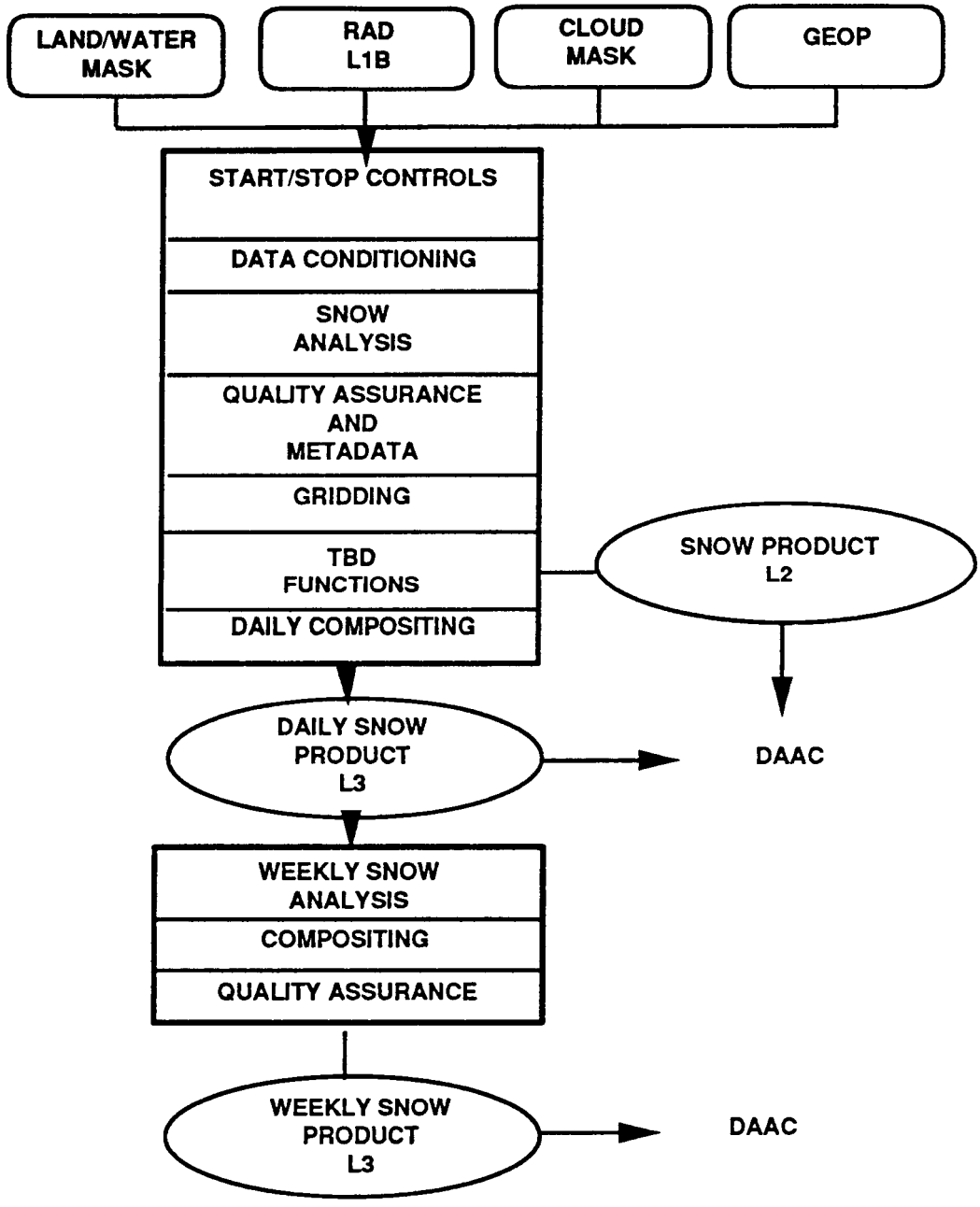

AN ANALYSIS OF THE NOAA SATELLITE-DERIVED SNOW COVER RECORD, 1972-PRESENT

David A. Robinson & Allan Frei
Department of Geography
Rutgers University
New Brunswick, NJ 08903

Introduction

The large-scale distribution of snow cover over northern hemisphere lands has been a topic of increasing attention in recent years. This interest has been spurred, at least in part, by concerns associated with potential changes in the global climate system associated with anthropogenic and natural causes. Satellite observations using visible satellite imagery permit a hemispheric analysis of snow extent. For almost three decades the National Oceanic and Atmospheric Administration (NOAA) has been using visible imagery to produce weekly charts depicting the extent of snow cover over northern hemisphere lands. These charts constitute the longest satellite-derived environmental dataset available on a continuous basis and produced in a consistent manner. We will briefly describe the NOAA charts and then provide an update on the variability of snow extent over the hemisphere from January 1972 through August 1995. Concentration will be on snow kinematics, as found formerly in Matson & Wiesnet (1981), Dewey & Heim (1982), Barry (1990), Robinson et al. (1991), Iwasaki (1991), Gutzler & Rosen (1992), and Masuda et al. (1993). Recent studies that use NOAA snow data to investigate snow cover synergistics within the climate system include, for example, Leathers & Robinson (1993; 1995), and Karl et al. (1993).

NOAA Snow Charts

Weekly snow charts produced by NOAA depict boundaries between snow-covered and snow-free land surfaces. They are produced from visual interpretation of photographic copies of visible-band satellite imagery, primarily Advanced Very High Resolution Radiometer (AVHRR) data. Charts show snow boundaries on the last day that the surface in a given region is observed. Since cloud cover can mask the surface, this is often not the last day of the chart week. On average, charts tend to represent the fifth day of a week. Charts are digitized on a weekly basis to the National Meteorological Center Limited-Area Fine Mesh (LFM) grid (cf. Matson et al., 1986, and Robinson, 1993 for further details on NOAA charts). While NOAA charts have been produced since 1966, early ones tended to underestimate snow extent, particularly during fall. Charting accuracy improved considerably in 1972, when VHRR and later AVHRR data began to be used. Data since 1972 are considered to be of high enough quality for use in climate studies (Wiesnet et al., 1987).

For our investigation, monthly means of snow cover area are calculated using a routine described fully in Robinson (1993). The Rutgers routine calculates weekly areas from the digitized snow files and to then obtain a monthly value, weights them according to the number of days of a chart week falling in the given month. A chart week is considered to center on the fifth day of the published chart week. Prior to the calculations, the digital files are standardized to a common land mask that includes those and only those LFM cells at least half covered by land. This corrects an inconsistency in the original NOAA files.

Snow Cover: 1972-present

Mean annual northern hemisphere snow cover is 25.4 million km^2. On average, 14.7 million km^2 lies over Eurasia and 10.6 million km^2 over North America (including Greenland). In figure 1, the variability of snow cover over the Northern Hemisphere between January 1972 and August 1995 is expressed through anomalies of individual months and twelve-month running means. Monthly anomalies of greater than 4 million km^2 have been observed occasionally throughout the past 24 years, although they are generally less than 2 million km^2.

Two pronounced snow regimes are evident during the period of record. Between 1972 and 1985, twelve-month running means of snow extent fluctuated around a mean of approximately 25.9 million km^2. A rather abrupt transition occurred in the 1986/87 period to a new regime from 1988 to the present where snow extent fluctuates around a running mean of about 24.2 million km^2. This recent interval is marked by a decrease in spring and early summer snow extent compared to the earlier period (figure 2). Changes are evident over both North America and Eurasia. Individual years of fall and winter snow cover vary around means that have remained more stable during the satellite era.

Zones exhibiting year-to-year variability in snow cover extent have been identified for each month of the year. Figure 3 shows these "action" areas for November and April, defined as locations where the surface is snow covered between 10% and 90% of the time in at least one third of the years between 1972 and 1994. This rather broad criterion excludes those regions where snow cover is extremely common or rare during a particular month. The variable zone in November straddles the US/Canadian border from coast to coast, and plunges into the US Rockies and high Plains. The Eurasian zone lies within approximately 5° of the 50th parallel, except in Europe where it curves poleward. The Himalayan/Tibetan region also has variable cover, which is also the case in April. The variable zone in April across the remainder of Eurasia lies between approximately 50° and 60°N. April snow extent is also variable in southern Canada and the US Rockies, a considerably smaller North American zone than in November.

Within these variable zones, Principal Components Analysis (PCA) has been used to identify regions of coherent snow cover; that is, areas within which snow time series for grid points are highly correlated to each other. An orthogonal varimax rotation of the components has been performed to allow for more clear visualization. Regional signals are found to be dominant over continent-wide signals in all months. The first two components for November and April are shown in figure 3. Together, the two November components explain 26% of the hemispheric variance. Component 1 centers on the northern US Rockies and the northern US high plains and western Canadian prairie. Component 2 covers much of the variable zone in eastern Asia. In April, component 1 is found in western Asia, and component 2 covers a region spanning North America, along and just north of the US/Canadian border. Together, these two components explain 27% of the hemispheric variance in April.

Conclusions

Given the relatively short time in which hemispheric monitoring of snow cover has been possible from space, it is difficult to fully understand the significance of the apparent stepwise change in snow extent in the middle 1980s. It is certainly premature to ascribe the less-extensive regime in recent years to a global warming. However it is noteworthy that the extent of snow cover appears to be inversely related to hemispheric surface air temperature (Robinson & Dewey, 1990), and, particularly in spring, feedbacks associated with the extent of the snowpack may be strongly influencing temperature (Groisman et al., 1994). Further studies using the NOAA set in conjunction with other climatic information are needed to better understand the synergistic relationships between hemispheric-scale atmospheric circulation and thermal variations and continental snow extent before any meaningful projections of future climatic states can be made.

NOAA will soon be discontinuing production of the weekly snow charts and replace them with daily ones. While still incorporating visible imagery, the new product will rely heavily on satellite passive microwave-derived estimates of snow extent. Plans are to conduct at least a twelve-month comparative study of the two products before discontinuing the current visible-only one. The appearance of MODIS-derived snow charts later in this decade will be a welcome addition to hemispheric snow charting efforts. The MODIS channels will provide the ability to better discriminate between snow and clouds. And perhaps with the development of procedures incorporating multiple visible and near infrared channels, snow will be identified more accurately in cloud-free areas. Together, the NOAA and MODIS products will provide an unprecedented means of assessing the seasonal and interannual fluctuations of this influential component of the climate system.

Acknowledgments

Thanks to D. Garrett at the NOAA Climate Analysis Center for providing continuous updates of the raw digitized NOAA snow chart data, and to J. Wright for running the Rutgers routine on these files. This work is supported by NSF grants ATM-9314721 and SBR-9320786 and NASA grant NAGW-3568.

References

Barry, R.G., 1990: Evidence of recent changes in global snow and ice cover. *GeoJournal*, 20, 121-127.

Dewey, K.F. & R. Heim Jr., 1982: A digital archive of northern hemisphere snow cover, November 1966 through 1980. *Bull. Am. Met. Soc.*, 63, 1132-1141.

Groisman, P. Ya., T.R. Karl & R.W. Knight, 1994: Observed impact of snow cover on the heat balance and the rise of continental spring temperatures. *Science*, 263, 198-200.

Gutzler, D.S. & R.D. Rosen, 1992: Interannual variability of wintertime snow cover across the Northern Hemisphere, *J. Clim.*, 5, 1441-1447.

Iwasaki, T., 1991: Year-to-year variation in snow cover area in the Northern Hemisphere. *J. Met. Soc. Japan*, 69, 209-217.

Karl, T.R., P.Y. Groisman, R.W. Knight & R.R. Heim, Jr., 1993: Recent variations of snow cover and snowfall in North America and their relation to precipitation and temperature variations. *J. Clim.*, 6, 1327-1344.

Leathers, D.J. & D.A. Robinson, 1993: The association between extremes in North American snow cover extent and United States temperatures. *J. Clim.*, 6, 1345-1355.

Leathers, D.J. & D.A. Robinson, 1995: Abrupt changes in the seasonal cycle of North American snow cover. *Proc. Fourth Conf. Polar Meteor. Oceanog.*, Dallas, AMS, 122-126.

Masuda, K, Y. Morinaga, A. Numaguti & A. Abe-ouchi, 1993: The annual cycle of snow cover extent over the Northern Hemisphere as revealed by NOAA/NESDIS satellite data. *Geographical Reports of Tokyo Metropolitan Univ.*, 28, 113-132.

Matson, M., C.F. Ropelewski and M.S. Varnadore, 1986: *An Atlas of Satellite-Derived Northern Hemisphere Snow Cover Frequency.* NOAA Atlas, 75pp.

Matson, M. & D.R. Wiesnet, 1981: New data base for climate studies. *Nature*, 289, 451-456.

Robinson, D.A. ,1993: Monitoring northern hemisphere snow cover. *Snow Watch '92: Detection Strategies for Snow and Ice. Glaciological Data Report*, GD-25, 1-25.

Robinson, D.A. & K.F. Dewey, 1990: Recent secular variations in the extent of northern hemisphere snow cover. *Geophys Res. Lett.*, **17**, 1557-1560.

Robinson, D.A., F.T. Keimig & K.F. Dewey, 1991: Recent variations in Northern Hemisphere snow cover. *Proc. 15th Annual Climate Diagnostics Workshop*, Asheville, NC, NOAA, 219-224.

Wiesnet, D.R., C.F. Ropelewski, G.J. Kukla & D.A. Robinson, 1987: A discussion of the accuracy of NOAA satellite-derived global seasonal snow cover measurements. *Large Scale Effects of Seasonal Snow Cover*, IAHS Publ. 166, 291-304.

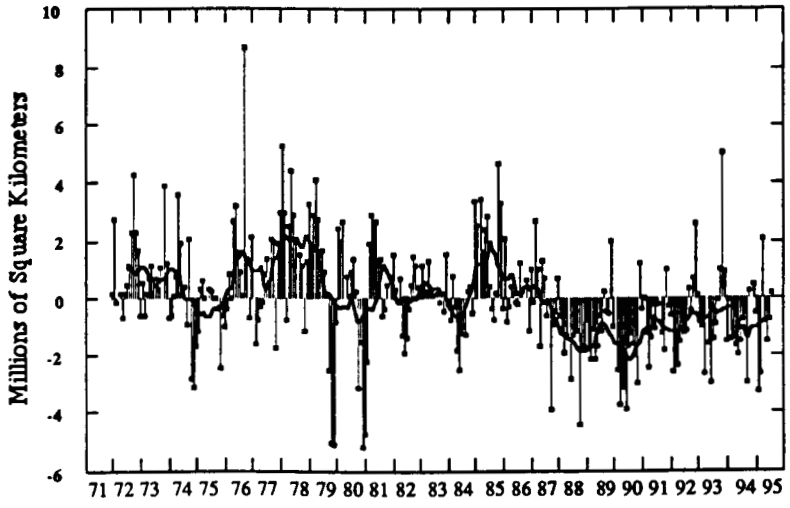

Figure 1. Anomalies of monthly snow cover extent over northern hemisphere lands (including Greenland) between January 1972 and August 1995. also shown are twelve-month running anomalies of hemispheric snow extent, plotted on the seventh month of a given interval. Anomalies are calculated from a mean hemispheric snow extent of 25.4 million km^2 for the full period of record.

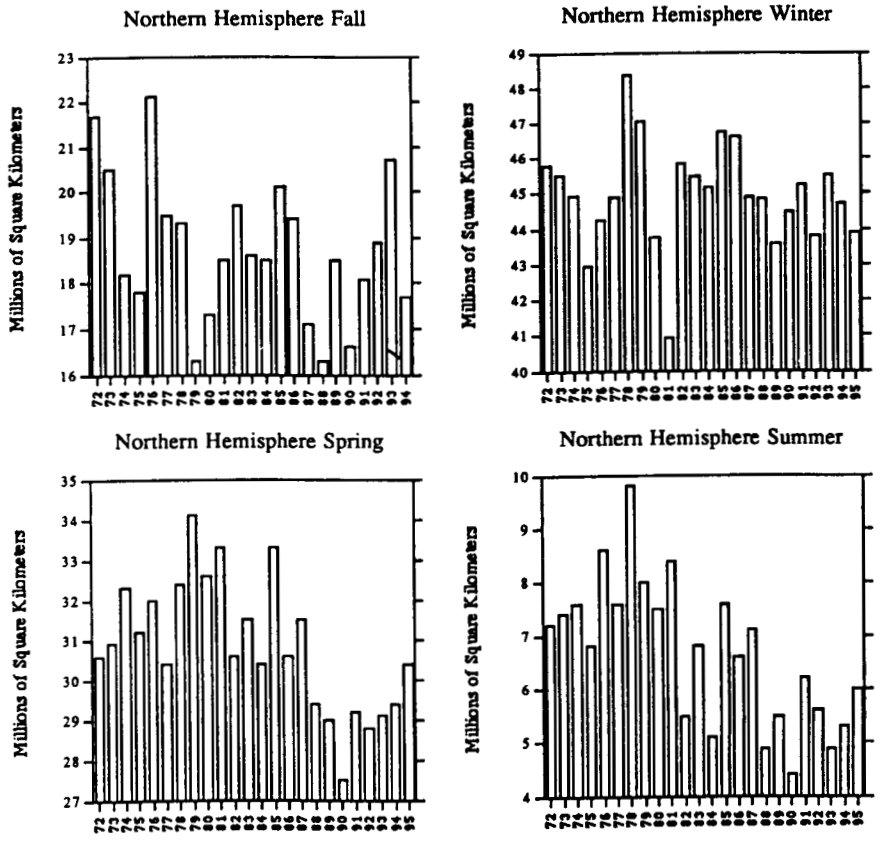

Figure 2. Extent of seasonal snow cover over northern hemisphere lands (including Greenland) since 1972.

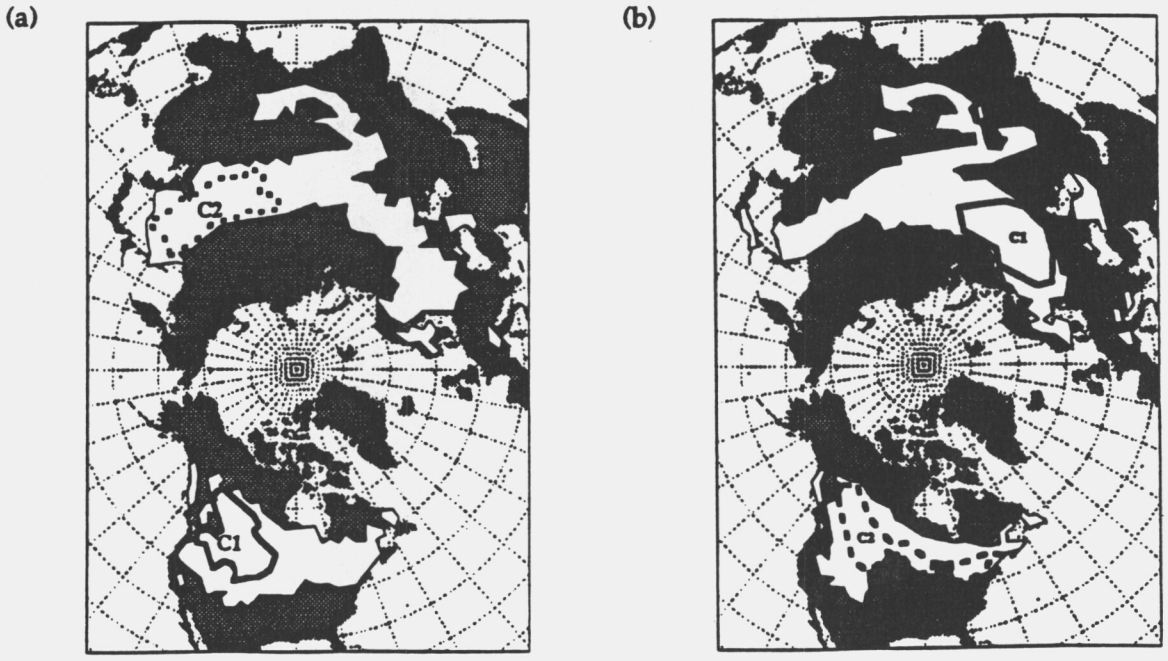

Figure 3. Land areas in white are zones of variable snow extent in November (a) and April (b) (cf. text for explanation). Contours within these zones show the first (solid) and second (dashed) principal components. Contours are plotted at 0.1 increments, starting at r^2=0.3.

MEASUREMENT OF THE SPECTRAL ABSORPTION OF LIQUID WATER IN MELTING SNOW WITH AN IMAGING SPECTROMETER

Robert O. Green[1,2] and Jeff Dozier[2]

[1]Jet Propulsion Laboratory, California Institute of Technology, Pasadena, CA 91109
[2]University California at Santa Barbara, CA 93106

1. INTRODUCTION

Melting of the snowpack is a critical parameter that drives aspects of the hydrology in regions of the Earth where snow accumulates seasonally. New techniques for measurement of snow melt over regional scales offer the potential to improve monitoring and modeling of snow-driven hydrological processes. In this paper we present the results of measuring the spectral absorption of liquid water in a melting snowpack with the Airborne Visible/Infrared Imaging Spectrometer (AVIRIS).

AVIRIS data were acquired over Mammoth Mountain, in east central California on 21 May 1994 at 18:35 UTC (Figure 1). The air temperature at 2926 m on Mammoth Mountain at site A was measured at 15-minute intervals during the day preceding the AVIRIS data acquisition. At this elevation, the air temperature did not drop below freezing the night of the May 20 and had risen to 6 degrees Celsius by the time of the overflight on May 21. These temperature conditions support the presence of melting snow at the surface as the AVIRIS data were acquired.

2. OPTICAL PROPERTIES OF LIQUID WATER AND ICE

The basis for the spectral measurement of liquid water is derived from the optical properties of liquid water in the 400- to 2500-nm range. To spectrally measure liquid water in snow, its absorption must be separable from the absorption due to frozen water. The complex refractive indices (Warren, 1982; Kou et al., 1993) were used to model the spectral properties of liquid water and ice. The complex refractive indices of these two phases of water are similar in overall magnitude and spectral trend. However, in detail these physical constants differ due to the different molecular bond energies of water in the liquid and solid state.

To investigate the contrast in spectral absorption between liquid water and ice, the transmittance of a 10-mm path through these materials was calculated (Figure 2). The spectral absorptions are overlapping, but displaced in both the 1000- and 1200-nm spectral regions. The 1000-nm spectral region is selected for this research because snow is more reflective at these wavelengths and path lengths of 10 mm are expected in the snowpack (Dozier, 1989).

3. AVIRIS MEASUREMENTS AND TRANSMITTANCE MODEL

AVIRIS measures the upwelling spectral radiance from 400 to 2500 nm at 10-nm intervals and collects images of 11 by up to 1000 km at 20-m spatial resolution. AVIRIS radiance spectra acquired over Mammoth Mountain were inverted to apparent spectral reflectance (Green, 1990; Green et al., 1993). An equivalent path transmittance model was developed for liquid water and ice in the 1000 nm spectral region. The model was inverted using a nonlinear least squares fitting routine to derive the equivalent path length transmittance of liquid water and ice for each spectrum measured by AVIRIS. A linear spectral albedo term is included in the model to compensate for illumination. For the AVIRIS spectrum in open snow below and adjacent to site A, the inverted spectral model returned values of 1.9 ± 0.1 mm liquid water and 13.3 ± 0.7 mm ice (Figure 3). The presence of liquid water due to surface melting at this elevation is consistent with the temperature prior to the AVIRIS acquisition. For site B to the north of the summit of Mammoth Mountain, the inverted model returned equivalent path transmittance of 0.0 mm liquid water and 20.1 ± 0.9 mm (Figure 4). At the 3362 m summit, the temperature is calculated to be 2.6 degrees Celsius colder. Snow at these higher elevations and north facing slopes had not commenced surface-melting at the time of AVIRIS data acquisition.

This equivalent path transmittance model was inverted for the entire AVIRIS scene of Mammoth Mountain (Figure 5). Absorption due to ice in snow is measured at Mammoth Mountain and to the higher elevations in the northwest. At this late spring date, absorption due to ice was not measured at the lower elevations to the east and in the valley to the west of the mountain. The equivalent path transmittance due to liquid water was derived for the AVIRIS scene (Figure 6). Liquid water is measured in the AVIRIS spectrum in the snow at the lower elevations at Mammoth Mountain. As expected, liquid water is absent at the highest elevations of Mammoth Mountain where the snow is fully frozen. At low elevations, liquid water is also measured in the leaves of vegetation (Green et al., 1991). Liquid water in melting snow is

spectrally distinguishable from liquid water in vegetation, based either on the absorption of ice in snow or chlorophyll in vegetation.

4. CONCLUSION

Examination of the optical constants of liquid and solid water shows that in the 1000 nm region these two phases of water are separable, based upon their spectral properties. Measurement of these two phases of water requires spectral modeling of the overlapping absorptions of the liquid water absorption centered at 970 nm and the ice absorption at 1030 nm. An equivalent-path transmittance model was developed for liquid water and ice. This model was inverted using a nonlinear, least-squares spectral fitting approach for Mammoth Mountain AVIRIS data. Liquid water and ice were measured in melting snow below 2926 m based on spectral properties. Near the summit at 3362 m, only the absorption due to ice was measured. The occurrence of fully frozen snow at high elevations and melting snow at intermediate and low elevations is consistent with measured temperatures and elevations at the time and date of the AVIRIS acquisition.

This first-time remote measurement of the spectral absorption of liquid water in a melting snowpack will lead to new algorithms for the measurement, modeling and monitoring of snow-driven hydrological processes.

5. FUTURE WORK

Future research will focus on development of a radiative transfer model of the snowpack when both the liquid and solid phases of water are present. In 1995 additional AVIRIS flights with in situ measurements will be used to further validate the measurement of these two phases of water in the snowpack.

6. ACKNOWLEDGMENTS

This research was carried out at the Jet Propulsion Laboratory, California Institute of Technology, under contract with the National Aeronautics and Space Administration. Computational resources of the Center from Remote Sensing and Environment Optics (CRSEO), University of California, Santa Barbara, CA, were used.

7. REFERENCES

Dozier, J., 1989, "Remote Sensing of Snow in Visible and Near-Infrared Wavelengths," in Theory and Applications of Optical Remote Sensing, G. Asrar, ed., pp. 527-547, Wiley and Sons.

Green, R. O., 1990, "Radiative-transfer-based retrieval of reflectance from calibrated radiance imagery measured by an imaging spectrometer for lithological mapping of the Clark Mountains, California," SPIE Vol. 1298, Imaging Spectroscopy of the Terrestrial Environment.

Green, Robert O., James E. Conel, Jack S. Margolis, Carol J. Bruegge, and Gordon L. Hoover, 1991, "An Inversion Algorithm for Retrieval of Atmospheric and Leaf Water Absorption From AVIRIS Radiance With Compensation for Atmospheric Scattering," Proc. Third AVIRIS Workshop, JPL Publication 91-28, Jet Propulsion Laboratory, Pasadena, California, pp. 51-61.

Green, R. O., J. E. Conel, D. A. Roberts, 1993, "Estimation of Aerosol Optical Depth, Pressure Elevation, Water Vapor and Calculation of Apparent Surface Reflectance from Radiance Measured by the Airborne Visible/Infrared Imaging Spectrometer (AVIRIS) using a Radiative Transfer Code," SPIE, Vol. 1937, Imaging Spectrometry of the Terrestrial Environment, p. 2-11.

Kou, L., D. Labrie, and P. Chylek, 1993, "Refractive indices of water and ice in the 0.65- to 2.5-μm spectral range," Applied Optics, Vol. 32, No. 19, P. 3531-3540.

Warren, S. G., 1982, "Optical Properties of Snow," Reviews of Geophysics and Space Physics, vol. 20, pp. 67-89.

8. FIGURES

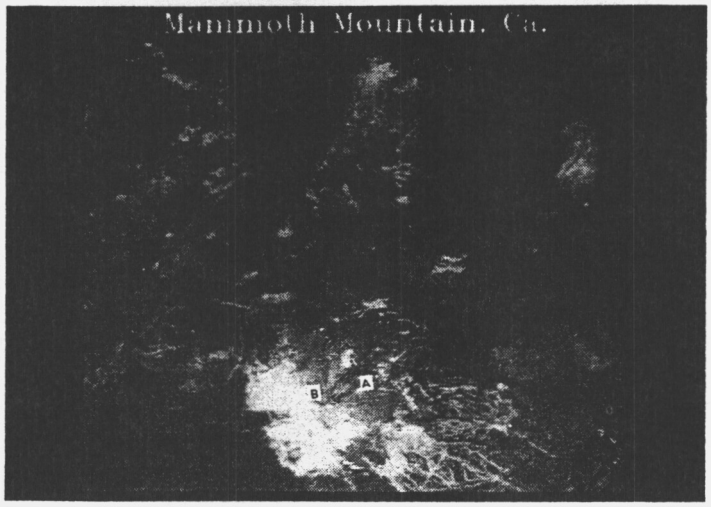

Figure 1. AVIRIS image of Mammoth Mountain with ski runs in the lower center of the image. North is to the top. (See AVIRIS Workshop Slide 4.)

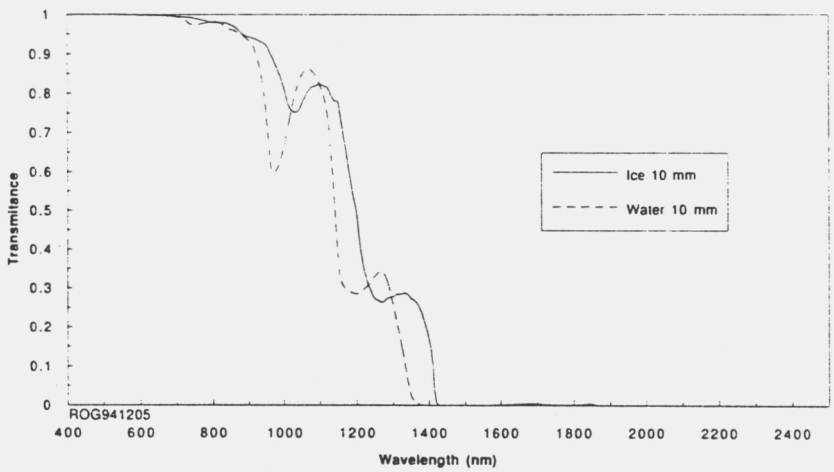

Figure 2. Transmission of light through 10 mm of water and ice.

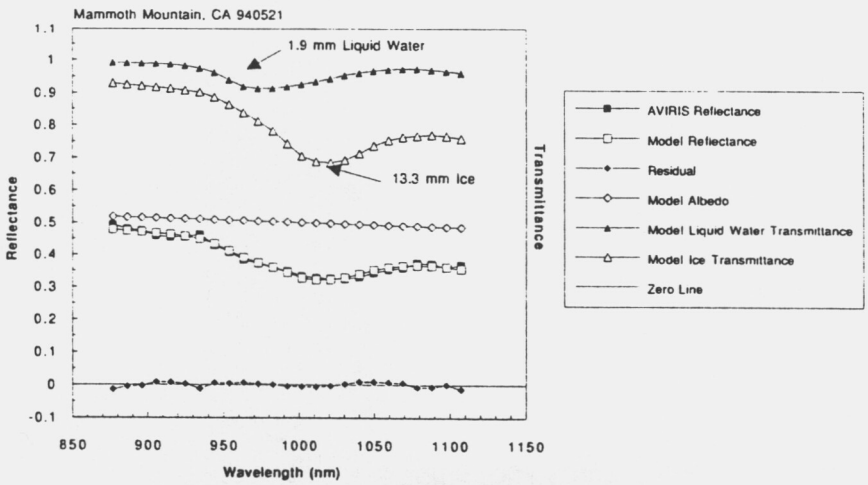

Figure 3. For site A at Mammoth Mountain, CA, the AVIRIS-measured spectrum and modeled spectrum when both liquid water and ice are present. Also shown is the residual disagreement and components of the model.

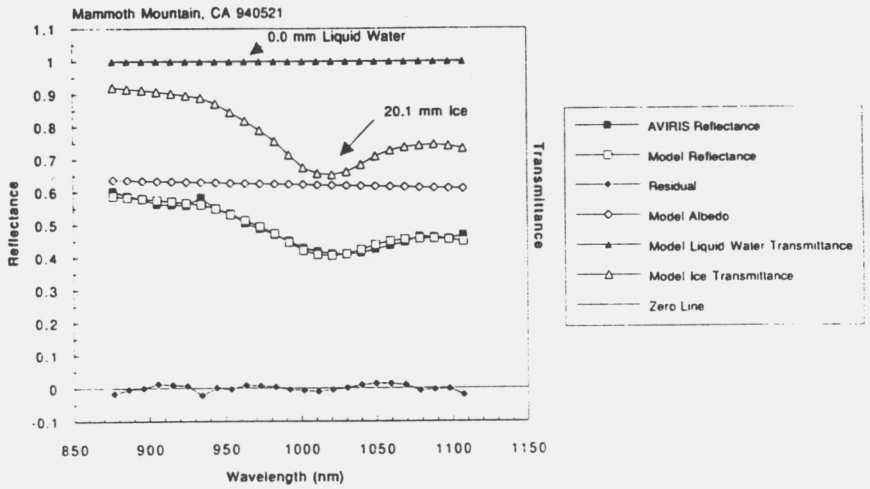

Figure 4. For site B, the AVIRIS-measured spectrum and modeled spectrum when ice is present, but liquid water is absent.

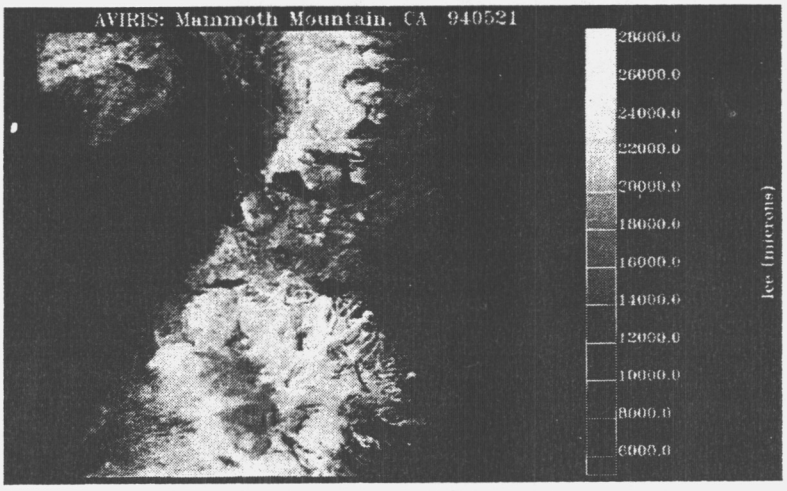

Figure 5. AVIRIS-derived path equivalent transmittance image for ice at Mammoth Mountain, CA. Ice is present only on the higher elevation in the May data set. (See AVIRIS Workshop Slide 4.)

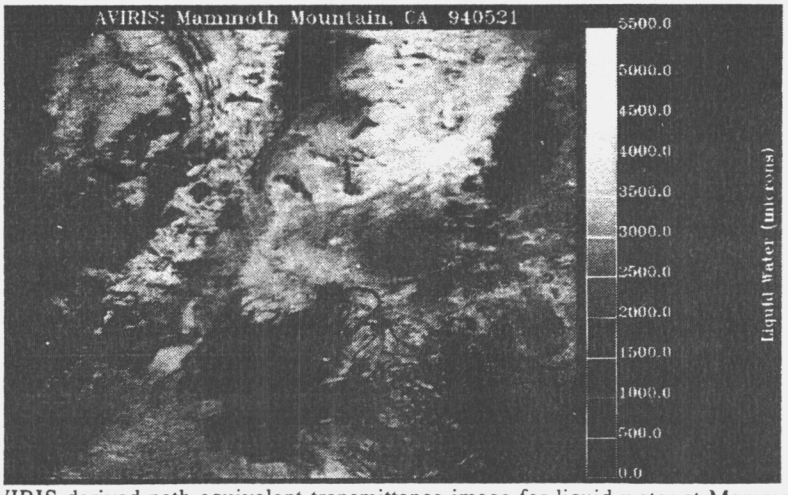

Figure 6. AVIRIS-derived path equivalent transmittance image for liquid water at Mammoth Mountain, CA. Liquid water is present on the lower snow slopes of the mountain where the snow is melting. Liquid water is also measured in healthy vegetation. (See AVIRIS Workshop Slide 4.)

SESSION III: MAPPING ICE AND CLOUDS WITH OPTICAL SENSORS

ESTIMATING CLOUD AND SURFACE PARAMETERS AT HIGH LATITUDES WITH AVHRR DATA

Jeff Key
Department of Geography
Boston University

1. INTRODUCTION

The EOS interdisciplinary project entitled Polar Exchange at the Sea Surface (POLES; D. Rothrock, PI) has as its goal the quantitative understanding of the exchanges of energy, momentum, and water in the atmosphere-ice-ocean system of the polar regions. Models of this complex system are being developed and are driven by or validated with geophysical fields estimated using satellite data. Several planned MODIS products are of interest to POLES: sea ice albedo, cloud cover, cloud top height, cloud transmissivity, sea ice edge, and sea surface temperature. Sea ice motion and sea ice concentration, though usually estimated using active and passive microwave sensors, could be generated using MODIS data and would also be useful to POLES.

While we look forward to a steady stream of MODIS data in the years to come, we need these geophysical fields now. We have therefore become engaged in a significant effort to develop algorithms for the retrieval of surface and cloud parameters using AVHRR and TOVS data. With AVHRR, methods have been developed to estimate

- surface temperature of snow and ice,
- surface albedo of snow and ice,
- cloud amount,
- cloud optical depth,
- cloud particle effective radius,
- cloud top temperature,
- downwelling shortwave and longwave fluxes at the surface.

These algorithms are not discussed here; see Key and Haefliger (1992), DeAbreu et al., (1994), and Key et al. (1994) for a discussion of the surface property retrievals, and Key and Barry (1989), Key and Stone (1995), Key (1995b), Key et al. (1994), and Schweiger and Key (1994) for details on the cloud and surface radiative flux retrieval procedures and validation.

2. APPLICATION

These algorithms have been applied to data collected during LEADEX (March-April 1992 in the Beaufort Sea), and also to a year-long time series of AVHRR data covering the Beaufort Sea region north of Alaska. Figure 1 shows the retrieved fields of cloud optical depth, downwelling shortwave and downwelling longwave radiative fluxes for a daytime image acquired during LEADEX. Surface radiative fluxes are within about 5% of those reported at the base camp. Surface temperature and albedo cannot be compared for this image because they are only retrieved for clear sky pixels; the camp is under the cloud deck shown in the lower center portion of the image.

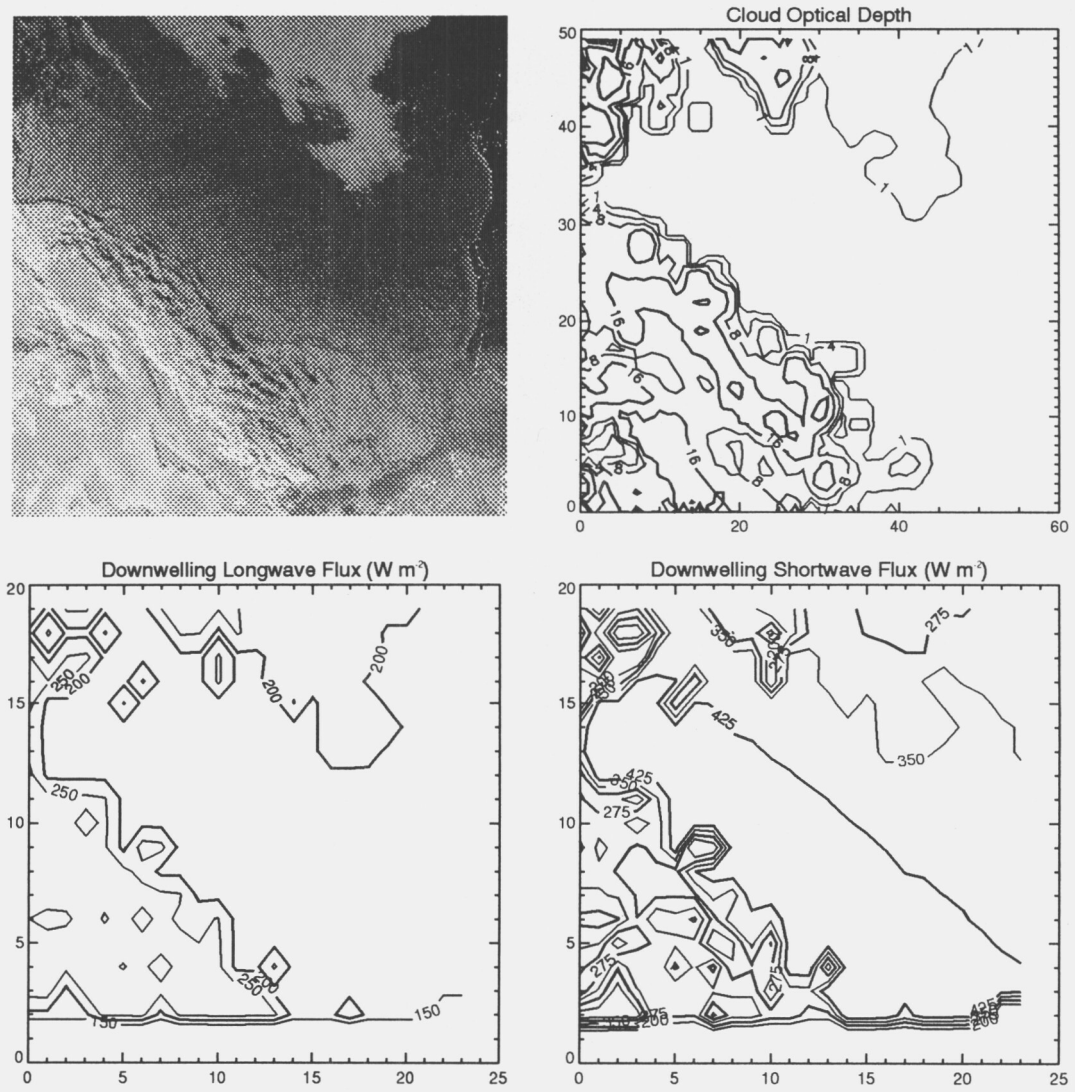

Fig. 1. Cloud properties and radiative fluxes retrieved from daytime AVHRR data (upper left) during LEADEX, April 18, 1992.

Figure 2 provides a similar example for a nighttime (January) image of the Beaufort Sea. The relative frequency histogram of cloud particle effective radius indicates that most of the particles are ice (effective radii greater than about 20 μm), though there is a significant portion of liquid droplets as well (effective radii from 5-20 μm). The cloud mask shows that, at least qualitatively, most of the cloud is being correctly identified.

Figure 3 shows the application of the retrieval procedures to a large data set. Nearly 300 daily (near 2300Z) AVHRR images were processed to generate these time series. Annual cycles of clear sky surface temperature, all sky broadband albedo, cloud particle effective radius and cloud optical depth are shown, where values are averages over $(1000\ km)^2$. The change in cloud particle

phase from summer to winter is clear, as is the decrease in surface albedo with the onset of melt.

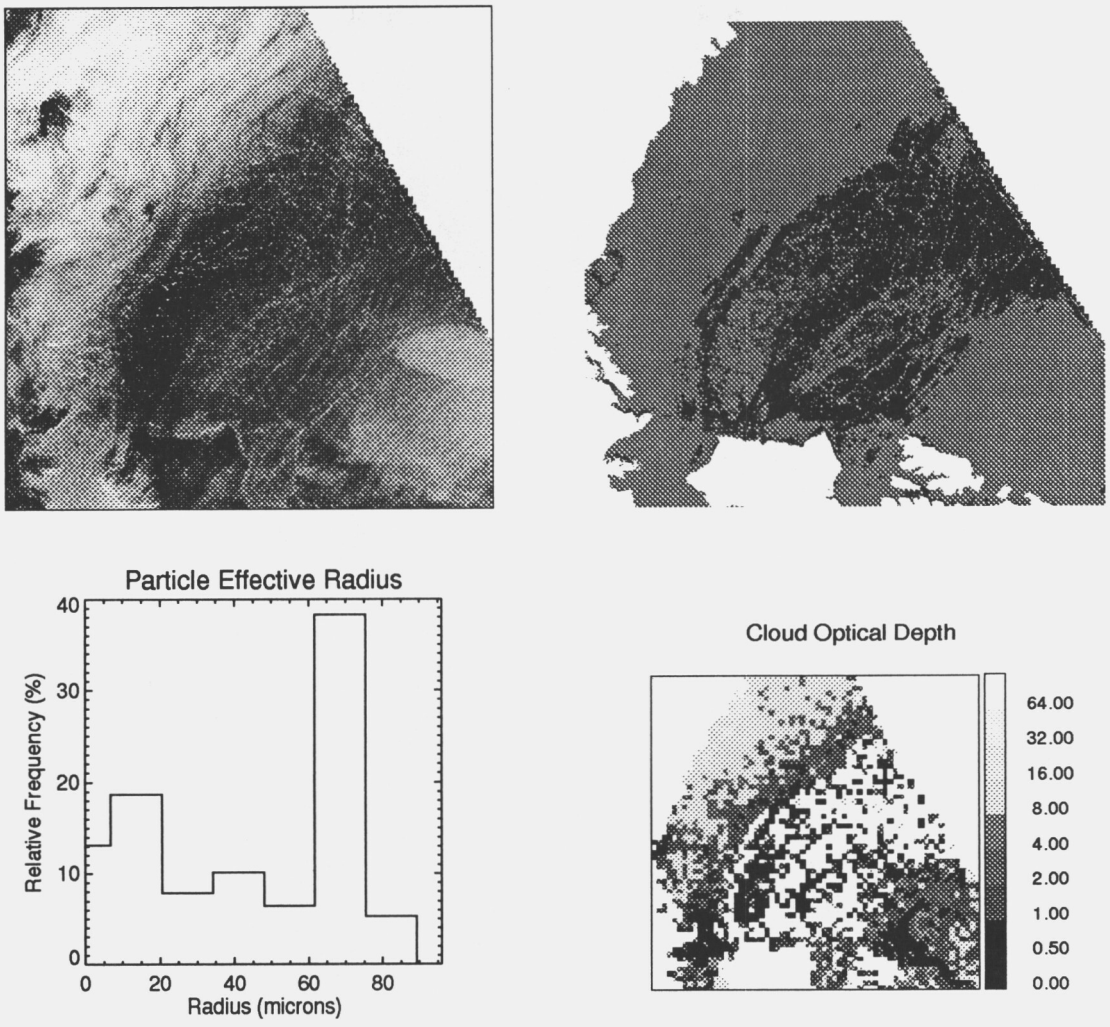

Fig. 2. Cloud properties retrieved from the nighttime (1/5/93) AVHRR image in the upper left. The cloud mask is shown in the upper right.

3. Conclusions

We plan to continue refining these procedures for use with the AVHRR, and to extend their applicability to include MODIS. This will be done to ensure that polar-specific problems receive due attention. If the MODIS algorithms as described in current and future ATBDs are found to be adequate for polar applications, we will happily switch to MODIS standard products.

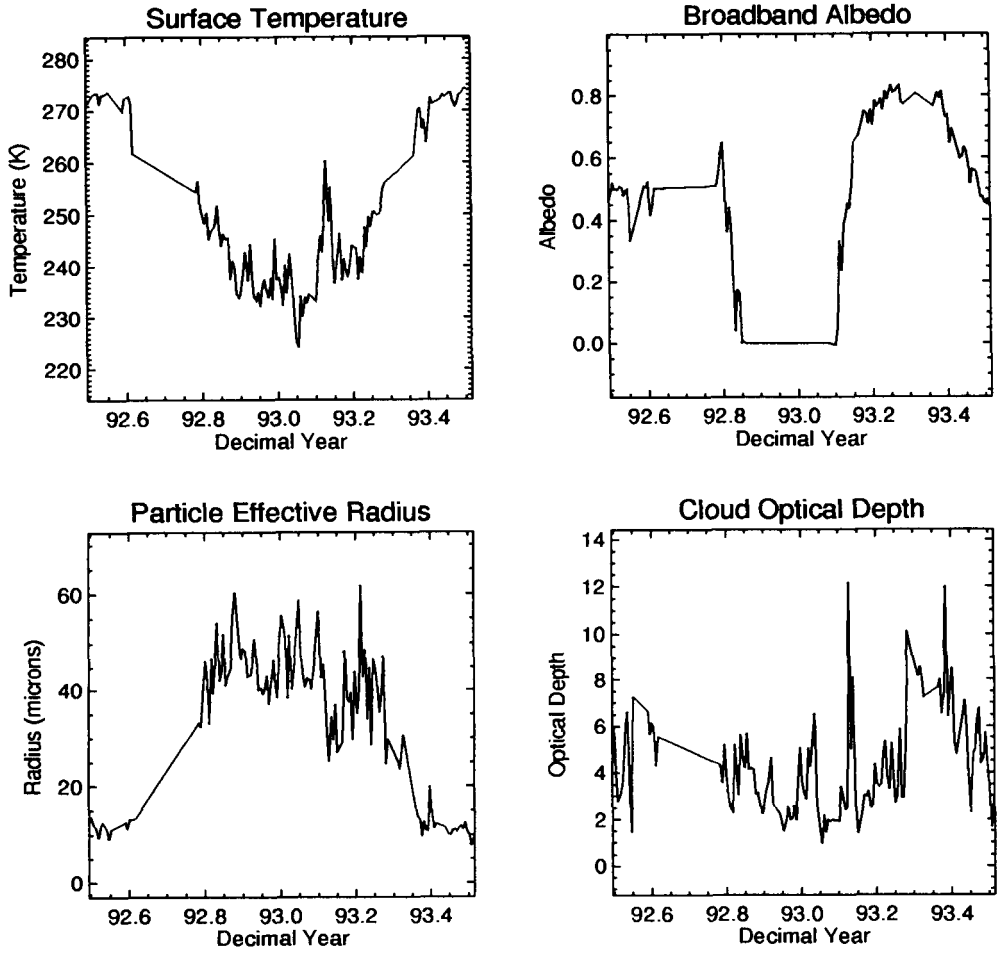

Fig. 3. Annual cycles of clear sky surface temperature, all sky broadband albedo, cloud particle effective radius and cloud optical depth derived from AVHRR data over the Beaufort Sea. Values are averages for $(1000\ \text{km})^2$ images.

4. Software Tools

Two software tools were used in this work and are available to the public. A radiation model, called *Streamer*, has built-in liquid and ice cloud optical properties, aerosols, standard profiles, and surface albedo models. It can compute irradiances or radiances using two or more streams, for 24 shortwave and 105 longwave spectral bands. It has a flexible user interface that provides looping capabilities and customizable output. The retrieval algorithms described above, including the estimation of surface properties and radiative fluxes, have been collected together in a toolkit called the Cloud and Surface Parameter Retrieval (*CASPR*) System for polar AVHRR data. The algorithms are integrated into a user-friendly, flexible environment that includes on-line help and a multitude of options for estimating geophysical parameters and visualizing the results. *Streamer* and a test version of *CASPR* are available via anonymous FTP. See the Web page at *http://stratus.bu.edu*.

5. REFERENCES

DeAbreu, R.A., J. Key, J.A. Maslanik, M.C. Serreze, and E.F. LeDrew. Comparison of in situ and AVHRR-derived surface broadband albedo over Arctic sea ice. *Arctic*, 47(3), 288-297, 1994.

Key, J., 1994. *Streamer*, version 2.0p: user's guide, Cooperative Institute for Research in Environmental Sciences, University of Colorado, Boulder, 68 pp. (unpublished).

Key, J., 1995a. The Cloud and Surface Parameter Retrieval (*CASPR*) System User's Guide, University of Colorado, 60 pp. (unpublished).

Key, J., 1995b. Retrieval of cloud optical depth and particle effective radius at high latitudes using visible and thermal satellite data. *Proceedings of the European Symposium on Satellite Remote Sensing II*, Paris, September 1995.

Key, J. and R.G. Barry, 1989. Cloud cover analysis with Arctic AVHRR, part 1: cloud detection. *J. Geophys. Res.*, 94 (D15), 18521-18535.

Key, J. and M. Haefliger, 1992. Arctic ice surface temperature retrieval from AVHRR thermal channels. *J. Geophys. Res.*, 97(D5), 5885-5893.

Key, J., R. Stone, and M. Rehder, 1994. Estimating high latitude radiative fluxes from satellite data: problems and successes. *IGARSS'94 Proceedings*, Vol. 2, 8-12 August, Pasadena, 1018-1020.

Key, J., J.A. Maslanik, T. Papakyriakou, M.C. Serreze, and A.J. Schweiger, 1994. On the validation of satellite-derived sea ice surface temperature. *Arctic*, 47(3), 280-287.

Key, J. and R.S. Stone, 1995. Accuracies of satellite-derived cloud and surface parameters in the polar regions and their effect on radiative flux estimates. *Proceedings of the Fourth Conference on Polar Meteorology and Oceanography*, Dallas, January 1995, 32-37.

Schweiger, A.J. and J. Key, 1994. Arctic Ocean radiation fluxes and cloud forcing based on the ISCCP C2 cloud data set, 1983-90. *J. Appl. Meteorol.*, 33(8), 948-963.

Potential MODIS Applications for Ice Surface Studies based on AVHRR Experience

Konrad Steffen
CIRES
University of Colorado
Campus Box 216
Boulder, CO 80309-0216

Ice Concentration

Tie Point Algorithm

The tie point algorithm assumes the presence of only two surface type classes: ice and ice free. This assumption is valid for sea ice areas during summer with air temperatures above the freezing point. Tie points are locations where a known state of surface type is assumed (i.e. 100 % white ice, 100% ice free). The ice concentration for any pixel location can be calculated as following:

$$Ic = (Dx-D1)/(Dh-D1) * 100$$

with Dx being the brightness values representing ice concentrations, D1 the brightness value for open water, and Dh the brightness value for white ice (including first-year and multi-year ice). The algorithm has sub-pixel resolution, as for an individual pixel, the associated grey-level value (digital number) between the two tie points (ice free and white ice) will be assigned an ice concentration value between 0 and 100%. However, the tie point algorithm is only applicable during the summer and early fall, when air temperatures are above the freezing point and no young and new ice types are present.

Threshold Algorithm

For most of the year, different ice types such as nilas, grey ice, grey-white ice, thin first-year ice, medium first-year ice, thick first-year ice, second-year ice, and multi-year ice are present in the ice pack. There is presently no satellite based algorithm that classifies all the above ice types (ice thickness classes). However, a classification based on the surface reflectance of solar radiation reveals the four different ice types: dark/light nilas, grey ice, grey-white ice, and white ice (including multi-year ice). This type classification was demonstrated in a supervised classification of Landsat thematic mapper data for the Beaufort Sea (Steffen and Heinrichs, 1994). The spatial resolution of the threshold algorithm is limited to the satellite pixel size (instantaneous field of view (IFOV)). Further, the method assumes that all the ice types have a spatial eaxtent of at least one pixel, as the mixed pixel of i.e., 20% ice free, 50% grey ice, 30% white ice will be mis-classified as grey-white ice. This error becomes crucial for large IFOV (i.e. AVHRR sensors); for the 250 m IFOV of MODIS the resultant classification error is probably

crucial in highly dynamic ice areas such as the marginal ice zone or polynyas (floe size <<250 m).

Planetary and Surface Albedo

Satellite derived albedo values are useful for estimating the short-wave radiation balance over large areas under clear sky conditions. Multispectral narrow-band radiometric scanners from satellites (i.e. MODIS) with small fields of view, need proper adjustments, so that their data can be used to estimate top-of-the-atmosphere albedo values (Steffen et al., 1993). The conversion of short-wave narrow-band data into average planetary albedo requires adjustment of the spectral expansion from filtered narrow-band to unfiltered broadband radiance of the short-wave spectrum (300-3000 nm). To derive surface albedo values from satellite narrow-band radiance measurements, the scattering and absorption of the atmosphere has to be included. If surface albedo values are required over snow and ice regions, atmospheric computations (i.e. LOWTRAN) are required to correct for scattering and absorption as demonstrated by Haefliger et al. (1993).

In the analysis of narrow angle nadir-recorded satellite imagery, such as Landsat thematic mapper (TM), it is usually assumed that radiance variations caused by small off-nadir angles are negligible. This may not hold true for large field of view (FOV) scanners such as MODIS (FOV +/- 55°), when pointing in directions with stronger reflectance gradients than in the nadir region. The assumption that snow reflection is isotropic and independent of wavelengths is not valid. While the reflectivity from freshly fallen snow is almost isotropic (negligible specular component for the reflectance zenith angles of MODIS), the specular component increases with the age of snow, and in particular, with the number of melting and refreezing processes.

References

Haefliger, M., K. Steffen and C. Fowler, AVHRR surface temperature and narrow-band albedo comparison with ground measurements for the Greenland ice sheet, *Ann. Glaciol., 17, 49-54, 1993.*

Steffen, K., W. Abdalati, and J. Stroeve, Climate sensitivity studies of the Greenland ice sheet using satellite AVHRR, SMMR, SSM/I, and in situ data, *Meteorol. Atmos. Phys., 51, 239-258, 1993.*

Steffen, K., and J. Heinrichs, Feasibility of sea ice typing with Synthetic Aperture Radar: merging of Landsat Thematic mapper and ERS-1 SAR satellite imagery, *J. Geophys. Res., 99(C11), 22,413-22,424, 1994.*

CLOUD MASKING AND SURFACE TEMPERATURE DISTRIBUTIONS IN THE POLAR REGIONS USING AVHRR AND OTHER SATELLITE DATA

Joey C. Comiso
Ocean and Ice Branch, Code 971, Laboratory for Hydrospheric Processes
NASA/Goddard Space Flight Center, Greenbelt, MD 20771
e-mail: comiso@joey.gsfc.nasa.gov; FAX: 301-286-1761; Tel: 301-286-9135

1. Introduction

Surface temperature is one of the key variables associated with weather and climate. Accurate measurements of surface air temperatures are routinely made in meteorological stations around the world. Also, satellite data have been used to produce synoptic global temperature distributions. However, not much attention has been paid on temperature distributions in the polar regions. In the polar regions, the number of stations is very sparse. Because of adverse weather conditions and general inaccessibility, surface field measurements are also limited. Furthermore, accurate retrievals from satellite data in the region have been difficult to make because of persistent cloudiness and ambiguities in the discrimination of clouds from snow or ice.

Surface temperature observations are required in the polar regions for air-sea-ice interaction studies, especially in the calculation of heat, salinity, and humidity fluxes. They are also useful in identifying areas of melt or meltponding within the sea ice pack and the ice sheets and in the calculation of emissivities of these surfaces. Moreover, the polar regions are unique in that they are the sites of temperature extremes, the location of which is difficult to identify without a global monitoring system. Furthermore, the regions may provide an early signal to a potential climate change because such signal is expected to be amplified in the region due to feedback effects (Budyko, 1966).

In cloud free areas, the thermal channels from infrared systems provide surface temperatures at relatively good accuracies. Previous capabilities include the use of the Temperature Humidity Infrared Radiometer (THIR) onboard the Nimbus-7 satellite which was launched in 1978. Current capabilities include the use of the Advance Very High Resolution Radiometer (AVHRR) aboard NOAA satellites. Together, these two systems cover a span of 16 years of thermal infrared data. Techniques for retrieving surface temperatures with these sensors in the polar regions have been developed (Key and Haefliger, 1992; Steffen et al., 1993; Comiso, 1994; Massom and Comiso, 1994). Errors have been estimated to range from 1K to 5K mainly due to cloud masking problems. With many additional channels available, it is expected that the EOS-Moderate Resolution Imaging Spectroradiometer (MODIS) will provide an improved characterization of clouds and a good discrimination of clouds from snow or ice surfaces.

2. Cloud Masking

Microwave systems have been used to monitor the polar regions primarily because of almost all weather capability. Unfortunately, they cannot be used for surface temperature measurements because the snow surface is transparent to microwave radiation. Thermal infrared systems may be the only way to obtain spatially and temporally coherent surface temperatures. Accurate retrievals, however, may not be possible until an effective cloud masking technique is developed.

The techniques that have so far been used for masking clouds in the polar regions are: (a) spectral thresholding; (b) statistical and clustering; (c)

textural; and (d) a combination of spectral, statistical and textural. The merit of each technique has been evaluated by Welch et al., (1992). The most popular option has been to use a combination of the first and the second because of ease in implementation. Textural techniques have been used for the difficult cases, but despite the introduction of sophisticated methods, (i.e., neural network, fuzzy logic, etc.), ability to masked out clouds consistently has not been achieved. Such techniques are also computationally very demanding.

This work utilizes primarily the first two techniques. The areas of emphasis are sea ice surfaces and continental ice sheets, but the technique is expected to be effective in the adjacent open water and land areas as well. Thresholding is usually done using the radiances of either channel 1 or channel 2, or the differences of the radiances between channels 3 and 4, and/or between channels 4 and 5. To gain insight into the effectiveness of this technique, a scatter plot of channel 1 radiances versus the differences between channels 3 and 4 is presented in Figure 1a while a scatter plot of the differences between channels 4 and 5 versus the differences between channels 3 and 4 is shown in Figure 1b. The data points are from an AVHRR image in the Central Arctic region (western side) on July 17, 1992. The plots show distinct clusters, labeled A, B, and C. The data points in cluster A are usually from sea ice covered regions, while those from cluster B are from ice free open water. The data points in cluster C and those distributed almost at random in non-cluster areas, represents cloud covered areas. Setting up a threshold (of say 10 and above) along the abscissa for (channel 3-4) would basically eliminate much of the cloud covered areas. Also, channel 1 (or channel 2) can be utilized to further remove cloud cover effects not removed by the channel 3-4 threshold. The channel 4-5 difference (see Figure 1b) can be similarly utilized to remove remaining cloud cover that has not been masked. The clusters A and B are distinct when channel 1 is utilized but are indistinguishable when the difference between channels 4 and 5 is used. With channel 1, the thresholds can thus be optimized separately for the ocean and ice surfaces.

In general, the utilization of a combination of channels as outlined above do not mask out all the clouds. Further masking is done by taking advantage of the fact that the cloud cover moves. By taking the difference between two orbits, further cleaning up of cloud covered areas is possible as was done in Comiso (1994). Additional procedure for open ocean areas was also utilized using co-registered SSM/I data. Weather effects are easily identified with the latter over the open ocean and was therefore used as additional mask when necessary.

Cloud masking is generally most effective for AVHRR data when done in a supervised manner. The thresholds must be set such that clear sky scenes are not inadvertently masked out for otherwise the data set will be full of gaps.

3. Polar Surface Temperatures

Historical orbital AVHRR data have been preserved in the GAC format but only a limited fraction is readily available in the full resolution LAC format. The resolution of the GAC data is about 4 km while that of the LAC data is about 1 km at nadir. For a global surface temperature data set, the difference in resolution is not critical in most scientific applications. However, it is important to know whether the LAC data provide significantly different results from the GAC data. Scatter plots similar to that of Figure 1 were generated for both GAC and LAC data and the results indicate very similar clusters for both of them. Also, it was found that there was no need to readjust the thresholds. The resulting surface temperatures were also found to be almost identical.

To minimize gaps due to the masking of persistent clouds, weekly surface temperatures are usually the final product. Cloud masking is done on an orbit to orbit basis. Only the data from the middle 351 are chosen from the 409 AVHRR measurements that goes from -55^{o} to +55^{o} from nadir. Daily maps are created from all available orbital data during the day. Difference maps between days are then created to further mask out clouds which were not successfully masked out previously. Surface temperatures are generated from each daily map using a regression technique similar to that used for open ocean (McClain et al., 1985).

Examples of AVHRR polar maps during winter in the northern and southern hemispheres are shown in Figure 2. The maps show details that are not available from climatological maps which are usually generated from sparsely spaced historical data. Figure 2a shows that on July 19-25, 1988, the coldest area in the southern hemisphere is located, as expected, in the Antarctic plateau, but not at the Vostoc station where the coldest temperature on earth was previously observed. The coldest temperature in the northern hemisphere on January 17-23, 1988 is seen to have occured in the Greenland ice sheet. However, as shown by Comiso (1994), the coldest area could be over the Central Arctic or the Siberian region during other times of the year.

4. Summary

Thermal infrared satellite data could provide a useful climate data set of surface temperatures in the polar regions. Current capability provides data at average uncertainties between 1 to 5 K. However, the precision provided by the satellite sensor is much better (i.e., < 1K). The main cause of uncertainty is the inability of mask out clouds effectively because of ambiguities in the discrimination of clouds from snow or ice. Masking techniques have been developed and can only improve with time as more sophisticated methods becomes more mature. Also, the new AVHRR systems are expected to carry a 1.6 micron channel which can better discriminate clouds from snow and ice than the 3.7 micron (channel 3). With systems, like MODIS, the potential for effective cloud removal and for better discrimination of different types of clouds would even be greater.

5. References

Budyko, M.I., Polar ice and climate, In Proceedings of the Symposium of the Arctic Heat Budget and Atmospheric Circulation, ed. by J.O. Fletcher (ed), RM 5233-NSF, Rand Corporation, Santa Monica, CA, 3-21, 1966.

Comiso, J.C., Surface Temperatures in the Polar Regions using Nimbus-7 THIR, J. Geophys. Res.,99(C3), 5181-5200, 1994.

Key, J., and M. Haefliger, Arctic ice surface temperature retrieval from AVHRR Thermal Channels, J. Geophys. Res., 97(D5), 5885-5893, 1992.

Massom, R. and J.C. Comiso, Sea ice classification and surface temperature determination using Advanced Very High Resolution Radiometer Satellite Data, J. Geophys. Res.,99(C3), 5201-5218, 1994.

McClain, E.P., W.G. Pichel, and C.C. Walton, Comparative performance of AVHRR-based multichannel sea-surface temperature, J. Geophys., Res., 90(6), 11,587-11,601, 1985.

Steffen, K., R. Bindschadler, C. Casassa, J. Comiso, D. Eppler, F. Fetterer, J. Hawkins, J. Key, D. Rothrock, R. Thomas, R. Weaver, and R. Welch, Snow and ice applications of AVHRR in Polar Regions, Annals of Glaciology, 17, 1-16, 1993.

Welch, R.M., S.K. Sengupta, A.K. Goroch, P. Rabindra, N. Rangaraj, and M.S. Navar, Polar cloud and surface slassification using AVHRR imagery: An intercomparison of methods, J. Applied Met., 30, 405-420, 1992.

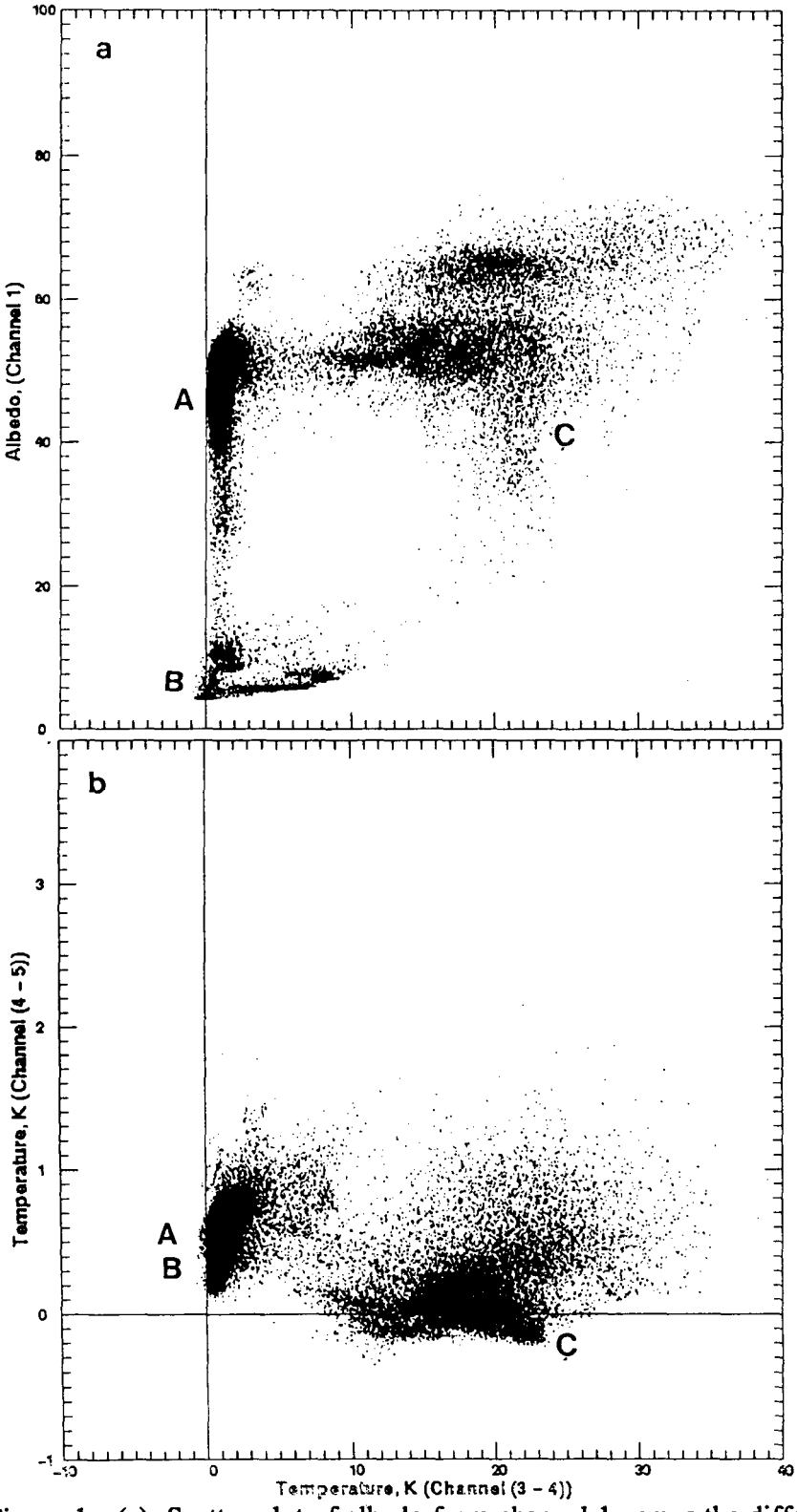

Figure 1. (a) Scatter plot of albedo from channel 1 versus the differences of the temperatures from channel 3 and 4 for data in the western Arctic region on July 17, 1992; (b) Scatter plot of the differences of the temperatures from channels 4 and 5 versus those from channels 3 and 4 for the same area and day.

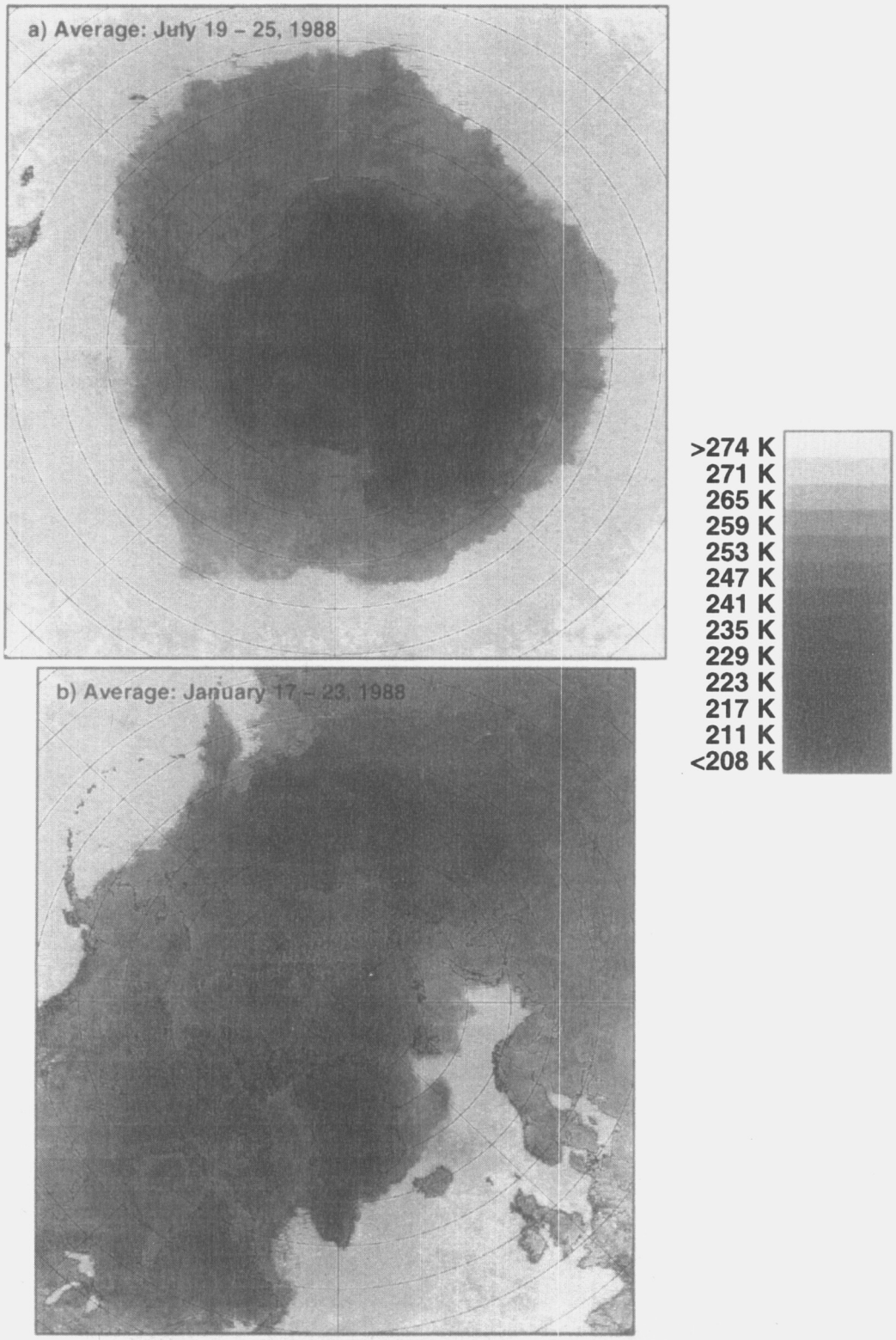

Figure 2. Surface ice temperatures retrieved from AVHRR GAC data in (a) the Southern Hemisphere on July 19 to 25, 1988; and (b) the Northern Hemisphere on January 17-23, 1988.

Satellite Mapping of Great Lakes Ice Cover

George A. Leshkevich

NOAA/Great Lakes Environmental Research Laboratory
Ann Arbor, Michigan 48105 USA

Much of the satellite ice interpretation algorithm development in the Great Lakes region began during the Extension to the Navigation Season Demonstration Study conducted during the 1970's. However, many of the early studies were done by visual interpretation of satellite and other remotely sensed data. Starting in the mid-1970's, a series of studies including field studies and computer digital image processing, explored techniques and algorithms to classify and map freshwater ice cover using Landsat, NOAA/AVHRR, and ERS-1 SAR data. The goal of much of this work is to develop an automated or semi-automated method to classify and map Great Lakes ice cover using satellite digital imagery.

Introduction

In his recommendations for Great Lakes ice research, Marshall (1966) concludes that "studies are needed to classify Great Lakes ice types, their distribution and drift during the winter, and the subtle changes in albedo and imagery which mark the gradual disintegration of the ice and the imminent breakup." Early investigations by various researchers were conducted to classify and categorize ice types and features (Chase,1972; Bryan, 1975), to map ice distribution (McMillan and Forsyth, 1976; Leshkevich, 1976), and to monitor and attempt to forecast ice movement with remotely sensed data (Strong, 1973; McGinnis and Schneider, 1978; Rumer et al.,1979; Schneider et al., 1981). Most of the early research on Great Lakes ice cover was done by visual interpretation of satellite and other remotely sensed data (Rondy, 1971; Schertler et al., 1975; Wartha, 1977). Because of the size and extent of the Great Lakes and the variety of ice types found there, the timely and objective qualities inherent in computer processing of satellite data make it well suited for such studies.

Northern Green Bay

Northern Green Bay ice cover on February 13, 1975 was analyzed from Landsat-1 digital data using computer image processing techniques. The purpose of this study was to investigate whether Landsat digital data can be used for objective classification of various types of Great Lakes ice cover. The major objectives were to determine if new ice (thin ice) could be differentiated from water, if ice could be differentiated from cloud cover, and if various ice types could be classified using a maximum-likelihood procedure. Secondary objectives included determining the percent coverage of each ice type and calculating the total percentage of water surface covered by ice.

Training sets, consisting of selected areas in the Landsat scene that represented various ice types, were entered based on the tone, texture, and location of the ice within the bay. The classification algorithm used in the analysis consisted of a modified maximum likelihood procedure using the multivariate Gaussian probability density function. It was found that seven

ice types could be differentiated in the ice cover, that new (thin) ice could be distinguished from water, and that ice could be distinguished from relatively thin cloud cover (Leshkevich, 1981). However, could this analysis be duplicated in another scene, and could it be automated?

Ice Albedos as Training Sets

In a second study, the purpose was to determine whether previously gathered reflectance values for various types of freshwater ice could be converted to digital numbers and used as training sets to classify Great Lakes ice cover using Landsat digital data. A method was developed and used to convert ground-measured freshwater ice albedos to Landsat-1 digital numbers indirectly corrected for atmospheric attenuation and path radiance. The method was tested by using the digital numbers as training sets to machine classify Landsat-1 digital ice cover data from a portion of the northern Green Bay scene imaged on Febuary 13, 1975. Results showed that the conversion algorithm produced digital numbers numbers that, when used as training sets, classified approximately 50% of the test area. The results of the classification are a verification of the algorithm and not an absolute classification of ice types in the test area. Differences between the classified test area and a previous machine classification of the Green Bay scene, as well as the percentage of unclassified area caused by lack of data for some surface types, pointed to the need for a more comprehensive, well-documented library of signatures representing Great Lakes ice types (Leshkevich, 1985a).

Airborne Measurements

In an attempt to compile such a library, field measurements of the spectral reflectance of major Great Lakes ice types were made in March, 1984 and again in March, 1985. The instrumentation and measurement technique used were basically the same in both years. Measurements made on March 26 and 27, 1984 were over large areas of surface types on southern Lake Huron including open water, refrozen slush ice, densely consolidated brash, large floes in a black ice matrix, and skim ice, and are described by Leshkevich and Reid (1984). Additional measurements were made on March 20, 1985 on Saginaw Bay (Lake Huron) over open water, old snow, and windrowed, snow-covered ice. The purpose of this study was to obtain airborne measurements (from an altitude of 300 m) of major freshwater ice types and combinations in the 400-1100 nm range for use in satellite interpretation and lakewide ice albedo estimates. The objective was to measure the spectral reflectance of relatively large homogeneous and heterogeneous areas of various freshwater ice types under clear skies.

A programmable band spectral radiometer was used to acquire data. The instrument and cassette data logger were powered by a 12 VDC battery, which allowed for the needed mobility. Using a three sector chopper wheel and a detector array, the instrument was capable of measuring radiance, irradiance, and dark current in about 3 seconds, which made measurement from a helicopter possible. Three measurements were made over each surface type and averaged. Simultaneous radiance and irradiance measurements were also made at the surface over a spray-painted barium sulfate reference panel and over snow and water. After determining the spectral reflectance of the snow and water, an algorithm was applied to calculate the spectral reflectance of the ice types measured from 300 m, corrected for atmospheric attenuation and path radiance (Leshkevich, 1985b).

However, Kimes and Kirchner (1982) and others noted that the assumption of a Lambertian reference panel was not necessarily valid. The non-Lambertian behavior of a reference panel can cause considerable error when its radiance data is used in the calculation of reflectance factors or in the characterization of irradiance conditions. Goniometric measurements of the spray-painted barium sulfate reference panel were made to determine its Lambertian characteristics in the visible and near-infrared (400-1100 nm) range for zenith angles from 0 to 80 degrees. Errors in Lambertian response varied with zenith angle and wavelength and ranged from 0 to 52% in the visible and .03 to 30% in the near-infrared (Leshkevich, 1988a). A technique to correct calculated reflectance factors of field targets collected under clear sky conditions for the non-Lambertian response of the spray-painted barium sulfate reference panel was used to correct the airborne reflectance measurements made over Saginaw Bay (Leshkevich, 1988b).

Bi-directional Reflectance

Although the NOAA series of satellites with high temporal and broad spacial coverage are well suited for Great Lakes ice monitoring , the large scan angles inherent in AVHRR data may hinder interpretation based on nadir-looking measurements. Ott et al. (1984) demonstrated the value of angular (directional) reflectance data or "angular signatures" in the interpretation of aircraft and satellite sensor data. To improve the interpretation of surface cryospheric albedo from satellite sensor data, diurnal measurements of the spectral bi-directional reflectance of a commonly-found fresh-water ice type were made, from which hemispherical reflectance can also be derived. The purpose of this study was to document its clear-sky, bi-directional reflectance characteristics in the visible (650-670 nm) and near-infrared (810-840 nm) region, assess the diurnal nature of the reflectance, and quantify the surface anisotropy. Bi-directional reflectances of the re-frozen slush ice (white ice) measured show a spectral dependence and changed significantly with solar zenith angle. Considerable variation occured at each view angle and among view angles throughout the day. Although diurnal reflectance patterns were similar in both bands, magnitudes varied greatly, being highest in the visible and lowest in the near-infrared region. With the exception of peak saturated (specular) values in the forward scatter direction, bi-directional reflectance was generally highest in the morning when the surface and the illumination were most diffuse in character (Leshkevich et al., 1990).

A database containing such measurements, acquired for different ice and snow surface types, could improve interpretation of these different surface types using satellite sensor data and improve the estimation of hemispheric reflectance from satellite observations of the Earth-atmosphere system (Kimes et al., 1987), a parameter needed for climate and radiation budget models for the shortwave spectrum.

GLERL Contribution No. 981

References

Bryan, M.L. (1975), A comparison of ERTS-1 and SLAR data for the study of surface water resources, Final Report, ERIM No. 193300-59-F, prepared for the National Aeronautics and Space Administration by the Environmental Research Institute of Michigan, Ann Arbor, MI under Contract No. NAS5-21783, 104 pp.

Chase, P.E. (1972), Guide to ice interpretation: Satellite imagery and drift ice, Final Report prepared for the U.S. Department of Commerce by The Bendix Corp, Aerospace Systems Division, Ann Arbor, MI, under Contract No. 2-35372, 24 pp.

Kimes, D.S., and Kirchner, J.A. (1982), Irradiance measurement errors due to the assumption of a Lambertian reference panel, *Remote Sens. Environ.,* 12:141-149.

Kimes, D.S., Sellers, P.J., and Diner, D.J. (1987), Extraction of spectral hemispherical reflectance (albedo) of surfaces from nadir and directional reflectance data, *Int. J. Remote Sensing,* 8(12), 1727-1746.

Leshkevich, G.A. (1976), Great Lakes ice cover, winter 1974-75, NOAA Technical Report ERL 370-GLERL 11, National Technical Information Service, Springfield, VA 22161, 42 pp.

Leshkevich, G.A. (1981), Categorization of northern Green Bay ice cover using Landsat-1 digital data--a case study, NOAA Technical Memorandum ERL GLERL-33, National Technical Information Service, Springfield, VA 22161, 19 pp.

Leshkevich, G.A. and Reid, N.J. (1984), Airborne measurements of freshwater ice albedos, Proceedings of the Eighteenth International Symposium on Remote Sensing of Environment, Environmental Research Institute of Michigan , Ann Arbor, MI, pp.1677-1687.

Leshkevich, G.A. (1985a), Machine classification of freshwater ice types from Landsat-1 digital data using ice albedos as training sets, *Remote Sens. Environ.,* 17(3), 251-263.

Leshkevich, G.A. (1985b), Airborne measurements of the spectral reflectance of freshwater ice, Proceedings of the Third International Colloquium on Spectral Signatures of Objects in Remote Sensing, ESA SP-247, pp. 245-248.

Leshkevich, G.A. (1988a), Goniometric measurements of a spray-painted barium sulfate reference panel, *Remote Sens. Environ.,* 24:287-296.

Leshkevich, G.A. (1988b), Non-Lambertian reference panel effect on spectral reflectance measurements of freshwater ice, *Int. J. Remote Sensing,* 9(4), 825-832.

Leshkevich, G.A., Deering, D.W., Eck, T.F., and Ahmad, S.P. (1990), Diurnal patterns of the bi-directional reflectance of fresh-water ice, *Annals of Glaciology* 14:153-157.

Marshall, E.W. (1966), Air photo interpretation of Great Lakes ice features, Great Lakes Research Division, Special Report No. 25, University of Michigan, Ann Arbor, MI, p. 89.

McMillan, M.C., and Forsyth, D.G. (1976), Satellite images of Lake Erie ice, January-March 1975, NOAA Technical Memorandum NESS-80, National Technical Information Service, Springfield, VA 22161, 15 pp.

McGinnis, D.F., and Schneider, S.R. (1978), Monitoring river ice breakup from space, *Photogramm. Eng. Remote Sens.* 44(1):57-68.

Ott, W., Pfeiffer, B., and Quiel, F. (1984), Directional reflectance properties determined by analysis of airborne multispectral scanner data and atmospheric correction, *Remote Sensing Environ.,* 16(1), 47-54.

Rondy, D.R. (1971), Great Lakes ice atlas, NOAA Technical Memorandum NOS LSCR 1, National Technical Information Service, Springfield, VA, 22161, 48 pp.

Rumer, R.R., Crissman, R., and Wake, A. (1979), Ice transport in Great Lakes, Water Resources and Environmental Engineering Research Report No. 79-3 prepared for the Great Lakes Environmental Research Laboratory by the State University of New York at Buffalo, Department of Civil Engineering, and the Center for Cold Regions Engineering, Science and Technology, under Contract No. 03-78-B01-104, 275 pp.

Schertler, R.J., Mueller, R.A., Jirberg, R.J., Cooper, D.W., Heighway, J.E., Homes, A.D., Gedney, R.T., and Mark, H. (1975), Great Lakes all-weather ice information system, NASA Technical Memorandum NASA TM X-71815, National Technical Information Service, Springfield, VA, 22161, 13 pp. and 16 pp. of figures.

Schneider, S.R., McGinnis, D.F., Jr., and Gatlin, J.A. (1981), Use of NOAA/AVHRR visible and near-infrared data for land remote sensing, NOAA Technical Report NESS-84, National Technical Information Service, Springfield, VA 22161, 48 pp.

Strong, A.E. (1973), New sensor on NOAA-2 satellite monitors during the 1972-73 Great Lakes ice season, Remote Sensing and Water Resources Management, Proceedings No. 17, American Water Resources Association, Urbana, IL, pp. 171-178.

Wartha, J.H. (1977), Lake Erie ice--winter 1975-76, NOAA Technical Memorandum NESS-90, National Technical Information Service, Springfield, VA, 22161, 68 pp.

An Introduction to the Cloud Mask for the MODIS

S. A. Ackerman, K. I. Strabala, R. A. Frey, C. C. Moeller and W. P. Menzel*

Cooperative Institute for Meteorological Satellite Studies, University of Wisconsin - Madison
*NOAA/NESDIS/ASPP

1. INTRODUCTION

The 36 channel MODerate resolution Imaging Spectrometer (MODIS) (King et al. 1992) on the Earth Observing System (EOS) AM-1 platform is scheduled for launch in 1998. In preparation for a MODIS day-1 cloud mask product, data from the AVHRR, HIRS/2 and MODIS Airborne Simulator (MAS) (King et al., 1995) are being used to develop a multispectral cloud mask algorithm. MAS flies on board NASA's high altitude ER-2 aircraft collecting 50 meter resolution data across a 37 km swath. The multispectral nature of MAS (and later MODIS) enhances cloud detection capability, especially for highly variant surface, atmospheric, and cloud characteristics present on the global scale. A three month global data set of collocated AVHRR and HIRS/2 observations is also being used to develop the algorithm. This collocated data set has the advantage of containing many IR observations that are similar to the planned MODIS channels. AVHRR LAC scenes are also being used to familiarize the algorithm with handling a large 1 km spatial resolution data set.

2. Inputs and Outputs

Input to the cloud mask algorithms is assumed to be calibrated and navigated level 1B radiance data in channels 1, 2, 3, 5, 6, 16, 18, 22, 26, 27, 29, 31, 32, and 35 (incomplete or bad radiometric data will create holes in the cloud mask). Additionally several ancillary data inputs are required for the cloud mask; they are:

- sun angle, azimuthal angle, and viewing angle
- land/water map at 1 km resolution
- topography
- ecosystems
  - 1 km map of ecosystems desired
- snow/ice from yesterday known at 1 km resolution
- surface temperatures (sea and land) and wind speed (sea) at best available resolution
  - Surface observations, NMC analysis or yesterdays MODIS observations
- yesterdays 1 km cloud mask from MODIS
  - ascending orbit distinguished from descending orbit
- clear sky radiance composite from last month
  - VIS ch 2 at 1 km resolution, IR ch 22 and ch 31 at 5 km

The output of the MODIS cloud mask algorithm will be a 32 bit word for each field of view. The bit structure is listed in the following table. Confidence flags (bits 2 and 3) convey strength of conviction in the outcome of the cloud mask algorithm tests for a given FOV. For example, as one approaches a threshold limit of spectral tests, the certainty or confidence in the outcome is reduced. Therefore, an individual test confidence flag, based upon proximity to the threshold value, is assigned and used to work towards a final quality flag determination for the FOV outcome. The initial FOV obstruction determination is then the product of the confidences of all applied tests. This determination will dictate whether additional testing (using spatial variability tests) is warranted to improve the confidence. The final quality flag determination will be clear or cloudy with a confidence level associated with it. This approach is being considered as a method of quantifying our confidence in the derived cloud mask for a given pixel. For MODIS application, spatial and temporal consistency tests will be invoked as a final check. Temporal consistency compares composited previous 30 day clear sky radiances and yesterday's cloud mask to today's clear sky single pixel results. Spatial consistency checks neighboring clear sky pixel radiances (same ecosystem). If any consistency test fails, the confidence in the final cloud/no cloud determination is reduced by 1 sigma level.

The MODIS cloud mask will indicate whether a given field of view (FOV) of the earth surface is unobstructed by clouds and additionally whether that clear view is affected by cloud shadows. A battery of spectral tests, which use methodology applied for APOLLO (Sanders and Kriebel 1988), ISCCP (Rossow 1993), CLAVR (Stowe et al. 1991),

decision	1	1 mask determined, 0 no decision
summary of all algorithms	2	unobstructed FOV (quality flag) 11 > 99% prob of clear 10 > 95% prob of clear 01 > 66% prob of clear 00 cloud
ancillary information	1	visible data (1 if usable, 0 if not)
	1	snow/ice (1 no, 0 yes)
	2	land/water (11 land, 10 wetland, 01 coastal, 00 water)
results from cloud algorithms	1	IR threshold did not find cloud,
	1	IR temp diff. did not find cloud
	1	CO2 high cloud test did not find high cloud
	1	near IR test did not find thin cirrus
	1	SWIR threshold did not find cloud
	1	VIS ratio did not find cloud
	1	cloud shadow was not found
additional tests if not sure (prob less than 95%)	1	passed temporal consistency test
	1	passed spatial continuity test
250 m mask from visible tests	16	1 clear, 0 cloudy for 16 FOVs in 1 km FOV

and SERCAA (Gustafson et al. 1994), are employed to identify cloudy FOVs. From these a clear sky confidence level (>99%, >95%, >66%, or < 1%) is assigned to each FOV. For inconclusive results, spatial and temporal variability tests are applied. The spectral tests rely on radiance (temperature) thresholds in the infrared and reflectance thresholds in the visible. These thresholds vary with surface type, atmospheric conditions (moisture, aerosol, etc.) and viewing geometry. A necessary part of the algorithm development will be to characterize the individual spectral test thresholds as a function of these dependencies. The MAS spectral tests are described as follows.

3.1 INFRARED (IR) TESTS

The 11 micron brightness temperature (BT_{11}) test indicates cloud when BT_{11} is less than the threshold (e.g., 270 K for ocean).

The $BT_{8.6}$-BT_{11} and BT_{11}-BT_{12} differences are used in complement to detect cloud. This tri-spectral test utilizes spectral variation of ice and water absorption coefficients for the 3 channels. Sensitivity to water cloud is greatest in the BT_{11}-BT_{12} quantity; $BT_{8.6}$-BT_{11} is sensitive to ice cloud. Cloud is indicated when BT_{11}-BT_{12} is less than a threshold and $BT_{8.6}$-BT_{11} exceeds a threshold. Thresholds for this test are a function of atmospheric moisture.

$BT_{3.9}$-BT_{11} indicates cloud under several conditions. For example, a large difference indicates a partial cloud or thin cloud. A negative difference is indicative of a thick cloud scene (lower cloud emissivity at 3.9 microns).

MODIS channel 35 (MAS channel 49, 13.9 micron) provides good sensitivity to the relatively cold regions of the atmosphere; negligible contributions come from the earth surface. Thus a threshold test for cloud versus ambient

atmosphere should reveal high clouds. Global histogram analysis from the Collocated HIRS/2 and AVHRR Products (CHAPS) processing indicates use of a threshold of 245 K for the HIRS 14 micron channel.

3.2 VISIBLE/NEAR INFRARED TESTS

A new approach to cirrus detection suggested by the work of Gao et al. (1993) utilizes the 1.38 micron channel to detect the presence of thin cirrus cloud in the upper troposphere under daytime viewing conditions. The strength of this cloud detection channel lies in the strong water vapor absorption in the 1.38 micron region. Reflectance from the ground is masked whereas high clouds are unobscurred in the channel and appear bright; while low and mid level clouds are partially attenuated. The MAS 1.88 micron channel, which has similar spectral characteristics, is used to investigate the capabilities of the MODIS 1.38 channel.

The visible reflectance threshold test uses low .67 micron channel reflectances to indicate clear skies in sun glint free daytime regimes.

The reflectance ratio test uses the .87 micron divided by the .67 micron channel. AVHRR data has indicated this ratio to be between 0.9 and 1.1 in cloudy regions and some desert regions.

4. IMPLEMENTATION OF THE CLOUD MASK ALGORITHM FOR DAYLIGHT OCEANIC AREAS

As an example of processing for the cloud mask, the procedure for evaluating daylight, ocean background conditions is shown and applied to a MAS data set. The hierarchical approach used in the MAS version of the cloud mask, which is similar to that proposed for MODIS, has the following stages:

(A) Note pixels that have sun glint (possible effect on visible tests).

(B) Note pixels that have high (> 85°) solar zenith angle (possible effect on visible tests).

(C) Apply single FOV spectral tests (section 2), and assign a confidence level to each result:

(D) Multiply individual test confidences together to get a FOV clear confidence value, and initial quality flag

(E) For uncertain pixels (FOV confidence less than 2 sigma), spatial variability tests are performed in 3 x 3 pixel regions.

Reset quality flag if successful in increasing confidence levels.

The daytime ocean cloud mask algorithm was applied to January 1995 MAS data, with results depicted in Figures 1 and 2. Figure 1 is an example of a relatively clear scene; Figure 2 is a generally overcast scene containing a wide variety of cloud types.

Thin cirrus is present in the top portion of Figure 1, with small popcorn cumulus dotting the bottom portion. These clouds are evident in the .67 and 11 micron imagery. The final panel is the result returned by the daytime ocean MAS cloud mask algorithm. The four shades in the image (black to white) represent the four clear confidence intervals (99%, 95%, 66% and 1%). The image is dominated by >99% clear confidence; both cloud types are detected almost completely, appearing primarily as <1% clear confidence. Very thin edges of the cirrus cloud show >66% clear confidence. The lower confidence clear regions along both edges of the cloud mask image result from longer atmospheric path lengths, which increase the Mie and Rayleigh scattering components. This effect will be corrected through scan angle dependent thresholds.

A stratus cloud deck dominates the top portion of the Figure 2 Gulf of Mexico flight segment. Thin cirrus overlying the stratus deck thickens towards the bottom of the image (panels 1 and 2). Panels 3 through 7 depict individual test results. Note that each test excels at identifying different cloud types and combinations of clouds. For instance, the infrared brightness temperature difference tests (panel 4) detect the low stratus deck near the top of the image and the cold, thick cirrus near the bottom, whereas the 1.88 micron reflectance test (panel 7) picks up predominately high clouds. Panel 8 shows the cloud mask image, a combination of all the individual tests, and uses the same confidence coding as Figure 1. In this case only a few isolated FOVs fall into the >66% probability of clear; most FOVs show less than a 1% probability of clear.

5.0 SUMMARY

The MAS cloud mask algorithm applied to two drastically different cloud scenes, demonstrates the feasibility of the hierarchical approach proposed for MODIS. In addition to the MAS data, the algorithm is also being developed using AVHRR and collocated AVHRR and HIRS data.

6.0 REFERENCES

Coakley, J. A. and F. P. Bretherton, 1982: Cloud cover from high-resolution scanner data: Detecting and allowing for partially filled fields of view. J. Geophys. Res., 87, 4917-4932.

Gao, B.-C., A. F. H. Goetz, and W. J. Wiscombe, 1993: Cirrus cloud detection from airborne imaging spectrometer data using the 1.38 micron water vapor band. Geophys. Res. Letter, 20, no. 4, 301-304.

Frey, R. A, S. A. Ackerman and B. J. Soden, 1995: Climate parameters from satellite spectral measurements part I: collocated AVHRR and HIRS/2 observations of spectral greenhouse parameter. Accepted by J. Geophys. Res.

Gustafson, G. B., R. G. Isaacs, R. P. d'Entremont, J. M. Sparrow, T. M. Hamill, C. Grassotti, D. W. Johnson, C. P. Sarkisian, D. C. Peduzzi, B. T. Pearson, V. D. Jakabhazy, J. S. Belfiore and A. S. Lisa, 1994: Support of Environmental Requirements for Cloud Analysis and Archive (SERCAA): Algorithm descriptions. Phillips Labratory Scientific Report No. 2, Hanscom Air Force Base, MA, 100 pp.

King, M. D., Y. J. Kaufman, W. P. Menzel and D. Tanre, 1992: Remote sensing of cloud, aerosol, and water vapor properties from the Moderate Resolution Imaging Spectroradiometer (MODIS). IEEE Trans. Geosci. Remote Sensing, 30, 2-27.

Rossow, W. B. and L. C. Garder, 1993: Cloud detection using satellite measurements of infrared and visible radiances for ISCCP. J. Climate, 6, 2341-2369.

Saunders, R. W. and K. T. Kriebel, 1988: An improved method for detecitng clear sky and cloudy radiances for AVHRR data. Int. J. Remote Sensing, 9, 123-150.

Stowe, L. L., E. P. McClain, R. Carey, P. Pellegrino, G. Gutman, P. Davis, C. Long, and S. Hart, 1991: Global distribution of cloud cover derived from NOAA/AVHRR operational satellite data. Adv. Space Res., 11, 51-54.

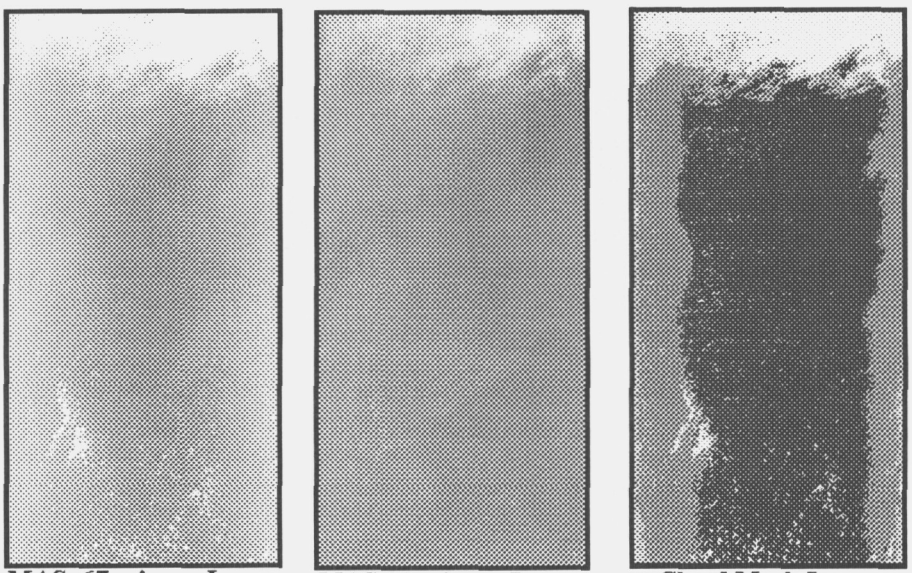

Figure 1. MAS visible (left panel), infrared (center panel) and cloud mask (right panel) image from the 13 January 1995 Gulf of Mexico ER-2 flight. Individual spectral threshold tests were combined to determine a clear sky confidence level. The resultant image represents the final clear confidence levels of >99% (black), >95% (dark gray), >66% (light gray) and <1% (white).

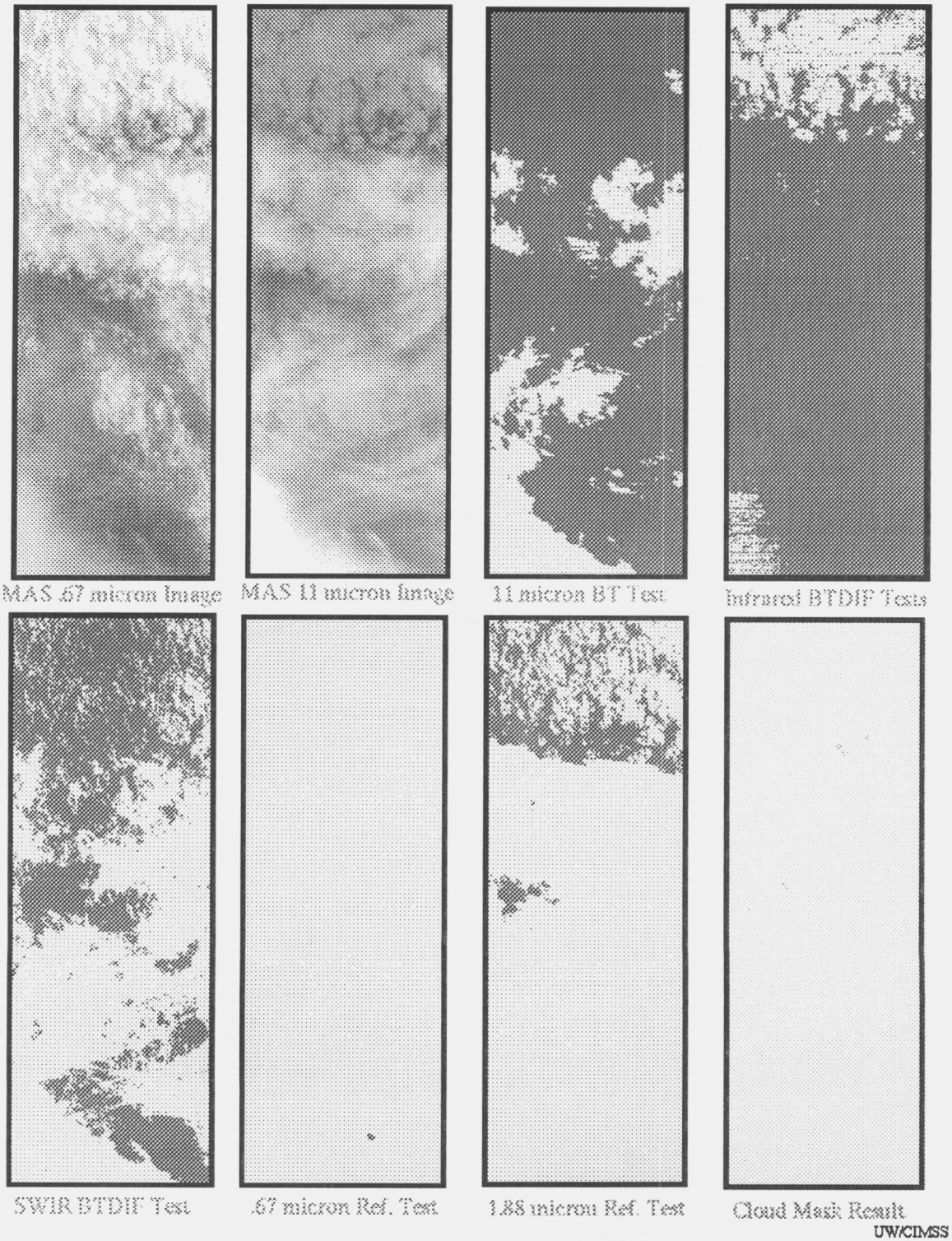

Figure 2. MAS visible image (top left, panel 1), infrared image (panel 2), threshold test results (panels 3-7, left to right, top to bottom), and cloud mask image (bottom right, panel 8) of a cloudy scene from the 6 January 1995 Gulf of Mexico ER-2 flight. The individual threshold tests result images are either light (test failed, low probability clear) or dark (test passed, high probability clear). They were combined to determine a clear sky confidence level. The cloud mask image represents the final clear confidence levels of >99% (black), >95% (dark gray), >66% (light gray) and <1% (white). In this case, the vast majority of the scene was coded as less than 1% probability of clear.

SESSION IV: MISCELLANEOUS TOPICS

SNOWSAT - OPERATIONAL SNOW MAPPING IN NORWAY

by Tom Andersen
STATKRAFT (Norwegian Energy Corporation)
P.O.Box 494
N-1322 HOVIK
Norway

Valuable snow data

Information on the amount of snow in drainage basins is very important to hydroelectric power companies in Norway, since all electricity generation in the country is based on water power and Norway has one of the world's most liberal laws for energy generation, trade and distribution. Relevant snow data is therefore classified as commercial (and non-public) data of high economic value.

A substantial part of the drainage basins is located in high mountain areas where more than 50% of the precipitation falls as snow. The amount and distribution of the snow is crucial information for planning of the power production. For several years Statkraft (the largest Norwegian hydroelectric power company) has performed analyses of images from the NOAA AVHRR sensors in order to determine the snow cover throughout the melting season. The results are used as input data to snow melting simulation models (e.g. the HBV model).

Difficult measurements

In the snow-accumulation period from November to April the snow water equivalent is measured at representative locations in all reservoir basins and the snow storage is calculated. However, in the snow-melting period such measurements cannot be carried out. In principle, this type of measurement problems could be solved using remote sensing which can provide frequent and low-cost data collection. Ideally, snow depth and density measurements should be taken over the whole drainage basin in the snow-melting period. This is not possible with state of the art operational remote sensing. The next best is to measure the snow-cover ratio: snow cover per unit area. This can be done by optical satellite sensors. The demand for frequent and low-cost data collection is not met by satellites such as SPOT or Landsat. The NOAA AVHRR fits the demands well, although the optimal spatial resolution would be in the range of 0.2-0.5 km.

Snow mapping by SNOWSAT

The data system for data acquisition and image processing, called SNOWSAT, has been under continous development since 1980 and was probably one of the first digital snow mapping system for operational use.

The data system is operated by a user-friendly interface that makes easy and fast operation of the complete system possible. The user interface is based on Motif X Windows under UNIX, and provides user interaction through menus and push buttons combined with display of image data and map products on the screen. Intelligent default values for user given parameters

combined, when practical, with options for automatic parameter estimation makes very efficient use possible.

The NOAA/AVHRR image data is acquired at the Tromso Satellite Station in Northern Norway. The relevant geographical part of the image data is extracted from band 2 (near infrared), and then geometrically corrected to UTM map projection. The resulting image is transmitted over a computer data network to Statkraft near Oslo. The SNOWSAT system is divided into two main parts: classification, and map generation. There are three types of map products that can be generated: Snow-cover, snow-cover by elevation, and seasonal snow-cover development. All the map products are derived from the classified image. The classification algorithm is based on an empirical reflectance-to-snow-cover model developed by Statkraft (Andersen 1982). All pixels are seen as partly snow covered from 0 to 100 per cent snow cover. The model is calibrated by providing two points on the reflectance function: maximum reflectance for 0% snow cover and lower reflectance for 100% snow cover. These values can be given either by the user, based on ground truth information, or by an automatic calibration procedure. The latter method uses a set of calibration areas of stable and known reflectance to relate image pixel values to the real reflectance values.

Satellite derived snow maps

The maps generated are a combination of information derived from the classified image and digital map information. The snow-cover map product shows snow coverage in colour codes, the drainage basin borders and a table of coverage for each drainage basin. The snow-cover-by-elevation map shows snow cover as a function of elevation. To make it easy to perceive the map information, only two categories of snow coverage are shown (below and above 50%). The elevation data is derived from an elevation model with same map projection and resolution as the AVHRR image. The seasonal snow-cover map shows how the snow cover has changed through the melting season, from late April to August. The map product is based on all or most of the classified AVHRR images that season. The map shows how the 50% snow-cover border moves through the season.

New developments

A continuous problem with optical satellite sensor monitoring is the requirement for a clear sky. At Norwegian latitudes there can be weeks between completely cloud-free days. However, the regions of interest are often only partly cloudy, so at least parts of the image data could be used. To provide more continuous monitoring, a system that can make use of partly clouded images are under development. The development has to be focused on two subjects: cloud detection, and combination of image information from a time series of image data. The idea is to detect and remove the cloudy parts, and then combine the remaining areas to give complete maps for a certain period. To be able to show the snow-cover situation for a given date, the data must be combined with a snow melting model to estimate snow cover in areas not covered at the time of interest. As a first step a cloud classification model is implemented in the system based on a tresholding technique using four AVHRR channels.

Another problem is reflectance variations due to the combined effect of solar angle and terrain slope. For most basins in the high mountain plateau of Southern Norway this is found to be a minor problem. But in some areas with very rough terrain, this effect can be considerable. We Plans are therefore made to use an illumination model combined with a terrain model for correction of this effect.

Multisensor Analysis of Satellite Images for Regional Snow Distribution

Klaus Seidel, Cornel Ehrler and Jaroslav Martinec
Image Science Division - Communication Technology Laboratory ETHZ
Gloriastr. 35, CH 8092 Zürich/Switzerland
T: +41-1-632 5284 - F: +41-1-632 1251
Email: seidel@vision.ee.ethz.ch

ABSTRACT -- The method is presented to evaluate areal average water equivalents of the seasonal snow cover by periodical snow cover mappings from multispectral satellite recordings. As a refinement of earlier preliminary results, an extra-polation procedure is applied using GIS techniques in order to analyse image segments obscured by clouds or by forest canopy. In the Upper Rhine basin at Felsberg (3250 km^2, 560-3614 m a.s.l.), the snow water equivalent on 1 April in four different years was evaluated for 5 elevation zones in 9 partial areas. Conventional depletion curves of snow covered areas were derived from SPOT-XS, Landsat-MSS and Landsat-TM data and converted to the so called modified depletion curves which indicate the snow water equivalent. A comparison with terrestrial measurements is limited by the insufficient snow gauging network above 2000 m a.s.l. Areal water equivalents interpolated for 2000 m a.s.l. indicate that the snow accumulation is persistently greater in the weastern part of the Felsberg basin than in the eastern part. In the middle part, the North-South relation of the snow accumulation changed from year to year.

1. INTRODUCTION

Each winter, snow accumulates in mountain areas and stores water which is subsequently used for power generation, irrigation and municipal supply.

The regional distribution of snow in Alpine basins can hardly be assessed from conventional snow gauging networks, in particular in elevations above 2000 m a.s.l. The need for these evaluations has been recognized for a long time, for example in connection

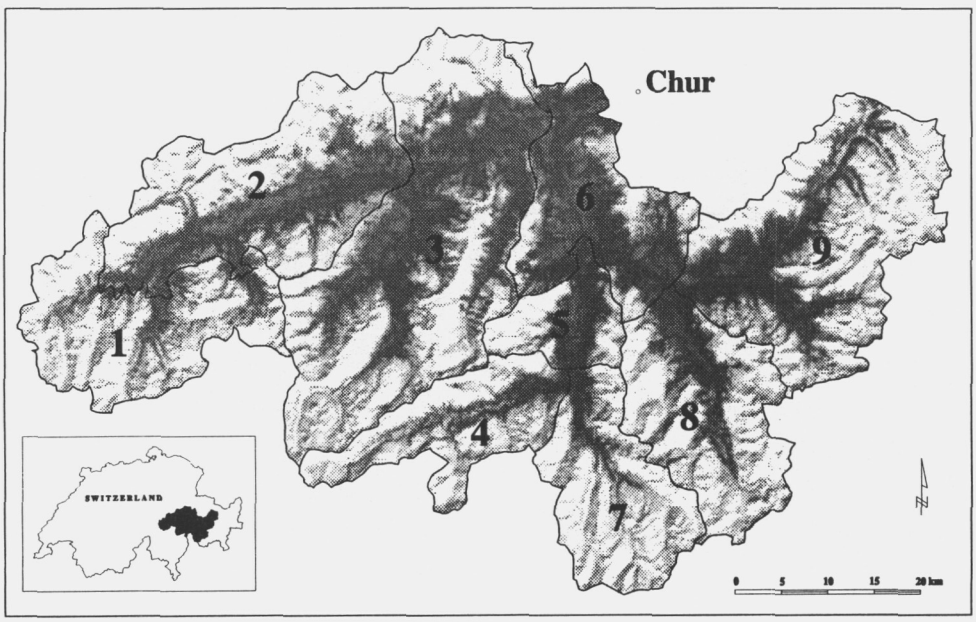

Fig. 1: Snow cover map on 29-APR-1994 as viewed by SPOT-XS and division of Rhein-Felsberg basin (3250 km^2, 560-3614 m a.s.l.) into 9 regions

TABLE 1. Areal water equivalents (Hw in cm) for 9 regions and 5 elevation zones of the basin Rhine/Felsberg on 1 April of the years 1982, 1985, 1993, 1994

Region	Zone A	Zone B	Zone C	Zone D	Zone E
(1) Tavanasa + Sedrun					
HW 1982	-	38.3	57.7	99.8	137.2
HW 1985	-	29.5	40.8	93.0	127.6
HW 1993	-	10.3	38.0	69.5	97.3
HW 1994	-	3.4	30.0	71.8	128.5
(2) Cadi, Surselva					
HW 1982	18.5	27.7	60.5	139.3	176.5
HW 1985	11.6	33.8	36.7	100.9	138.2
HW 1993	0.9	5.2	27.1	75.7	98.1
HW 1994	0	1.9	25.3	79.6	122.5
(3) Lugnez/Vals/ Safien					
HW 1982	16.1	25.3	43.9	82.6	82.8
HW 1985	20.1	30.4	32.4	63.5	70.3
HW 1993	0.7	4.8	28.8	52.1	62.5
HW 1994	0	1.4	16.9	56.4	71.4
(4) Rheinwald					
HW 1982	-	25.0	48.1	91.3	127.9
HW 1985	-	26.3	52.8	112.5	133.3
HW 1993	-	5.1	32.3	67.5	96.0
HW 1994	-	3.2	25.6	80.7	133.8
(5) Schams					
HW 1982	14.2	16.8	46.0	77.7	71.0
HW 1985	18.2	18.8	34.3	72.1	100.9
HW 1993	0	3.3	30.2	55.5	68.1
HW 1994	0	0.1	19.5	51.0	73.8
(6) Domleschg					
HW 1982	2.5	19.3	41.8	84.0	95.6
HW 1985	3.0	25.5	29.8	56.4	61.0
HW 1993	0.6	6.1	38.4	51.0	58.9
HW 1994	0	0.1	20.0	49.8	92.5
(7) Avers					
HW 1982	-	12.5	37.8	66.0	78.3
HW 1985	-	15.0	33.4	76.0	104.5
HW 1993	-	4.0	32.0	47.4	69.6
HW 1994	-	0.1	19.9	50.6	94.3
(8) Oberhalbstein					
HW 1982	14.9	40.0	39.8	69.0	75.1
HW 1985	5.3	19.8	24.2	66.5	88.2
HW 1993	0.8	7.7	35.1	50.1	58.5
HW 1994	0	0.1	17.9	53.7	75.8
(9) Albula/Davos "Tiefencastel"					
HW 1982	12.8	14.1	33.2	80.3	100.8
HW 1985	12.6	14.4	18.3	68.2	95.6
HW 1993	0.1	4.9	27.1	57.0	71.6
HW 1994	0	0.3	15.7	58.1	81.9

TABLE 2. Point measurements of the snow water equivalent Hw (meas) compared with the areal average at corresponding altitudes (na = not available)

Station [m a.s.l.]	Partial Area	Hw [cm]: 1 April 1982		Hw [cm]: 1 April 1985		Hw [cm]: 1 April 1993		Hw [cm]: 1 April 1994	
		meas	areal	meas	areal	meas	areal	meas	areal
Weissfluhjoch 2540	9	100.6	94	60.5	84	72.5	64	70.5	70
Büschalp 1960	9	60.1	40	31.9	24	32.9	32	37.9	22
Davos 1560	9	41.9	18	16.6	15	16.6	10	13.0	4
Bivio 1770	8	35.1	34	28.8	25	11.7	28	22.7	13
Zervreila 1735	3	47.1	38	36.4	34	23.2	22	32.9	13
San Bernadino 1630	(4)	37.9	33	39.3	34	na	9	21.7	7
Splügen 1460	4	21.1	23	29.5	25	7.7	5	14.0	3
Sedrun 1420	2	39.4	30	20.1	28	6.0	9	na	2
Disentis 1170	2	8.4	22	9.5	19	na	3	0	0

with seasonal runoff forecasts (Rango, 1994). Further emphasis for this problem has been recently added in view of the expected climate change and predictions of the resulting future snow conditions.While efforts to measure areal water equivalents of snow by microwaves are in progress, but not yet operational, results are presented of a different approach using optical remote sensing sensors. Areal water equivalents for the respective regions and elevation zones are evaluated at the point of the maximum accumulation of the seasonal snow cover. To this effect, the so called modified depletion curves of the snow coverage are used which are derived from the periodical snow cover mappings during the snowmelt season. Evalu-

ated have been the years 1982 and 1985 (Martinec et al., 1991) and, now in addition, with an improved method using high resolution satellite data, the years 1993 and 1994. As mentioned earlier, the spatial resolution of the sensor has to be adequate to the size of the basin (Baumgartner et al., 1987). For the present investigations SPOT-XS and Landsat-TM data has been used.

2. SNOW COVER ANALYSIS BASED ON GIS TECHNIQUES

The seasonal depletion of the snow cover in Alpine regions is monitored most effectively by multispectral remote sensing satellites (Seidel et al., 1989). Data acquired by different sensors have to be taken into account in order to make possible the evaluation of the varying snow distribution during the runoff season.

A model-based snow cover analysis approach is used: the raw data from the different sensors are geocoded according to the national coordinate system and integrated into a geographic information system (GIS). This GIS contains firstly basic entities such as a digital elevation model (DEM: elevation, slope and exposition) and secondly thematic entities such as the regions of interest (basin boundaries), elevation zones and gauge station values. Finally, detailed information concerning the land cover type or "ground nature" (forest, vegetation, glacier, permafrost, etc.) was made available and integrated into the GIS. Snow cover maps have been derived from multispectral satellite recordings by an hierarchical interpretation algorithm assigning for each pixel within the basin the affiliation to the categories "snow covered", "transition zone" or "snowfree" (=aper). The image processing task has been carried out using PCI software components. The snow interpretation algorithm has been put under the PCI environment and is now available from the PCI menu system.

For cloud covered or "unvisible" pixels the allocation to these classes is evaluated statistically in a post-processing step using GIS techniques. Another example and a more detailed description of the rather sophisticated extrapolation technique is given by (Ehrler and Seidel, 1995). The application of periodical snow cover mapping for snowmelt runoff modelling (SRM) and real-time runoff forecasts utilizing the SRM-ETH Menu System is described in (Seidel et al., 1995).

3. AREAL WATER EQUIVALENT FROM PERIODICAL SNOW COVER MAPPING

The method is applied in the upper Rhine basin at Felsberg (3250 km^2, 560-3614 m a.s.l.). Fig. 1 shows the snow cover on 29-APR-1994 as viewed by SPOT-XS and partial areas 1-9 in which the basin was subdivided. Areal water equivalents of the snow cover were computed separately for each partial area and for the following elevation zones A-E:

A	560-1100 m a.s.l.	D	2100-2600 m a.s.l.
B	1100-1600 m a.s.l.	E	2600-3614 m a.s.l.
C	1600-2100 m a.s.l.		

Detailed data on the elevation ranges, mean hypsometric altitudes and sizes of the regions and elevation zones are published in an earlier paper together with preliminary results (Martinec et al., 1991).

An example of conventional depletion curves (CDC) of snow covered areas based on satellite snow cover monitoring is shown in Fig. 2. The snow cover in the high zone E lasts longer than in the low zone A not only due to a larger accumulation of snow, but also due to the temperature lapse gradient. In addition, snow lasts evidently longer in a cold summer than in a warm summer. Consequently, as explained in more detail elsewhere (Hall and Martinec, 1985), conventional depletion curves cannot unequivocally indicate the initial snow reserves. The so-called modified depletion curves (MDC), which are illustrated in Fig. 3, can be derived for this purpose. In these curves, snow covered areas from conventional depletion curves are related to snowmelt depths computed daily by the degree-day method and totalized to the respective dates. The area below a MDC indicates the initial areal water equivalent of the snow cover. Naturally, intermittent snowfalls during the summer season do not belong to the seasonal snow cover on 1 April which is set as a starting date. Therefore melt depths of the new snow are excluded from the totalized snowmelt. Automatic plotting of the MDC curves and computation of water equivalents is included in the computer program of the SRM model (Martinec et al., 1994) as well as in the SRM-ETH version (Seidel et al., 1995). A detailed description of the numerous options in the ETH-SRM menu is available as Technical Report (Brüsch, 1995).

By this procedure, water equivalents of the snow cover have been evaluated in all partial areas as areal averages for the respective elevation zones. Results for the years 1982, 1985, 1993, and 1994 are listed in Table 1.

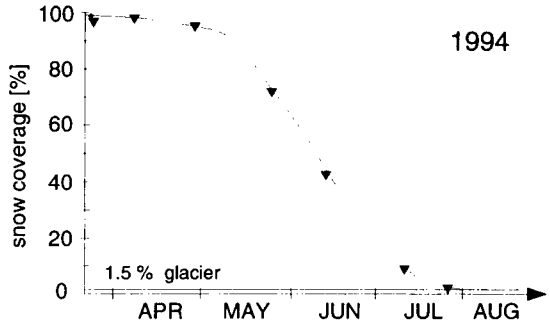

Fig. 2: Conventional depletion curve (CDC) for the subbasin SEDRUN within region 1 and Elevation range D

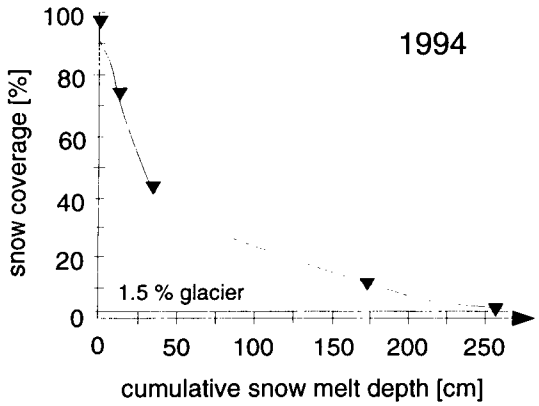

Fig. 3: Modified depletion curve (MDC) for the same basin and elevation range as in Fig. 2

The water equivalents in 1993 and 1994 are based on an improved snow cover mapping techniques in comparison with the values for 1982 and 1985 which have been published earlier (Martinec et al., 1991). In order to compare data from Table 1 with regular point measurements, it is necessary to interpolate the water equivalents to the altitudes of the respective snow gauging stations with the use of relations between water equivalent and altitude in each region. Results are listed in Table 2.

In the regions 1, 5, 6, 7 there is no snow gauging station for comparison. In the regions 2, 3, 4, 8, a comparison is possible only in the lower half of the elevation range. Only the region 9 is adequately covered thanks to the position of the Federal Institute of Snow and Avalanche Research (SLF) at Weisfluhjoch and in Davos. With regard to the altitude, the situation is also unfavourable: There is just one station in the zone D (1160 km^2) of the Felsberg basin and no measurements at all in the zone E (435 km^2). Evidently, representative snow water equivalents in mountainous regions can hardly be evaluated even from exceptionally well equipped snow gauging networks.

4. REGIONAL DISTRIBUTION OF SNOW IN TERMS OF WATER EQUIVALENT

In Fig. 4abcd, selected ranges of areal snow water equivalents are represented by gray tones. With regard to 9 regions and 5 elevation zones, there are altogether 42 partial areas (zone A is missing in the regions 1, 4 and 7) with an average size of 77 km^2 for which the snow water equivalents are evaluated. The spatial resolution in Fig. 4 abcd is further simplified because some partial areas belong to the same range of snow water equivalents. It should be noted that a fine spatial resolution of snow water equivalents should be accompanied by a refined computation of snowmelt depths in deriving the modified depletion curves. A study is in progress (Kustas et al., 1994) enabling the radiation component to be included in snowmelt computations. With the use of a digital terrain model, snow water equivalents could then be evaluated not only with regard to the altitude and temperature lapse rate, but also to the exposure of partial areas. The present evaluations reveal a general increase of the snow accumulation with the altitude so that the mountain relief is clearly indicated in Fig. 4abcd.

It may be noted that the highest areal water equivalents of the seasonal snow cover on 1 April occur near the North-West border of the Felsberg basin. This coincides with the zone of above-average long term maximum of snow accumulation overlapping to the Felsberg basin from North-West, as published in the Hydrological Atlas of Switzerland (Spreafico et al., 1992). Lighter grey tones in the eastern part of the Felsberg basin agree with the below-normal zone of the Atlas map. This map could be corroborated and possibly improved by applying the presented method in other regions of the Alps. To this effect, it would be necessary to evaluate the relation between the snow accumulation in single years and the long term maximum, in the respective areas.

5. REGIONAL VARIATIONS OF SNOW ACCUMULATION IN VARIOUS YEARS

In order to eliminate the altitude effect from the regional abundance or lack of snow, the areal snow water equivalents of the zones C and D were interpolated to a unified altitude of 2000 m a.s.l.. In

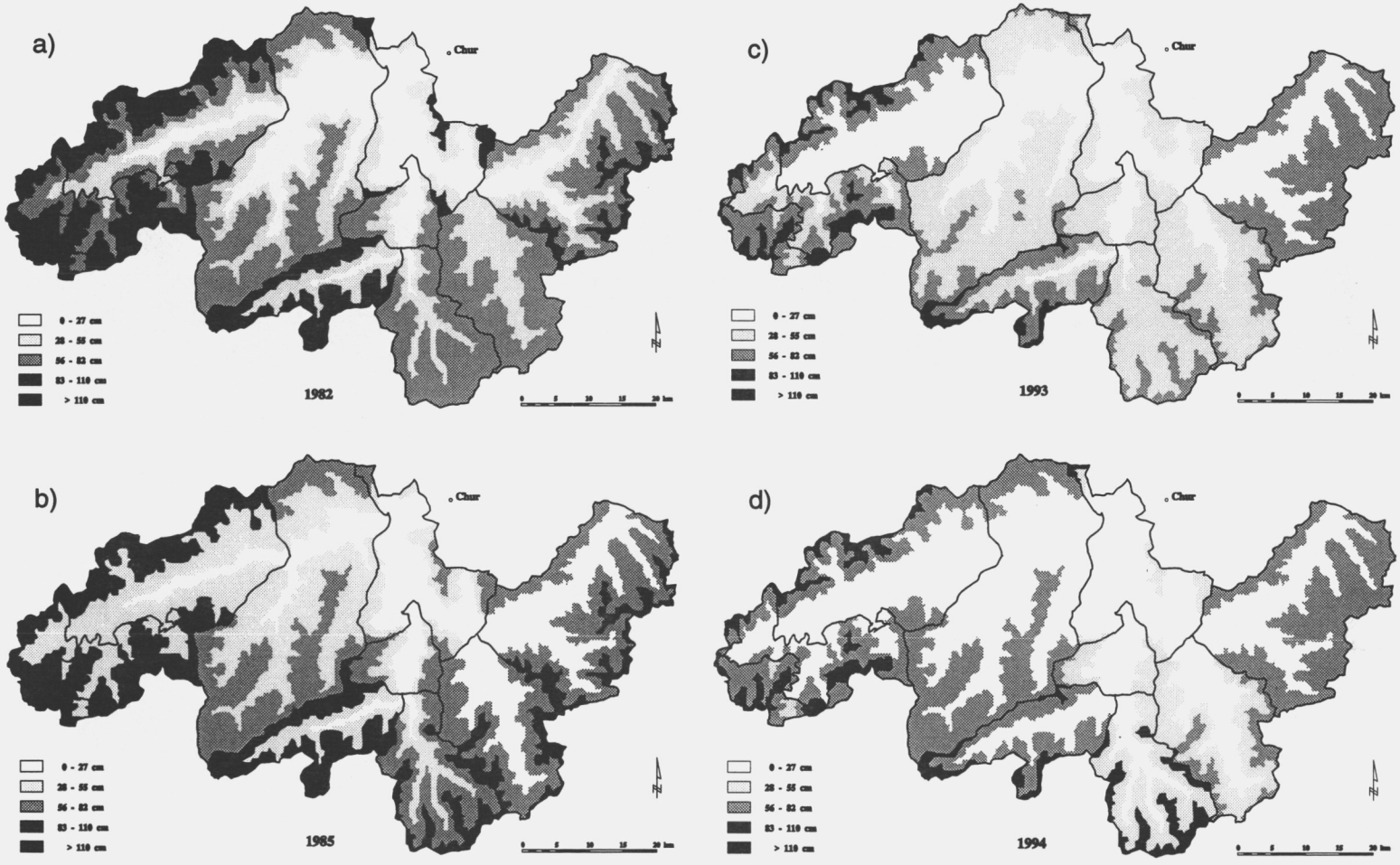

Fig. 4: Distribution of snow in terms of areal average water equivalent in the Rhine/Felsberg basin on 1 April 1982, 1985, 1993, and 1994
(region 1 devided into 1a SEDRUN and 1b TAVANASA)

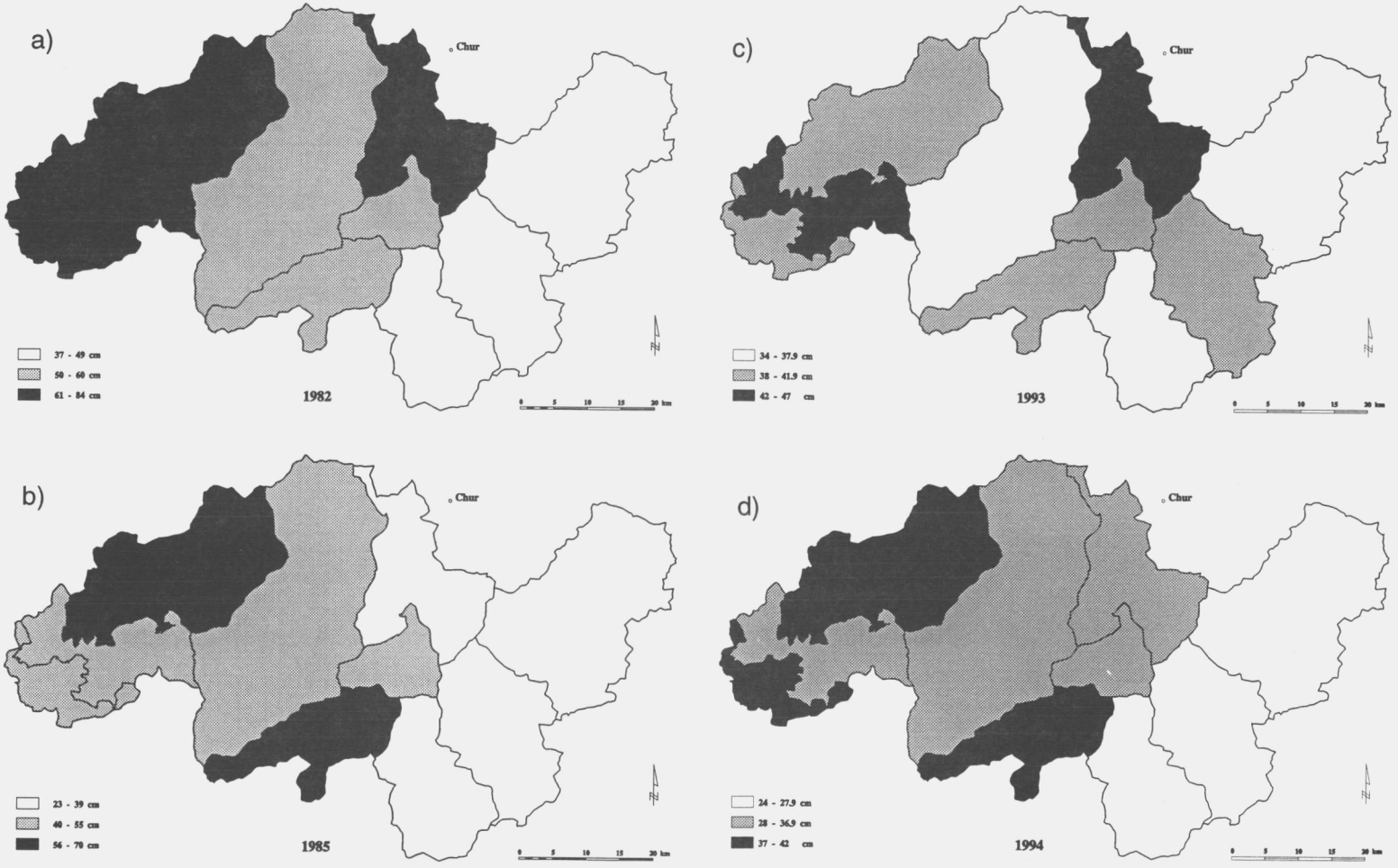

Fig. 5: Regional anomalies of the snow accumulation in terms of water equivalent at 2000 m a.s.l. on 1 April 1982, 1985, 1993, and 1994

Fig. 5abcd, the light grey area indicates an average accumulation of snow in the Felsberg basin at 2000 m a.s.l. in the respective year. The dark area indicates an accumulation above this average.

The western part of the Felsberg basin appears to have persistently more snow then the eastern part in all four years. The difference varies from year to year. It is for example larger in 1982 than in 1993 in absolute as well as in relative terms. Between these two extremes (West-East), average snow conditions prevail in the intermediate regions. Occasionally, heavy accumulation of snow may occur in the North (1982, 1993) or in the South (1985, 1994).

These regional variations must be taken into account when snow cover mapping is affected by clouds. The snow coverage under clouds should be extrapolated only from cloud-free areas with comparable snow conditions.

Another field of applications concerns the building standards in Switzerland with regard to expected snow loads on roofs and structures. The design snow loads have been evaluated from extreme snow water equivalents measured so far which generally increase with the altitude above sea level but also vary from region to region. Average areal water equivalents from the years 1982, 1985, 1993, and 1994 may serve for a tentative verification of the snow load chart of Switzerland (SIA, 1989) and of the mentioned map of regional snow water equivalents in the Felsberg basin. In these charts, the regional characteristics of the snow accumulation are indicated by four snow load or water equivalent zones (not elevation zones).

6. CONCLUSIONS

The evaluation of areal snow water equivalents from periodical snow cover mappings by satellites decisively improves the knowledge of the regional distribution of snow in the mountains, of altitude gradients of snow accumulation and variation of these conditions in different years.

It is useful for assessments of the representativeness of point measurements and snow courses as well as for comparisons with microwave measurements of the snow water equivalent (Rango et al., 1988). The regional assessment of snow accumulation is already used for an extrapolation of the snow coverage if satellite images are partially covered with clouds.

An improved evaluation of snow conditions, particularly above 2000 m a.s.l., is urgently needed for example for seasonal runoff forecasts (Seidel et al., 1990), (Seidel et al., 1993), (Paul et al., 1993) and for building standards concerning the snow loads on roofs (SIA, 1989).

Together with the SRM model, the satellite snow cover monitoring can produce runoff series in ungauged basins which is of particular importance in developing countries, for example in the Himalayan region, for the management of water resources.

A new field of application for the presented method is the emerging problem of climate change. A report of the Intergovernmental Panel on Climate Change (IPCC) (Street and Melnikov, 1990) notes the insufficiency of measurements at index points and states that "the areal distribution of seasonal snow cover, ice and permafrost need to be mapped on meaningful temporal and spatial scales to permit comparisons of changes in distribution under various climatic change scenarios".

7. REFERENCES

Baumgartner, M. F., Seidel, K., and Martinec, J. (1987). Towards Snowmelt Runoff Forecast Based on Multisensor Remote-Sensing Information. *IEEE Transactions on Geoscience and Remote Sensing*, GE-25:746–750.

Brüsch, W. (1995). SRM-ETH User's Manual. Technical Report TR Nr. 160, Computer Vision Laboratory - Institute for Communication Technology ETHZ.

Ehrler, C. and Seidel, K. (1995). Mutual effects of the climate change and the alpine snow cover and their influence on the runoff regime evaluated with the aid of satellite remote sensing. In Stein, T. I., editor, *IGARSS'95; Quantitative Remote Sensing for Science and Applications, Florence, Italy*, volume 3, pages 1973–1975.

Hall, D. K. and Martinec, J. (1985). *Remote Sensing of Ice and Snow*. Chapman and Hall, London - New York.

Kustas, W. P., Rango, A., and Uijlenhoet, R. (1994). Development and testing of a snowmelt-runoff forecasting technique. *Water Resources Research*, 30:1515–1527.

Martinec, J., Rango, A., and Roberts, R. (1994). Snowmelt Runoff Model (SRM) User's Manual. Geographica Bernensia P 29, Department of Geography—University of Bern.

Martinec, J., Seidel, K., Burkart, U., and Baumann, R.

(1991). Areal modelling of snow water equivalent based on remote sensing techniques. In *XX. General Assembly IUGG in Vienna 1991, IAHS-IUFRO Symposium Snow, Hydrology and Forests in High Alpine Areas*, pages 121–129. IAHS Publication No. 205.

Paul, P. R., Kumar, V. S., Rao, C. L. V. R., Seidel, K., and Haefner, H. (1993). Operational remote sensing for snowcover, runoff and avalanche applications in the Himalayas. In *Intern. Symposium "Operationalization in Remote Sensing"*, volume 4, pages 71–79. ITC Enschede NL.

Rango, A. (1994). Application of remote sensing methods to hydrology and water resources. *Hydrological Sciences -Journal- des Sciences Hydrologiques*, 39(4):309–320.

Rango, A., Martinec, J., Chang, A. T. C., Forster, J. L., and van Katwijk, V. (1988). Average areal water equivalent of snow in a mountain basin using microwave and visible satellite data. In *IGARSS '88 Symposium in Edinburgh, Scotland*, pages 447–448, Paris. ESA SP-284. Vol. 1.

Seidel, K., Brüsch, W., Steinmeier, C., Martinec, J., and Wiedemeier, J. (1995). Real time runoff forecasts for two hydroelectric stations based on satellite snow cover monitoring. In Askne, J., editor, *Sensors and Environmental Applications of Remote Sensing*, pages 253–258. 14th EARSeL Symposium 1994 in Göteborg, Sweden, A. A. Balkema Rotterdam/Brookfield.

Seidel, K., Burkart, U., Baumann, R., Martinec, J., Haefner, H., and Itten, K. I. (1989). Satellite data for evaluation of snow reserves and runoff forecasts. In *Hydrology and Water Resources Symposium, Christchurch, N.Z.*, pages 24–27.

Seidel, K., Martinec, J., Steinmeier, C., and Brüsch, W. (1993). Remote sensing of snow cover for operational forecasts. In *Intern. Symposium "Operationalization in Remote Sensing"*, volume 2, pages 134–144. ITC Enschede NL.

Seidel, K., Wiedemeier, J., and Martinec, J. (1990). Operationelle Überwachung von Schneeschmelzvorgängen: Möglichkeiten zur Prognose von Wasserabflussmengen (Operational Monitoring of Snowmelt Processes: Possibilities for Runoff Forecasts). *Bulletin SEV/VSE*, 81(10):9–17.

SIA (1989). SIA Norm 160 (Building Standards). Technical report, SIA, Zürich, Switzerland.

Spreafico, M., Weingartner, R., and Leibundgut, C. (1992). *Hydrologischer Atlas der Schweiz (Hydrological Atlas of Switzerland)*. Landeshydrologie und -geologie, EDMZ, CH-3003 Bern, 1 edition.

Street, R. B. and Melnikov, P. I. (1990). Seasonal snow cover, ice and permafrost (28 contributions). In *Potential Impacts of Climate Change, report for IPCC by Working Group*, chapter 7, pages 7–35. WMO-UNEP, Geneva, Switzerland.

MODIS Activities at the National Snow and Ice Data Center DAAC

Greg Scharfen
NSIDC, University of Colorado

MODIS Snow and Ice Workshop
14 September 1995

1) Introduction

The National Snow and Ice Data Center, at the University of Colorado in Boulder, is participating in EOSDIS as a Distributed Active Archive Center (DAAC) for snow and ice data products. The NSIDC DAAC is one of nine discipline and/or instrument-specific DAACs in EOSDIS. NSIDC is funded by NASA, NOAA and the National Science Foundation. The DAAC is NSIDC's largest project to date.

The NSIDC DAAC will produce and/or archive level 2 and 3 EOSDIS standard products pertaining to the snow and ice community as well as relevant in-situ data. NSIDC also intends to implement non-standard products developed by relevant Interdisciplinary Science (IDS) Teams such as Polar Exchange at the Sea Surface (POLES). These may be produced from data collected by several EOS sensors including: MODIS, GLAS, ASTER, AMSR and MISR. There are also several NOAA/NASA Pathfinder products being produced and archived at NSIDC.

NSIDC has been producing, archiving and distributing sea ice extent and concentration information derived from passive microwave satellite observations since the mid-1980s. The combined SMRR and SSM/I record now spans from 1979-94, and is available on CD-ROM. The annual cycle of sea ice extent shows some variation from year to year, and these data are being related to synoptic weather patterns by polar scientists (Serreze, in press). A combined sea ice/snow cover product from the passive microwave is under development.

2) MODIS products at the NSIDC DAAC

NSIDC will produce and/or archive the MODIS standard (at launch) snow and ice products developed by the MODIS Science Team. Currently these are the following:

Daily Snow Cover (MOD 10)
Level 2 Produced at GSFC Archived at NSIDC
Level 3 Produced at NSIDC Archived at NSIDC

Weekly Snow Cover (MOD 33)
Level 3 Produced at NSIDC Archived at NSIDC

Daily Sea Max Extent (MOD 29)
Level 2 Produced at GSFC Archived at NSIDC
Level 3 Produced at NSIDC Archived at NSIDC

Weekly Sea Ice Cover (MOD 42)
Level 3 Produced at NSIDC Archived at NSIDC

NSIDC will also implement relevant non-standard research products (post-launch) from MODIS. For example, several products are being considered by the POLES IDS Team: sea ice motion, ice surface temperature, albedo, cloud properties, surface radiative fluxes and snow cover.

3) Validation Data Sets at NSIDC

NSIDC maintains or is assembling several data sets which may be useful for validation of MODIS products: STOS Former Soviet Union Daily Snow Depth for 203 stations (distributed on CD-ROM), USDA SCS Snowtell Sites for the Western U.S. (planned monthly maps of snow water equivalent), NOAA/NWS forecast office snow depth observations (reviewed by D. Robinson), planned US Snow Depth Climatology (Snowtell and NWS sites combined), and the improved NOAA/NESDIS interactive multisensor snow and ice product (planned distribution to snow and ice community).

4) Grids for Level 3 MODIS Products

An important, and somewhat urgent, issue for consideration by the snow and ice community is the gridding of level 3 products. Current plans call for most EOSDIS level 3 products to be archived and distributed in a common grid suitable for displaying global data. Several groups are discussing this issue including the MODIS Land Group, the MODIS Science Team, the Science Working Group for the AM-1 Platform (SWAMP), and the CERES Science Team.

There are good reasons for a common gridding scheme, including the potential for greater processing efficiency and easier comparisons between the large number of geophysical parameters produced in the EOS system (Wolfe, 1995).

Several MODIS team members (whom I will refer to as the MODIS gridding group for the purposes of this report) are discussing this issue. According to this group, "the current proposed EOS grid is a binned, nested Sinusoidal grid" (Wolfe, 1995). There are at least two versions of this grid, a MODIS version which is equal area but not nested horizontally, and not binned at fine resolutions (Wolfe, 1995), and a CERES version which has an equal-area 'reference' grid with nestable equal angle subgrids (Green, 1995). Both are versions of the International Satellite Cloud Climatology Project (ISCCP) Grid.

For several reasons, neither of the proposed grids are ideal for use in the polar regions. Both are designed to have the desirable characteristic of being equal area, but the binning and nesting results in a loss of this characteristic at the poles. The sinusoidal projection and the usual form of the ISCCP grid either compress or stretch out the poles, but perhaps their most obvious drawback is that neither permit a polar-centric view. We have raised this issue with the MODIS Science Team, the MODIS Land Group and the MODIS gridding group.

If a second grid is needed for the polar regions, snow and ice products could be generated twice, on overlapping global and polar grids. Consideration must be given to how and where in the product generation system it is produced. If it is generated from the level 3 product, some information may be lost and artifacts introduced due to the resampling and rebinning of data. This could be avoided if both level 3 grids are generated from the level 2 data. More information is needed to determine the best approach.

The ability of the EOSDIS Science Data Production (SDP) Toolkit to provide a second grid is being investigated by NSIDC. The Toolkit is designed to provide an interface between instrument processing software and the production system environment (TK5 release announcement, 1995). There are Toolkit functions which perform geocoordinate transformations in the forward and inverse directions, ie. from geographical coordinates (latitude, longitude) to Cartesian coordinates (x, y) of the given

projection. But coordinate transformations are only one part of the problem; this tool does not resample or regrid!

To further discussion on the gridding needs of the polar science community, NSIDC is planning three near-term strategies:

1) NSIDC seeks the input of polar scientists on their requirements for grids for the level 3 MODIS snow and ice products. Individual comments can be provided to the MODIS Science Team or to NSIDC (email the author at scharfen@kryos.colorado.edu)

2) NSIDC will request that the MODIS gridding group consider alternative gridding schemes for polar products.

3) The MODIS snow and ice investigators and NSIDC propose to collaborate on a quantitative analysis of the potential degradation of information in regridding data from the level 3 global grid to a level 3 polar grid, vs. separately gridding level 2 data to both level 3 grids.

5) MODIS Science Software Integration and Test (SSI+T) at NSIDC

Another issue that NSIDC is addressing is the schedule for implementation of MODIS products at the DAAC. The AM-1 platform is scheduled for launch in June 1998. MODIS plans three releases of science software at the DAACs: Beta in January 1996, Version 1 "Engineering" in January 1997, and Version 2 "Operational" in August 1997.

According to MODIS, the purposes of the three deliveries is to learn the process of I&T (DAAC, IT, ESDIS, ECS), test out the evolving ECS system and the DAAC operations, learn the science algorithms, size the system (CPU, I/O, network, etc.), make changes in the system, science software etc. and be ready for production at launch. If NSIDC does not take part in the two earlier deliveries, no corrections or learning experiences based on these deliveries can be made (B. Putney, pers. comm.). Unfortunately, NSIDC is not scheduled to have ECS hardware, software and communications until Release B of the ECS in September 1997. NSIDC is the only AM-1 production DAAC not currently scheduled to take part in the three software deliveries!

Since NSIDC has a responsibility to the snow and ice community to

produce and distribute quality products we have undertaken steps to rectify this situation. NSIDC has requested a minimal configuration, early activation of ECS during the Release A timeframe to allow for MODIS SSI+T beginning with the release of Engineering Version 1 of MODIS software in January 1997. We seek support from concerned users on this issue (email messages to the author will be forwarded to the appropriate contacts).

6) Summary

The NSIDC DAAC is looking forward to implementing MODIS snow and ice products for the EOSDIS user community. We wish to bring two issues to the attention of the snow and ice community. First, NSIDC believes that the global projection EOS level 3 grid is inadequate for the polar regions, and suggests that a second grid is adopted and supported by EOSDIS for snow and ice products in the polar regions. Second, the current ECS schedule does not permit MODIS Science Software Integration and Test at the NSIDC DAAC, and we have asked ESDIS to implement an early activation of ECS at the NSIDC DAAC.

NSIDC seeks comment and the support of the user community on both of these issues. Please contact the MODIS Science Team, or the author at: NSIDC, Campus Box 449, University of Colorado, Boulder, CO. 80309; email: scharfen.kryos.colorado.edu.

7) References

Green, R. and Wielicki, B. "Selection of a Nestable Grid for EOS Products", DRAFT (June 29, 1995)

Putney, B., MODIS Science Data Support Team, pers. comm. May 22, 1995

Serreze, M., Maslanik, J., Key, J., Kokaly, R., Robinson, D. "Diagnosis of the Record Minimum in Arctic Sea Ice Area During 1990 and Associated Snow Cover Extremes", Geophysical Research Letters (in press)

Wolfe, R., Strahler, A., and Evans, B. "Proposed EOS Common Grid" DRAFT (June 19, 1995)

Science Data Production Toolkit Users Guide: URL http://edhs1.gsfc.nasa.gov:8001/waisdata/toc

Greg Scharfen
NSIDC DAAC
email: scharfen@kryos.colorado.edu
phone: 303-492-6197
fax: 303-492-2468

WORKING GROUP REPORTS

I. MODIS At-launch Snow Products - Michael Baumgartner, Chair

Participants: Tom Andersen
Richard Armstrong
James Foster
Dorothy Hall
Bruce Ramsay
Walter Rosenthal
Klaus Seidel

Themes

- Basic Questions
- Algorithm Questions
- Technical Questions

1. Basic Questions:

- Who is the audience/who needs global snow cover data?
  - Climatology/GCM
  - Snowmelt (hydroelectricity production, irrigation, energy balance models, natural hazards)

  Problem: Research is not always directed towards applications. Applications do not use remote sensing data. Reason: spatial resolution.

- Resolution: For most applications 250-500 m is optimal resolution (resolution is process dependent). This means using the advantage of MODIS! Even though costs are higher for the finer resolution. With today's development in computer technology, there is no major technical or financial limitation.

- Operational Considerations:
  - Daily products must be available within 24 to 48 hours. There is no concern related to climatological studies and research.

  Conclusion: 500 m/48 hours acceptable; applications better guaranteed compared to 1 km product.
  - Daily products are necessary in operational use due to clouds (basically, a weekly resolution would be acceptable, if no clouds exist).

- Temporal Aspects:
  - Daily product mandatory; base product
  - Monthly product for climatology
  - User has to decide which product he wants to derive from daily data (e.g. 5-, 7- or 10 day composites).

- Raw Data:
  - Should be easily accessible for global user community on network (low cost!)

- ESA launches MERIS (medium resolution imaging spectrometer) in 1999; comparison with AVHRR and MODIS?

- Metadata for User, Related to Products:
  - Carried through from raw data (orbit parameters; lat./long., resolution, calibration data, sun normalization, etc.).
  - Information is needed on how snow cover maps are produced (e.g. in a header)
  - User-friendly format
  - Query language

- Gridding Scheme:
  - Global grid is not acceptable to the polar community
  - Is there a single archive?
  - The user wants a grid which best serves him (equal area at highest latitudes).

2. Algorithm Questions:

- Regional algorithm, different for Rockies, Mid-West, Russia, Norway, Alps, etc.
  Problems: vegetation, topography, geology, shadows, forests!
- Regionalization
- Multiresolution, different for Rockies, Mid-west, Russia, Alps, etc.
  mountainous regions should leave a higher resolution than lowlands
  For each pixel, all information is needed in all possible resolutions
  user has to decide upon resolution
- Post-launch classification algorithm improvement
- Does the snow map include the cloud mask? Can user switch mask on/off?
- Accuracy: what are the errors, how large are they--to be determined for different regions of the world; level of confidence is important for user.
- Can the evening orbit be processed/is there a product available?

3. Technical Questions:

- Development of hardware is very fast; therefore, technical limitations (e.g. amount of data, CPU-time) are not critical and have no major influence on financial aspects.

Conclusions:

1. Basic Questions:

   - Who are the users?
     - Climatology
     - Hydrology

   - What is the optimal resolution?
     - 500 m/24-48 hours

   - Temporal Aspects:
     - Daily product as basis
     - User decides which other products he wants

   - Raw Data:
     - Accessible for all users (easily, cheap)

   - Metadata:
     - Carried through from raw data
     - Information, How snow cover data were derived?
     - User friendly

2. Algorithm Questions:

   - Regional algorithms: regionalization
   - Multiresolutions: high resolution of complex topography
   - Improvement of algorithm?
   - Accuracy? level of confidence

3. Technical Questions:

   - Hardware
   - Finances

II. MODIS At-launch Ice Products - Cheryl Bertoia, Chair

Participants:
Lawson Brigham
Donald Cavalieri
Joey Comiso
Dorothy Hall
Jeffrey Key
George Leshkevich
Claire Parkinson
Konrad Steffen

Is an ice/no ice product useful?

- Operational: conditional yes
- Research: not terribly useful

Essential: cloud mask, cloud type/thickness

MODIS vs other available sensors: What capabilities are added?

1. Good temporal frequency in Antarctica (vs SAR)
2. Better spectral resolution for fresh water ice typing (not much help with sea ice)

How often will a sea ice product actually be available?

- Climatological cloud cover - 70%
- If cloud mask permits--maybe could get a product 50% of the time.

When is a pixel labeled ice?

- Currently ~ 50%
- Prefer ~ 15%

Questions:

1. How soon after acquisition?
   R - 3-6 months
   0 - 6 hr. optimum
   2 day useful
   7 day no use

2. Composite maps
   - Prefer daily, monthly
   - Optimal: half daily

3. Most useful?
   - Imperative: cloud mask/type/thickness

   Ice products
   - Ice type/concentration
   - Temperature
   - Albedo

   (ice motion)

4. Use of products
   - Surface climatology
   - Polynya studies
   - Snow over ice
   - Validation of other products
   - Supplement (replace?) AVHRR temp fields-Great Lakes
   - Ice sheets-surface temperature and albedo
   - Validation/case studies: SSM/I
   - Operational ship support: high confidence product?

5. Metadata
   - Image id/lat. long./time/date
   - Image size (row/col.)
   - Cloud %, type, etc.

Understanding:

- Limited number of at-launch products

Recommendation:

- Substitute an ice type/concentration product for the current ice/no ice product. Increase resolution to 250-500 m for inland lake ice.

Action Items:

1. K. Steffen to obtain simulated MODIS data set. Use to test drive Landsat ice type algorithm.
2. Consult with other members of the sea ice community during the next PoDAG meeting.
3. Invite D. Hall (other MODIS folks?) to the next PoDAG meeting, October 17-18, Annapolis, Maryland.

III. Post-launch MODIS Snow and Ice Products - Ron Welch, Chair

Participants: Jeffrey Dozier
Robert Green
Jeffrey Key
Anne Nolin
George Riggs
Greg Scharfen
Larry Smith

Snow:

- Subpixel snow coverage (regional, global)
- Snow under trees (with MISR-angular)
- Spectral albedo
  (from grain size and contamination)
- Temperature
- Wetness

Ice Sheets:

- Spectral albedo

Sea/Lake Ice:

- Spectral albedo
- Temperature
- Open water fraction
- Ice Types: first year/multiyear
  bare/snow covered
  thin/thick
- Melt ponds
- Ice edge
- Ice motion (Radarsat?)

Time/Space Averaging:

- Monthly/1° spatial
- Corresponding to CERES Energy Budget
- For weekly composites, encode which days contributed--data legacy

- Must have best possible cloud mask
  - Validation
  - ASTER

Communities:

- Alpine snow hydrology
- Water Resources Management
  - hydroelectric
  - agriculture
- Meteorology
- Oceanography
- Biogeochemistry
- Transportation (ocean, lake, river)
  - ship routing
- Regional and global climate modeling
- Microwave Remote Sensing
  - improved interpretation

Gridding/Projections:

- Lack of knowledge
- Bring in experts
- Need flexibility
  - New ideas/algorithms
  - Reprocessing
- Should Level-3 data be archived
  - Subsetting
- Path to migrate IDS algorithms to MODIS Standard Products

IV. Utility of MODIS Snow and Ice Products - Anne Walker, Chair

Participants: Steven Ackerman
Michael Baumgartner
Tom Carroll
Ed Josberger
Al Rango
George Riggs
David Robinson

Users:

- Operational
- Research

MODIS Advantages:

- Resolution
- Cloud vs. snow discrimination

How soon after acquisition?
- 24-48 hrs. (radiances)
- Research

Composite maps?
None - DAAC should have flexibility to accommodate user requirements for different composites
  - Interactive software
- Difficult to determine at this point in time what ideal composite users would require

MODIS Products:

- At-launch
  - Daily gridded snow cover (1 km)
  - Level 2 snow cover
  - Monthly snow cover (?)

- Post-launch
  - End user processing system (multiple sensor products included)
  - MODIS/microwave SWE
  - Albedo
  - Fractional snow cover per pixel

Use of Products?

- Snow melt run-off model
- Large scale model parameterization
- Validation source for other snow cover products
- Climate analyses
- Monitoring, change detection
- Integration with other snow cover data sets for river/flood forecasting
- Ice navigation
- Ice jam monitoring
- Air/sea interactions

Metadata--needs vary with product (Level 2 vs. 3)

- Georeferencing
- Ephemeris data
- Calibration parameters
- Orbit parameters

Improvements to current snow and ice products?

- Software to generate user customized products

List of Attendees:

Steven Ackerman
CIMSS
University of Wisconsin
1225 West Dayton Street
Madison, WI 53706
Phone: (608) 263-3647
Fax: (608) 262-5974
E-mail: stevea@ssec.wisc.edu

Tom Andersen
Statkraft
P.O. Box 494
N-1322 H0VIK
NORWAY
Phone: +47-67-57-70-13
Fax: +47-67-57-79-91
N/A

Richard Armstrong
National Snow and Ice Data Center
CB 449, University of Colorado
Boulder, CO 80309-0449
Phone: (303) 492-1828
Fax: (303) 492-2468
E-mail: rlax@kryos.colorado.edu

Charles Bachmann
Naval Research Lab
Code 5365
Bldg. 56, Rm. 218
Washington, DC 20375-5336
Phone: 202-767-3240
E-mail: bachmann@radar.nrl.navy.mil

Roger Barry
National Snow and Ice Data Center
CB 449, University of Colorado
Boulder, CO 80309-0449
Phone: (303) 492-5488
Fax: (303) 492-2468
E-mail: rbarry@kryos.colorado.edu

Michael Baumgartner
Dept. of Geography
University of Berne
Hallerstrasse 12
3012 BERN
SWITZERLAND
Phone: ++ (31) 631-8020
Fax: ++ (31) 631-8511
E-mail: baumgartner@giub.unibe.ch

Cheryl Bertoia
U.S. National Ice Center
4251 Suitland Road FOB 4
Washington, D.C. 20395-5120
Phone: (301) 457-5314, ext. 302
Fax: (301) 457-5300
E-mail: cbertoia@icecen.fb4.noaa.gov
cbertoia@sar_ws.fb4.noaa.gov

Lawson Brigham
9902 Treetop Lane
Seabrook, MD 20706
Phone: 301-794-7759
Fax: 301-314-2023
N/A

Tom Carroll
Nat. Oper. Hydrologic Rem. Sens. Cntr.
Office of Hydrology
National Weather Service, NOAA
1735 Lake Drive West
Chanhassen, MN 55317-8582
Phone: (612) 361-6610, ext. 225
Fax: (612) 361-6634
E-mail: nohrsc@mcimail.com
tc@nohrsc.nws.gov

Donald Cavalieri
NASA/Goddard Space Flight Center
Code 971
Greenbelt, MD 20771
Phone: (301) 286-2444
Fax: (301) 286-0240
E-mail: don@cavalieri.gsfc.nasa.gov

Eugene Clothiaux
Penn State University
College of Earth and Mineral Sciences
Dept. of Meteorology
410 Walker Bldg.
University Park, PA 16802
Phone: 814-863-7834

Joey Comiso
NASA/Goddard Space Flight Center
Code 971
Greenbelt, MD 20771
Phone: (301) 286-9135
Fax: (301) 286-0240
E-mail: comiso@joey.gsfc.nasa.gov

Jeffrey Dozier
University of California
School of Environmental Science and Management
Santa Barbara, CA 93106
Phone: (805) 893-2309
Fax: (805) 893-2578
E-mail: dozier@icess.ucsb.edu

James Foster
NASA/Goddard Space Flight Center
Code 974
Greenbelt, MD 20771
Phone: (301) 286-7096
Fax: (301) 286-1758
E-mail: jfoster@glacier.gsfc.nasa.gov

Barry Goodison
Climate & Atmospheric Research
Atmospheric Environment Service
4905 Dufferin St.
Downsview, ONT M34 5T4
CANADA
Phone: 416-739-4345
Fax: 416-739-5700
E-mail: goodisonb@aestor.am.doe.ca

Robert Green
Jet Propulsion Laboratory
MS 306-438
4800 Oak Grove Drive
Pasadena, CA 91109-8099
Phone: (818) 354-9136
Fax: (818) 393-4406
E-mail: rog@gomez.jpl.nasa.gov

Dorothy Hall
NASA/Goddard Space Flight Center
Code 974
Greenbelt, MD 20771
Phone: (301) 286-6892
Fax: (301) 286-1758
E-mail: dhall@glacier.gsfc.nasa.gov

Ed Josberger
Ice and Climate Project
U.S. Geological Survey
University of Puget Sound
Tacoma, WA 98416

Phone: 206-593-6516
Fax: 206-383-7967
E-mail: ice@wayback.ups.edu

Jeffrey Key
Dept. of Geography
Boston University
675 Commonwealth Ave.
Boston, MA 02215
Phone: (617) 353-2841
Fax: (617) 353-8399
E-mail: jkey@bu.edu

Stephen Lehrman
Research Triangle Institute
60 Watch Hill
East Greenwich, RI 02818
Phone: 401-885-3995
Fax: 401-884-7375
E-mail: s_lehrman@ids.net

George Leshkevich
NOAA/Great Lakes Environmental Research Lab.
2205 Commonwealth Blvd.
Ann Arbor, MI 48105-1593
Phone: 313-741-2265
Fax: 313-741-2055
E-mail: leshkevich@sparc.glerl.noaa.gov

Gregg Linebaugh
Goddard Space Flight Center
Code 974
Greenbelt, MD 20771
Phone: (301) 286-4738
Fax: (301) 286-1758
E-mail: linebaugh@hydro1.gsfc.nasa.gov

Anne Nolin
CIRES
Campus Box 216
University of Colorado
Boulder, CO 80309-0216
Phone: (303) 492-6508
Fax: (303) 492-1149
E-mail: nolin@spectra.colorado.edu

Claire Parkinson
NASA/Goddard Space Flight Center
Code 971
Greenbelt, MD 20771
Phone: (301) 286-6507
Fax: (301) 286-1761
E-mail: clairep@neptune.gsfc.nasa.gov

Bruce Ramsay
Interactive Processing Branch (E/SP22)
NOAA Science Center (Rm. 510)
5200 Auth Road
Tm. 510, Stop H
Camp Springs, MD 20748
Phone: (301) 763-8142 ext. 128
Fax: (301) 763-8131
E-mail: bramsay@ssd.wwb.noaa.gov

Albert Rango
Hydrology Laboratory
USDA/ARS/BARC-W
Bldg. 007, Rm. 104
Beltsville, MD 20705
Phone: (301) 504-8700
Fax: (301) 504-8931
E-mail: alrango@hydrolab.arsusda.gov

George Riggs
Research & Data Systems Corp.
7855 Walker Drive, Suite 460
Greenbelt, MD 20770
Phone: (301) 286-6811
Fax: (301) 982-3749
E-mail: griggs@ltpextreme1.gsfc.nasa.gov

David Robinson
Dept. of Geography
Rutgers University
New Brunswick, NJ 08903
Phone: (908) 932-4741
Fax: (908) 932-0006
E-mail: drobins@gandalf.rutgers.edu

Walter Rosenthal
Institute for Computational Earth System Science
P.O. Box 7457
Mammoth Lakes, CA 93546
Phone: (619) 935-4464
Fax: (619) 935-4867
E-mail: walter@icess.ucsb.edu

Vincent Salomonson
NASA/Goddard Space Flight Center
Code 900
Greenbelt, MD 20771
Phone: (301) 286-8601
Fax: (301) 286-1738
E-mail: vinces@esd.gsfc.nasa.gov

Greg Scharfen
National Snow and Ice Data Center
University of Colorado
Campus Box 449
Boulder, CO 80309
Phone: (303) 492-6197
Fax: (303) 492-2468
E-mail: scharfen@kryos.colorado.edu

Klaus Seidel
Institut fuer Kommunikationstechnik ETHZ
Gloriastr. 35
CH 8092 Zuerich
SWITZERLAND
Phone: +41-1-632-5284
Fax: +41-1-632-1251
E-mail: seidel@vision.ee.ethz.ch

Larry Smith
Cornell University
Dept. Geological Sciences
Snee Hall
Ithaca, NY 14853-1504
Phone: (607) 255-2673 (lab), (607) 255-6329 (office)
Fax: (607) 254-4780
E-mail: lsmith@geology.cornell.edu

Konrad Steffen
CIRES
University of Colorado
Campus Box 216
Boulder, CO 80309-0216
Phone: (303) 492-4524
Fax: (303) 492-1149
E-mail: koni@seaice.colorado.edu

Anne Walker
Atmospheric Environment Service
Climate Research Branch
4905 Dufferin Street
Downsview, Ontario M3H 5T4
CANADA
Phone: (416) 739-4357
Fax: (416) 739-5700
E-mail: walkera@aestor.am.doe.ca

Ron Welch
Institute of Atmospheric Sciences
South Dakota School of
Mines and Technology
Rapid City, SD 57701
Phone: (605) 394-2291
Fax: (605) 394-6061
E-mail: welch@cloud.ias.sdsmt.edu

REPORT DOCUMENTATION PAGE

Form Approved
OMB No. 0704-0188

1. AGENCY USE ONLY *(Leave blank)*	2. REPORT DATE	3. REPORT TYPE AND DATES COVERED
	October 1995	Conference Publication

4. TITLE AND SUBTITLE
Proceedings of the First Moderate Resolution Imaging Spectroradiometer (MODIS) Workshop on Snow and Ice

5. FUNDING NUMBERS
Code 974

6. AUTHOR(S)
Dorothy K. Hall, Editor

7. PERFORMING ORGANIZATION NAME(S) AND ADDRESS(ES)
Hydrological Sciences Branch, Code 974
Laboratory for Hydrospheric Processes
Goddard Space Flight Center
Greenbelt, MD 20771

8. PERFORMING ORGANIZATION REPORT NUMBER
96B00001

9. SPONSORING/MONITORING AGENCY NAME(S) AND ADDRESS(ES)
NASA Aeronautics and Space Administration
Washington, D.C. 20546-0001

10. SPONSORING/MONITORING AGENCY REPORT NUMBER
CP-3318

11. SUPPLEMENTARY NOTES
The first day of the workshop was held in conjunction with the Arctic Climate Systems Study (ACSYS) Worskhop.

12a. DISTRIBUTION/AVAILABILITY STATEMENT
Unclassified-Unlimited
Subject Category: 43
Report available from the NASA Center for AeroSpace Information, 800 Elkridge Landing Road, Linthicum Heights, MD 21090; (301) 621-0390

12b. DISTRIBUTION CODE

13. ABSTRACT *(Maximum 200 words)*

This document is a compilation of summaries of talks presented at a 2-day workshop on Moderate Resolution Imaging Spectroradiometer (MODIS) snow and ice products. The objectives of the workshop were to: inform the snow and ice community of potential MODIS products, seek advice from the participants regarding the utility of the products, and determine the needs for future post-launch MODIS snow and ice products. Four working groups were formed to discuss at-launch snow products, at-launch ice products, post-launch snow and ice products and utility of MODIS snow and ice products, respectively. Each working group presented recommendations at the conclusion of the workshop.

14. SUBJECT TERMS
Moderate Resolution Imaging Spectroradiometer (MODIS), Ice, Snow

15. NUMBER OF PAGES
133

16. PRICE CODE

17. SECURITY CLASSIFICATION OF REPORT	18. SECURITY CLASSIFICATION OF THIS PAGE	19. SECURITY CLASSIFICATION OF ABSTRACT	20. LIMITATION OF ABSTRACT
Unclassified	Unclassified	Unclassified	Unlimited